THE UNIVERSITY OF QUEENSLAND

Bachelor of Engineering Thesis

Finite Element Study of the Effects of Characteristic, Geometric Variables in Handpan Designs and Performance

Student Name: Liam O'DONNELL

Student Number: 42936060

Course Code: MECH4500

Supervisor: Bill Daniel

Submission date: 27th of October, 2017

A project report submitted in partial fulfilment of the requirements of the course: MECH4500 Engineering Thesis

UQ Engineering

Faculty of Engineering, Architecture and Information Technology

School of Mechanical and Mining Engineering

Abstract

Handpans are a recently developed percussive instrument that share similarities with the steel drum. Current literature has not developed an understanding of how geometry, the only variable in a handpan, affects performance. Demand currently exceeds productive capacity of the manufacturers due to the labour intensive nature of building the instrument. Understanding the system response based on geometry is desired as this may provide insight to the instrument and improve manufacturability.

An examination of geometric changes on the instrument's response is the primary concern of this thesis. Peripheral work represents a large portion of work done and covers the development of a robust and variable CAD model, testing of actual handpans to determine their harmonic response and theoretical plate vibration analysis. Key geometric variables are to be identified and analysed.

An FEA analysis is performed on the CAD model in both modal and transient settings. Results from the two analysis types are compared. Comparison to actual handpan outputs and theoretical plate vibrations are also made. Discrepancies are analysed and reasons for differing output between the instruments in their physical testing are hypothesised.

Non-linear effects are highly significant and current methodologies of modelling need improvement. Handpans are highly sensitive to geometry and all information generated shows this. Small changes in geometry create large changes in harmonic response and design details can alter system output significantly. CAD geometry creation process and model ideology is sufficient, however, the fidelity of the geometry needs to be, and can be, improved.

Using the recommendations of this report as points of improvement, the current modelling process should soon be able to accurately and precisely model handpans with very low error. Once this is the case, fully predictive modelling is possible. At this point a more complete investigation into the geometry of handpans can be conducted.

Acknowledgements

This year has been interesting and tumultuous, to say the least. A number of people helped me with this thesis and a number more helped me get through the year.

First and foremost, to Bill; you have been a great supervisor. Whenever I needed anything you were there with an informative and useful answer. It was never a hassle and you never made it seem difficult. I would also like to extend my thanks to Belinda, Bill's wife, whose handpans were used extensively in this thesis. She was always generous with letting me have them for study even though she is rather fond of them and they are expensive pieces of equipment.

To Matthew Edwards and David Cusack; without your help and advice this thesis would likely not have happened. It was good fun spending the odd Friday working in SolidWorks with Matt. It was equally enjoyable seeing Dave once a week, bouncing ideas off him and learning about his PhD as he asked about my project.

To Dan Hatch, for providing me with fresh tunes to study to and a good chat every couple of weeks. International geopolitical tensions to lifting were often discussed, with a side of University and your mateship helped keep me going. See you Sydney side. And Mitch and Jesse, you blokes made me appreciate that there is a light at the end of the tunnel.

My girlfriend, Grace Harris; you've been really great about my stress and ups and downs. You've helped me get this thesis done and your input is throughout this document. Along with Mum, Dad and Sarah, you have kept me on track and functioning during this year.

Finally, to Jack, Brendan, Rylie, Steve, Chris, Andy and all the other mates who were always there for beers when they were needed most; cheers. It has been a hell of a ride. Good luck getting rid of me, gentlemen.

Thank you.

CONTENTS

List of Figures

List of Tables

1 INTRODUCTION

1.1 Motivation

Handpans (Figure 1) are a relatively new percussive musical instrument with increasing usage (Google 2017) since its invention in 2000 (Rohner and Schärer 2007). Basic designs are a conical shell with small idents or raised sections around the circumference of the shell. These indents are tuned so as to vibrate locally when struck, producing notes of a specific tone and scale. Current design and manufacture rely on a guess and check method (Morrison and Rossing 2007, Rohner and Schärer 2007). Comparing the effects of design changes to develop an understanding of the instrument workings is desired, as well as the generation of working digital models.

Figure 1: Handpans Being Played ((Paniverse 2017))

Notes, and thus the musical scale, on a handpan are restricted by the number of indents that can fit around the circumference. The notes are also limited by the mode of vibration that an indent can operate in. Furthermore, the vibration of one indent (or note) can interfere with its

neighbours if not adequately spaced and this is often the limiting design factor (Rossing, Morrison et al. 2007).

Many manufacturers use different geometries of the shell and indents to unknown effect. To understand why a manufacturer might use a rotated ellipse shape instead of a hemisphere, for example, is a primary motivator. Essentially, the author and supervisor are curious as to the why and how of manufacturing these fascinating new instruments.

1.2 Problem Definition

Design and build methodology of handpans is heavily guess and check, with only a limited number of investigations delving into theoretical modelling. Design elements such as indent spacing, size and orientation are highly dependent on the individual manufacturer of the handpan. Consistent classification of design parameters and why they are used is not available and the effect of most possible changes in design is not known (a brief example would be the elliptical indents provided by some manufacturers). Rigour in classifying and predicting the effects of design changes is the end goal of this project.

The function of finite element analysis (FEA) is to examine structures computationally and learn their predicted behaviour in real life. FEA allows us to alter designs quickly and easily via a computer aided design (CAD) tool to observe changes to the structure. This method can sometimes be limited if the manufacture of the structure is not consistent. Thus a test of real response of a handpan and a comparison to a FEA model will be needed to validate the FEA/CAD model.

Spectral analysis via MATLAB of an existing handpan provides the start point of investigations. From here it is hoped that an ANSYS FEA model of the existing pan can be created that mimics the response of the real pan. Once this meeting of physical and digital performance is achieved the ANSYS model can be modified and experimented with. Ultimately, the effects of changing the design (geometry) of the handpan and classifying the outcomes may be achieved. This lively

instrument may become far more prevalent if consistent performance of the product can be predicted and ensured. This project strives for that goal.

1.3 Scope

Currently the project runs two aspects simultaneously; the testing of the physical handpan and subsequent spectral analysis and the development of a theoretical model to examine the effects of changing the handpan design. The physical testing will aim to provide consistent data gathering and analysis techniques while the theoretical model will test variation of parameters that is not possible with the physical handpan. Physical testing also provides baseline information that can help inform the theoretical model analysis.

Desired lines of enquiry for the physical testing include developing consistent striking and sound recording methods. Theoretical model scope includes analysing the effect of geometric changes to the handpan.

1.4 Aims

Primary project goals:

1) Produce a repeatable method of testing the output of a physical handpan. This will include methods of measuring the sound, striking the pan and supporting the pan. Spectral analysis of the results will form a key part of this goal.
2) Develop a validated FEA model of the existing handpan that can provide a spectral vibratory response equivalent to the real device. Comparison of measured notes and their spectral response will be compared with the ANSYS model response and spectral output.
3) Use CAD and FEA to determine the effect of each design parameter on the output of the handpan. This will involve altering the CAD model, once it has been validated, and testing its spectral response for a standardised strike input. An ability to design a handpan based on theory to produce a certain note or scale would be an end goal.

1.5 Expected Outcomes

The following list outlines the desired outcomes of the project.

1) Develop a standard test procedure for analysing the resonant response of the hand pan when struck.
2) Identify and categorise any discrepancy between physical handpan and ANSYS model responses.
3) Understand the effects of each design element of a handpan and how altering these elements affects performance.
4) Suggest methods for achieving desired notes or handpan performance based on theoretical design.
5) Suggestions for further work.

2 LITERATURE REVIEW

The literature review comprises of two primary sections; Definitions and Analysis Techniques and Existing Literature. Definitions and Analysis Techniques is broken into multiple subsections comprising: Natural Frequencies and Modes, Damped Natural Frequencies, Finite Element Analysis, Fast Fourier Transform, Spectrograms and Plate Vibrations. Existing work examines Steel Pan and Handpan literature. The Definitions and Analysis Techniques segment draws on the academic works evaluated in the Existing Literature section. A Summary of Findings is provided to close out the review.

2.1 Definitions and Analysis Techniques

2.1.1 Natural Frequency and Modes

Natural frequency is the rate of oscillation of an unforced (free vibration) object. It is an inherent property of all physical objects and is affected by factors such as material type, geometry, boundary conditions and temperature. Each degree of freedom an object possesses corresponds to a natural frequency in radians per second denoted by ω_n, where subscript n represents the degree of freedom. This degree of freedom is called a mode and the way it vibrates is called its mode shape. Therefore, each natural frequency has a corresponding mode of vibration with a defined shape (Rao 2011).

ω_n (rad s^{-1}) is sometimes called the circular natural frequency and f_n (Hz) is called the natural frequency. The two are related via:

$$f_n = \frac{\omega_n}{2\pi}$$

Where:

- f_n = natural frequency in Hertz (Hz),
- ω_n = natural frequency, or circular natural frequency, in radians per second (rad/s) and,

- π is the geometric constant (approximately 3.14).

Certain modes of natural vibration can be excited by applying an impulse to an object. Based on where and how this impulse is applied, particular (already existing) natural modes of vibration, at their corresponding natural frequencies, can be made to oscillate. These modes have points called nodes, denoted by N, which are points of zero motion when that mode has been excited. Conversely, anti-nodes are points of maximum oscillation displacement under a given mode (Rao 2011) . Applying an impulse to a node of a mode will not excite that mode to oscillation. However, applying the same impulse to an anti-node will achieve the maximum excitation of that mode.

Figure 2 shows the first three modes of vibration for a cantilever beam of length (L), mass (m), second moment of area (I) (which is a geometric property of the beam cross section) and elastic modulus (E), which is an inherent material property that measures stiffness. Part (b), (c) and (d) of the figure show the first, second and third modes respectively with part (a) showing the beam setup. The analytical solution for the corresponding natural frequency is presented next to each mode.

A load or impulse applied at N_1 in part (c) of Figure 2 will not excite the second mode of vibration. Mode 2 has an anti-node is roughly hallway between the fixed support and N_1, and an impulse applied here would excite the mode to the fullest capability of the impulse, at frequency ω_2.

Methods for calculating natural frequency can be analytical or numerical, but for complex geometries it is found numerically. This is often performed by FEA packages. In physical systems it is measured, as in Morrison's paper which used holographic interferometry to analyse the first three modes of vibration of each note (Morrison and Rossing 2007). Even more simply, if the system generates a sound, this can be recorded by microphone and analysed to determine frequencies of modes present following excitation (Alon 2015).

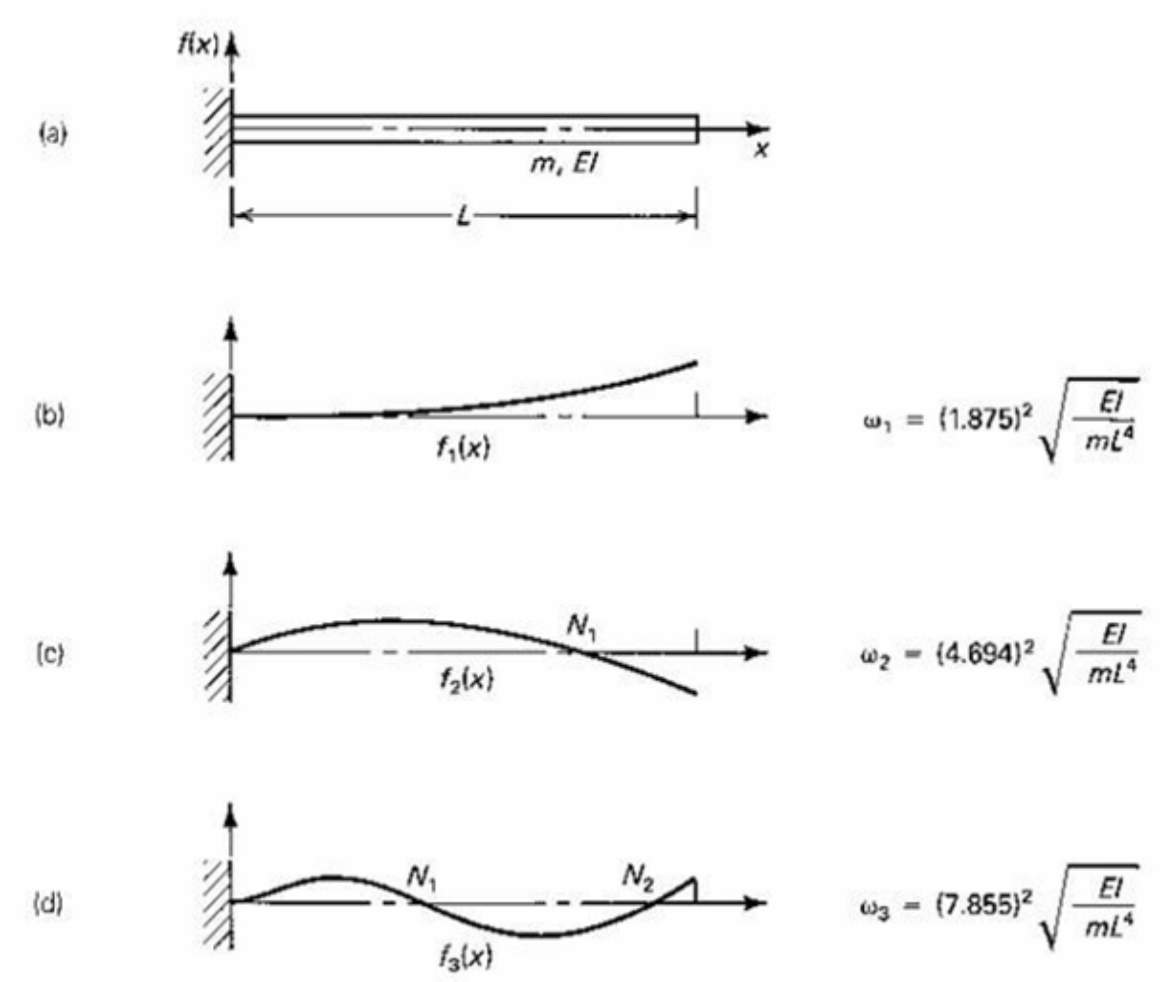

Figure 2: Vibration of a Cantilever Beam (ICT 2017)

2.1.2 Damped Natural Frequencies

A natural frequency can be damped or undamped depending on the amount of damping present in the system. This is often the most difficult part of a system to determine; where the damping is, how much is present and what types of damping are present (Rao 2011). Natural frequencies

of a system are largely unaffected by low levels of damping. However, if a system is what is known as critically damped or overdamped the natural frequency cannot occur. Existing studies on handpans and steel drums have not found damping to be considerably high and it is known these systems do vibrate readily (Achong 1996, Morrison and Rossing 2007, Rohner and Schärer 2007, Rossing, Morrison et al. 2007).

Damped natural frequency is given by:

$$\omega_d = \omega_n\sqrt{1-\zeta^2}$$

Where:

- ω_d is the damped natural frequency of a given mode,
- ω_n is the natural frequency of that mode and,
- ζ is the damping ratio of the system (or of that mode).

Damping ratio is a measure of the actual damping to the critical damping of a system. It is usually a very low number for continuous metal systems, ranging between 0.01 for metals on their own to 0.07 for metal structures with joints (Adams and Askenazi 1999).

2.1.3 Finite Element Analysis

Finite element analysis (FEA) and modelling is the process of dividing a system into small, discrete parts called elements. These elements can be described by individual properties such as material and geometry. Equilibrium equations can be applied over each element and assembled to recreate the full system (Gay 2008). Results such as stress and displacement on an object can be calculated in this manner.

Modal analysis is an extension of FEA. Frequencies, in the form of eigenvalues, and their displacements, in the form of eigenvectors, can be used to construct mode shapes (Alon 2015). This has been used extensively in existing handpan and steel drum literature.

An FEA package extracts this information using the underlying method of its solving algorithms. A simple, single degree of freedom system with no damping and no applied loading has the following matrix form equation of motion (EoM):

$$[M]\{\ddot{u}\} + [K]\{u\} = 0$$

Where:

- [M] = the mass matrix of the system,
- [K] = the stiffness matrix of the system,
- $\{u\}$ = the displacement vector of the system,
- $\{\ddot{u}\}$ = the acceleration vector (second derivative of displacement) of the system.

This matrix form the EoM for undamped free vibration. Assuming a harmonic solution to the displacement of form:

$$\{u\} = \{\phi\}\sin \omega t$$

Where:

- $\{\phi\}$ = the eigenvector or mode shape.

Differentiating Equation X twice and then substituting the result and the original function into Equation Y yields:

$$-\omega^2[M]\{\phi\}sin\omega t + [K]\{\phi\}sin\omega t = 0$$

Which simplifies to:

$$([K] - \omega^2[M])\{\phi\} = 0$$

This is now in the form of the eigenequation. More often this is shown in the form:

$$[A - \lambda I]X = 0$$

Where:

- A = square matrix,
- λ = eigenvalues,
- I = identity matrix,
- X = eigenvector.

Thus, when written in terms of K, ω, and M the eigenequation is the physical representation of natural frequencies and mode shapes of a system, with $\omega^2 = \lambda$. Analytically, the eigenequation is solved using the determinant of $([K] - \omega^2[M])$ to solve for each ω_i^2 and then solve for each mode shape (Software 2011). Numerically, it is solved by iteration on an initial guess of the eigenvectors.

FEA packages can perform this analysis for complex systems and limit their solution space to minimise computation time. Thus, for large and complex systems, early modes of vibration and their natural frequencies can be extracted.

2.1.3.1 Transient Analysis

Transient dynamic analysis is a technique used to determine the dynamic response of a structure under time-dependent loads. Sometimes, this is called time-history analysis or transient structural analysis. Under standard static structural analysis or modal analysis, time dependent effects and non-linearities are not accounted for. These include inertial effects, which are often significant in thin membrane structures (Han and Petyt 1997), geometric stiffness considerations or changing load over time.

2.1.4 Fast Fourier Transform

Once a recording of a vibrating has occurred, be it acoustically, via accelerometer or optically, analysis of frequencies present is essential. Fourier transforms are used to do this. Fourier transforms are found by:

$$X(f) = \int_{-\infty}^{\infty} x(t) \times e^{-i2\pi ft}\, dt$$

X(f) is the Fourier transform of the time domain signal, x(t), and f is the frequency (Rao 2011).

Most commonly a fast Fourier transform (FFT) is used to do this. It separates time series data into the frequency domain, allowing the dominant frequencies present to be identified. It is inherently a numerical method performed on discrete data points and this transform is called the discrete Fourier transform (DFT), of which an FFT is an efficient method of computation (Alon 2015). Figure 3 shows an example FFT of the C note on the PiDrum handpan with peaks in relative power at dominant frequencies. The primary spike corresponds to 523 Hz, the expected pitch of C5.

This method has some limitations. Namely, the Nyquist frequency, which is the equal to half the sampling frequency. This means that frequencies over half of the sampling frequency cannot be identified. Frequencies above the Nyquist frequency will be displayed but will be a mirror of those below the Nyquist, with the Nyquist frequency being the plane of symmetry. Figure 4 shows the mirror effect, the Nyquist frequency in this case is 24 kHz with sample rate 48 kHz. Thus a sufficient sampling frequency must be present. However, this is complicated by the inverse relation between sampling frequency and sampling time gap. Thus there is always a trade-off between time-domain and frequency-domain resolution (Achong 1996).

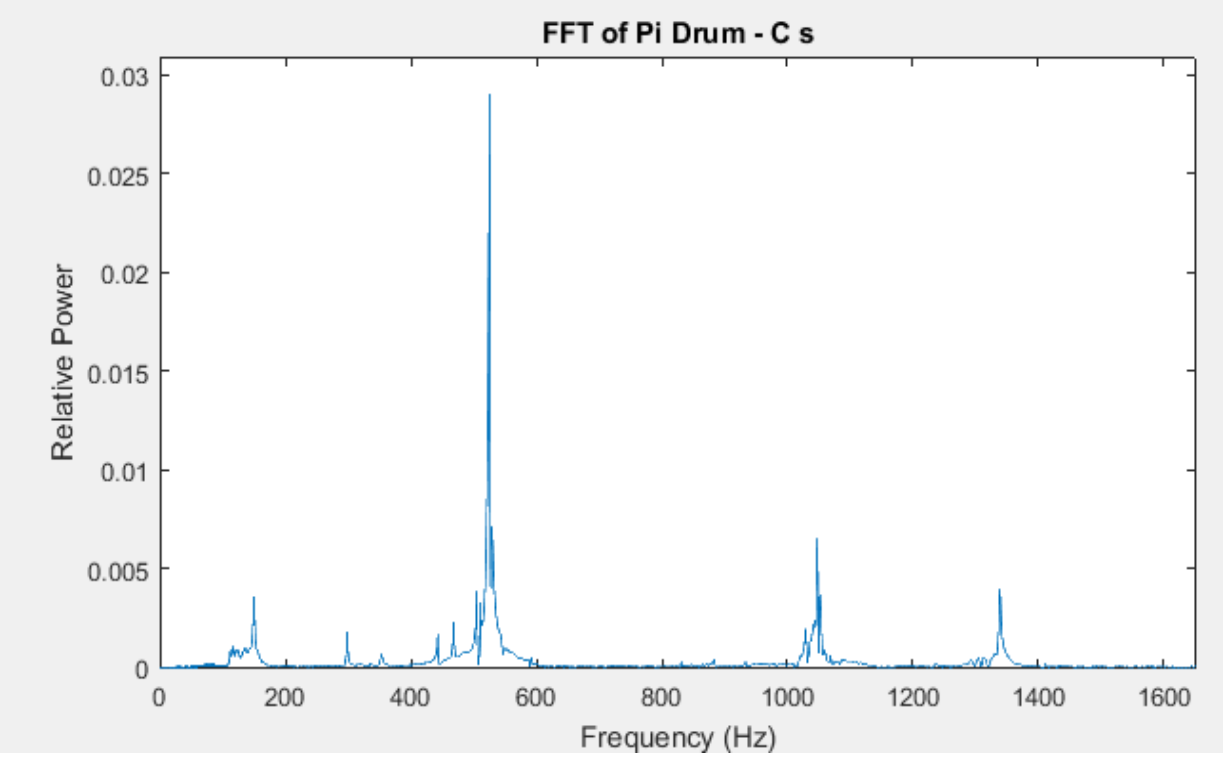

Figure 3: Example FFT

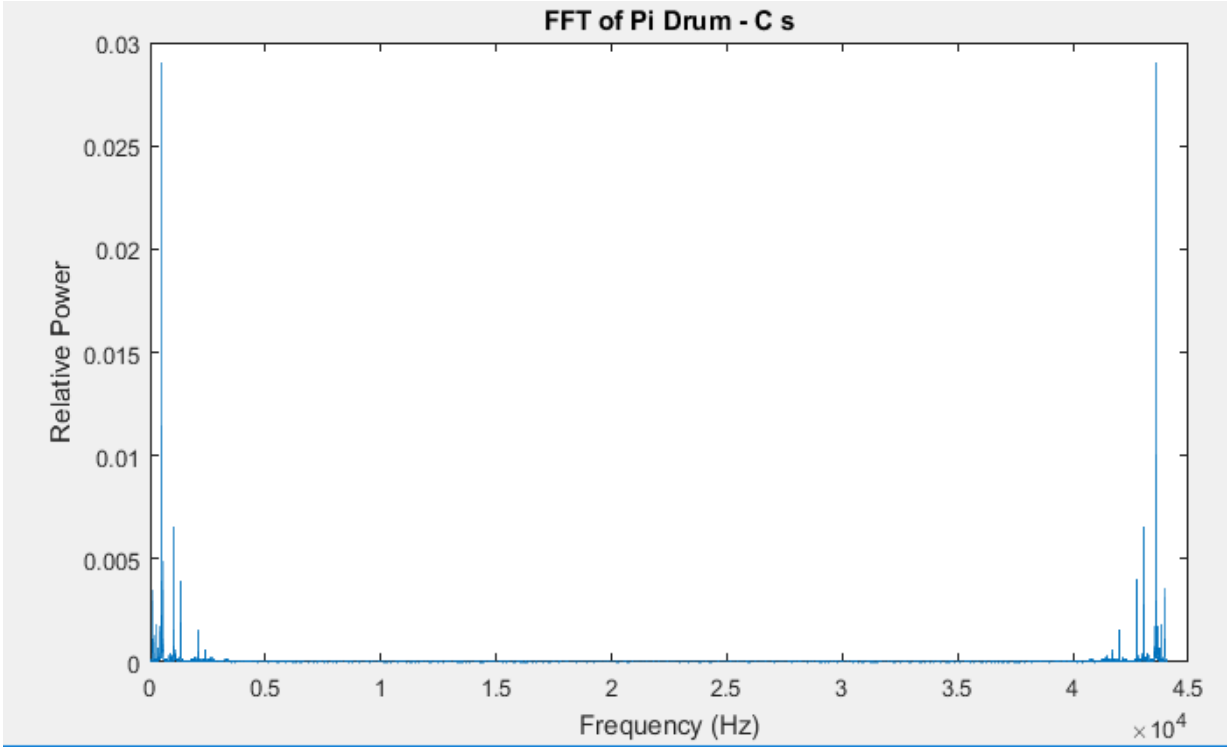

Figure 4: Mirror Around Nyquist Frequency

2.1.5 Spectrogram

An extension of the FFT can be applied to spectral analysis and development of spectrograms. Spectrograms take multiple, short term Fourier transforms (STFT) and plot them over time with sound level intensity. This is very useful for seeing how certain vibrational modes behave over time, after excitation (Alon and Murphy 2015). The effects of time-domain and frequency-domain trade-offs become apparent with spectrograms.

MATLAB has useful built in spectrogram functions. Specifically, spectrogram(x, window, noverlap, f, fs) returns the spectrogram at the defined parameters:

- x is the time-domain data,
- window is how many points are taken to use in the STFT,
- noverlap is the amount of overlapping data points between $STFT_1$ and $STFT_2$,
- f is frequency range to analyse and,
- fs is the sampling frequency of the data.

Figure 5 and Figure 6 are a spectrogram of the same C note from Figure 3 with changed window parameters. Firstly, the dominant frequencies as seen in Figure 3 can be seen in both figures as coloured lines in yellow and green, this time along the y-axis. How long the note remains for after initial excitation is plotted along the time axis and the decay of the note can be seen by changing colour.

Window sizes of 1024 (2^{11}) and 4096 (2^{13}) data samples were used in each STFT for Figure 5 and Figure 6 respectively. The dominant 523 Hz frequency can be seen in yellow on both spectrograms. However, Figure 5 has a lower resolution (more spread out sections) in the frequency domain, as shown by the width of the yellow 523 Hz line. Conversely, Figure 6 shows the 523 Hz frequency as a thinner line (higher resolution in frequency) but has lower

resolution in the time domain, as shown by the width of the individual segments while moving along the time axis.

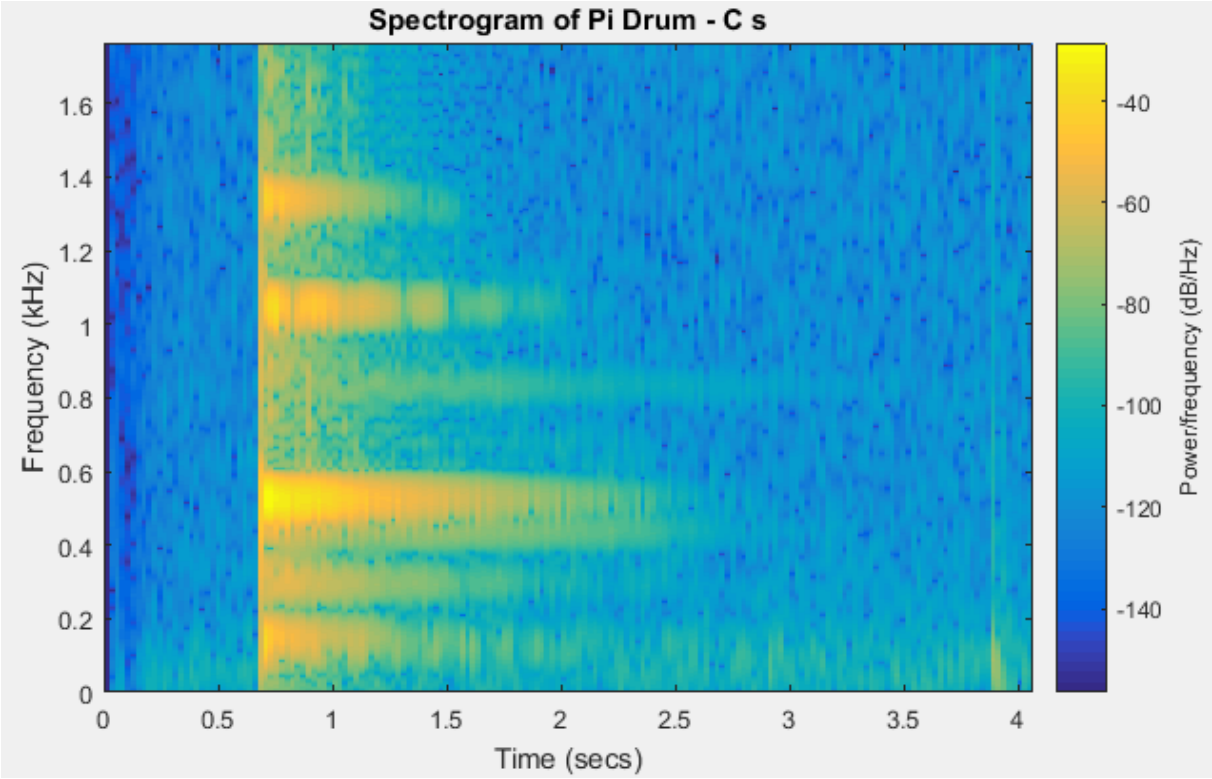

Figure 5: Spectrogram with 1024

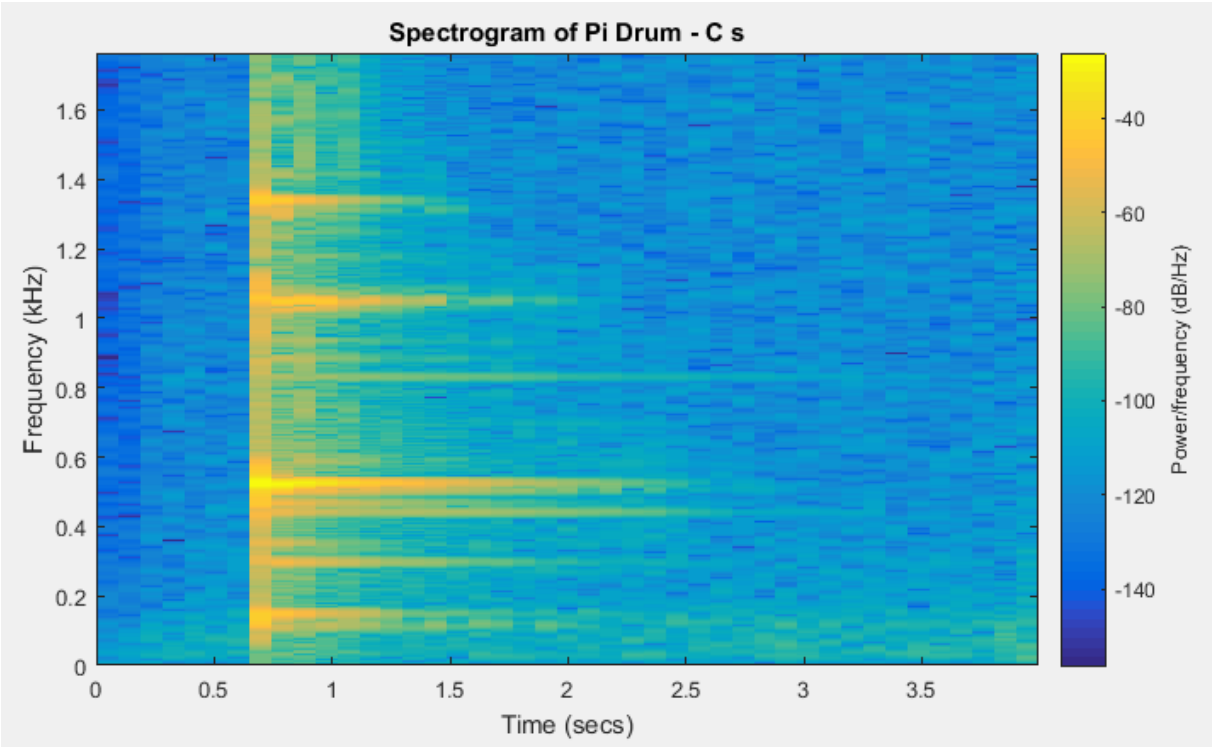

Figure 6: Spectrogram with 4096

2.1.6 Plate Vibrations

Analytical solutions exist for plate vibrations under various boundary conditions (Leissa 1969, Leissa 1973, Shi, Shi et al. 2014). Simplest solutions involve using tables of values and prescribed equations.

2.1.6.1 Rectangular Plates

A brief overview of important rectangular plate equations of interest follows.

For a rectangular plate of constant thickness the following equation describes the natural frequency (Leissa 1969):

$$\omega^2 = \frac{\pi^4 D}{a^4 \rho} \frac{K}{N}$$

Where:

- a = length of the plate (m)
- ρ = density ($\frac{kg}{m^3}$)
- K = constant from Figure 22 that depends on aspect ratio of plate and boundary conditions
- N = constant from Figure 22 that depends on boundary conditions
- $D = \frac{Eh^3}{12(1-\nu^2)}$
- h = thickness of plate (m)
- ν = Poisson's ratio of material

Figure 22 (contained in Appendix A) in Leissa's 1969 paper for NASA contains the boundary conditions and relevant K and N values for that condition. Aspect ratio (the ratio of length to width) is an important variable. If the width of a plate is denoted b then aspect ratio is a/b.

2.1.6.2 Circular Plates and Annular Plates

Leissa presents tables of critical values of a constant called λ^2 for the various possible modes of circular and annular plate vibrations with varying boundary conditions (Appendix A). Relationship between variables already established for circular and annular plates is:

$$\lambda^2 = \omega a^2 \sqrt{\frac{\rho}{D}}$$

Where:

- $\lambda^2$is a constant found in various tables from Leissa (Appendix A),
- a is the plate outer radius.

In tables values for λ^2 are presented for various values of n and s. These constants are not important for the purposes of this paper as they are both taken to be zero.

Annular plates have one further variables which is *b/a*, where *b* is the inner radius of the annulus. Interpolation between the presented *b/a* values would be required as they are not presented to a high resolution.

2.2 Existing Literature

2.2.1 Steel Drums

Much informative ground work has been performed on the steel drum, a father to the handpan. "The steelpan as a system of non-linear mode-localized oscillator" part 1(Achong 1996) and part 2 (Achong and Sinanan-Singh 1997) represent the most rigorous mathematical analysis of the steel drum. Much of the theory utilised and presented in these papers forms a basis of theories of interaction for the investigation; specifically, the use of STFT to analyse frequency domain data from time-domain information alone.

Significant effort was undertaken by Achong to look at the interactions and bifurcations of the steel drum system. One key point of the Achong papers was to show, with rigour, that coupling of notes is not a large consideration and analysis of the system can be done as a single note analysis, if natural frequencies are not very close to each other. While the coupling of modes and mathematical predictions are interesting and, in some regards, useful, it does not help answer the central question of this paper. It does, however, provide some insight into the complexities of systems with limited geometry and their interactions.

"Nonlinear vibrations of steelpans: analysis of mode coupling in view of modal sound synthesis" (Monteil, Touzé et al. 2013), is one paper to examine the sue of FEA in analysing the steel drum. Importantly, it rigorously identifies the need to examine non-linear effects when analysing the steel drum. It does not examine the effects of changing geometry, merely how to effectively model an existing geometry. One final point is the alignment of theoretical and physical results was a strong focus of the paper. This is of note because it is perhaps the only paper to attempt to correlate the two with accuracy and precision. Full correlation of the two is not achieved as there are some discrepancies but, overall, the trend of the physical system was able to be predicted by the theory.

These two papers are the most informative and other works build on their basis without much extension.

2.2.2 Handpans

"Modes of vibration and sound radiation from hang" (Morrison and Rossing 2007) focuses exclusively on measurement of the modes of vibration and natural frequencies, including visualisation in the form of holographic interferometry. Holographic interferometry projects light onto the surface of a vibrating objects and the resulting phase shifts in light caused by the movement of the surface can be detected by a received and displayed. Images using this method visualise vibrational modes with great accuracy and provide a method for comparing theoretical

model modes to tested, existing modes, of a similar instrument. Other similar works (Rohner and Schärer 2007, Rossing, Morrison et al. 2007) help provide direction for physical testing but report no work on changing geometry.

This holographic technique provides information of mode shapes present and about the effect of changing strike intensity. Figure 7 and Figure 8 show the mode shapes of the first three modes of the top ding and F note of the handpan they used in their study. It shows in the top row of images the small amplitude strike and in the second row the large amplitude strike. These images will be useful when comparing to FEA model results as a verification step.

Some brief observations about the images. Firstly, mode shapes are simple and what is to be expected at the fundamental mode but increase in complexity for both the top ding and the side note with increasing mode number. Secondly, and importantly, small amplitude vibrations excite mostly the local note struck. This changes with increasing the amplitude and areas away from the struck note become excited. This is especially evident with the top ding. The

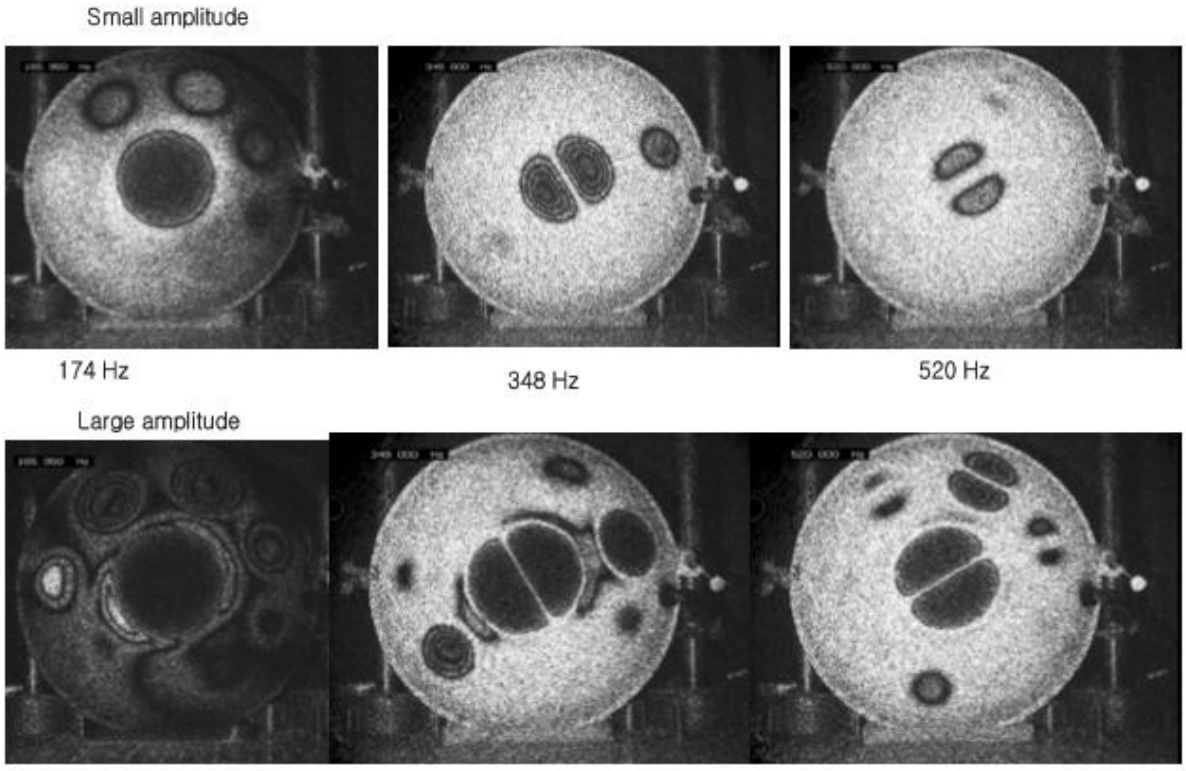

Figure 7: Holographic Image of Top Ding Mode Shape (Rossing, Morrison et al. 2007)

fundamental mode of the F note at 368 Hz excites the top ding when struck with large amplitude which has a resonance at 348 Hz, more than 5% different.

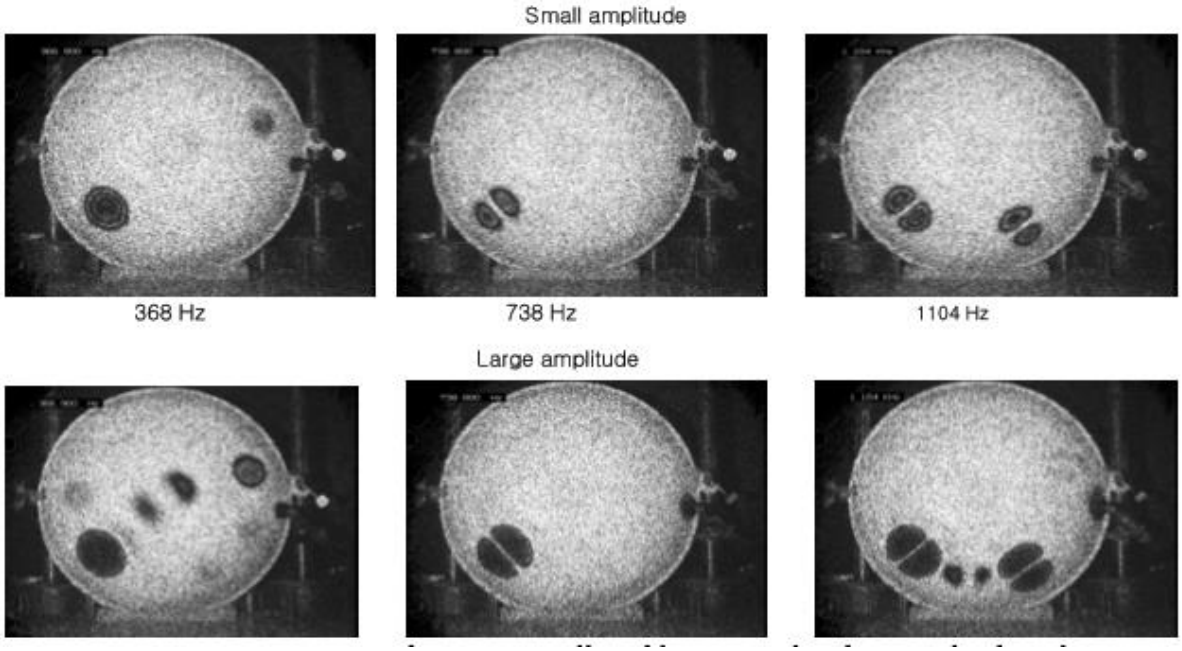

Figure 8: Holographic Image of F Note Mode Shape (Rossing, Morrison et al. 2007)

"Analysis and Synthesis of the Handpan Sound" (Alon 2015), represents the most complete body of work on analysing handpan response to changing input factors. This single paper informs much of the current analysis. Primarily this paper was focused on testing and analysis of the physical system, with no digital modelling performed. No investigation of changing geometry, with the exception of entirely changing the instrument was made. While rigorous, methodical and a complete study, it does not provide much of the insight the author craves.

To date, no work has been found investigating the geometric effects of the handpan on note generation. Similarly, no work has been found that focuses on handpan design before manufacture or the ability to produce handpans industrially instead of by hand. Existing works focus on the measurement of physical systems and the methods of analysing these systems.

2.3 Summary of Findings

Existing literature focuses heavily on steel drums, as opposed to handpans. Current literature on both, however, does not examine the effects of changing geometry, even though use of FEA models can be seen. Furthermore, literature on handpans themselves is limited to a few articles and the very useful thesis by (Alon 2015). Methods of analysing both physical and digital systems, as well as data gathered from both, has comprehensively been presented. Three options are presented for validating results; physical testing, theoretical plate vibration solutions and digital modelling via FEA. Usage of the FFT is key to analysis of data from the physical testing and transient analysis of the system.

Despite claims on the contrary from papers, modal interactions appear to be significant as shown by Figure 7 and Figure 8. Non-linear effects and modal interactions are exacerbated by increasing the amplitude of vibration (which is expected) and this may provide a significant point of interest.

3 PHYSICAL TESTING

3.1 Introduction

Acquiring data on the actual instruments available and developing a methodology for attaining accurate and consistent results are a project requirement and goal respectively. Data for both the Meridian and Pi Drum handpans was gathered for each note as well as for the instrument being on or off a stand. Originally, a tool to deliver a consistent strike to the instrument was to be created. However, this produced inconsistent and artificially high pitched notes and so was abandoned.

3.2 Instrumentation

The following is required:

1. Handpan (two varieties were available; the Meridian and the Pi Drum)
2. Microphone
3. Audio Recording Software
4. Portable device for recording (laptop or phone)
5. Stand for instrument
6. Some cloth to sit under the instrument
7. Anechoic chamber
8. Index finger

3.3 Methodology

A brief methodology is presented.

1. Place the handpan in the middle of the anechoic chamber either on the stand or on a piece of cloth.
2. Place the microphone on the floor about 30cm away from the note being struck.

3. Keep the mobile device close to the microphone for access.
4. Perform a few test strikes with finger until a “good” sounding note is achieved (that is, not off note or with discrepancies).
5. Begin recording the audio and immediately strike the desired note. Wait until it has faded away entirely and stop recording.
6. Play note back to ensure no noise pollution has entered the recording.
7. Save note using a specific naming convention (the author used the name of the instrument, the note and if it was on or off the stand).
8. Repeat steps 2 to 7 for all notes on the instrument.
9. Change the instrument from stand to floor or vice versa and repeat steps 2 to 8.
10. Change instruments and repeat steps 2 to 9.
11. Use the code in Appendix B (Figure 28) to analyse the data.

3.4 Results

Table 1 and Table 2 contain the measured and expected values for the first, second and third modal frequencies for each note for each instrument respectively. The percentage error is also presented. Appendix B contains the Spectrograms (Figure 29 to Figure 60) for each note on each instrument; both on and off a stand. A list of observations along with the raw data for each note is also presented in Appendix B (Table 12 to Table 15).

Table 1: Pi Drum Tested Modal Frequencies

Tested Modal Frequencies for Pi Drum With and Without Stand

Note		**No Stand**			**Stand**		
	Mode Number	**1**	**2**	**3**	**1**	**2**	**3**
D4	Measured (Hz)	297.9	-	884.8	294.3	588.3	884.4
	Expected (Hz)	293.66	587.32	880.98	293.66	587.32	880.98
	% Error	-1.42%	-	-0.43%	-0.22%	-0.17%	-0.39%

E4	Measured (Hz)	335.2	662.2	-	333	662.4	-
	Expected (Hz)	329.63	659.26	988.89	329.63	659.26	988.89
	% Error	-1.66%	-0.44%	-	-1.01%	-0.47%	-
F4	Measured (Hz)	353.1	-	1047	351.7	699	1047
	Expected (Hz)	349.23	698.46	1047.69	349.23	698.46	1047.69
	% Error	-1.10%	-	0.07%	-0.70%	-0.08%	0.07%
G4	Measured (Hz)	394.5	-	-	393.2	786.1	1173
	Expected (Hz)	392	784	1176	392	784	1176
	% Error	-0.63%	-	-	-0.31%	-0.27%	0.26%
A4	Measured (Hz)	443.5	884.7	1339	442.4	884	1339
	Expected (Hz)	440	880	1320	440	880	1320
	% Error	-0.79%	-0.53%	-1.42%	-0.54%	-0.45%	-1.42%
Bb4	Measured (Hz)	-	933.3	-	467.4	933.4	-
	Expected (Hz)	466.16	932.32	1398.48	466.16	932.32	1398.48
	% Error	-	-0.11%	-	-0.27%	-0.12%	-
C5	Measured (Hz)	525.3	1050	-	524.8	1048	-
	Expected (Hz)	523.25	1046.5	1569.75	523.25	1046.5	1569.75
	% Error	-0.39%	-0.33%	-	-0.30%	-0.14%	-
D5	Measured (Hz)	588.9	-	-	589	1175	-
	Expected (Hz)	587.33	1174.66	1761.99	587.33	1174.7	1761.99
	% Error	-0.27%	-	-	-0.28%	-0.03%	-

Table 2: Meridian Tested Modal Frequencies

Tested Modal Frequencies for Meridian With and Without Stand

Note		**No Stand**			**Stand**		
	Mode Number	**1**	**2**	**3**	**1**	**2**	**3**

G3	Measured (Hz)	194.8	391.2	-	195.4	-	-
	Expected (Hz)	196	392	784	196	392	784
	% Error	0.62%	0.20%	-	0.31%	-	-
Ab3	Measured (Hz)	208.4	414.8	-	207.9	415	-
	Expected (Hz)	207.65	415.3	830.61	207.65	415.3	830.61
	% Error	-0.36%	0.12%	-	-0.12%	0.07%	-
C4	Measured (Hz)	263.1	524.1	1046	262.1	521.7	1046
	Expected (Hz)	261.6	523.3	1046.5	261.6	523.3	1046.5
	% Error	-0.57%	-0.15%	0.05%	-0.19%	0.31%	0.05%
Eb4	Measured (Hz)	311.2	622.5	-	310.1	622.4	-
	Expected (Hz)	311.1	622.25	1244.5	311.1	622.25	1244.5
	% Error	-0.03%	-0.04%	-	0.32%	-0.02%	-
F4	Measured (Hz)	350.8	698.3		347	698.2	-
	Expected (Hz)	349.2	698.4	1396.9	349.2	698.4	1396.9
	% Error	-0.46%	0.01%	-	0.63%	0.03%	-
G4	Measured (Hz)	391.2	-	-	390.8	783.1	-
	Expected (Hz)	392	784	1568	392	784	1568
	% Error	0.20%	-	-	0.31%	0.11%	-
Bb4	Measured (Hz)	464.8	-	-	464.8	-	-
	Expected (Hz)	466.2	932.3	1864.7	466.2	932.3	1864.7
	% Error	0.30%	-	-	0.30%	-	-
C5	Measured (Hz)	524.1	1044	-	520.3	-	-
	Expected (Hz)	523.3	1046.5	2093	523.3	1046.5	2093
	% Error	-0.15%	0.24%	-	0.58%	-	-

3.5 Discussion

Results, particularly the FFTs and Spectrograms, show that interactions occur in the instrument. This is easily seen by the double peak phenomena that can be seen in the FFTs and by the excitation of modes close to the frequency being played in the raw data. While it may be the C4 note being played, C5 shows excitation because notes from it come through. Even more interesting is the G4 and D5 interactions that appear. Because of this, it is the opinion of the author that interactions are significant but not changing of the fundamental modes present, merely that extra notes can be present which often provides a richness of sound. This may also be an instrument tuning issue and could be resolved, if desired, if modelling methods are sufficiently accurate.

Maximum deviation from the ideal note was –1.66% on the E4 note of the Pi Drum without a stand and 0.63% for the Meridian F4 note with the stand. Overall the error of the Meridian was less than that of the Pi Drum and the error without a stand was higher than with a stand. This is too be expected as the Meridian is a better made instrument. This is informative in two useful ways. Firstly, the method of supporting the instrument does not have a large effect on performance. Secondly, it tells us about the difference in construction of the instruments and the effect this has.

A key point of interest is the sustain times of the two instruments. On average the Meridian had a sustain period of almost double that of the Pi Drum. This suggests that there is significant damping in the Pi Drum compared to the Meridian. It is likely the joint between the two halves of the shell causing this difference. On the topic of damping, as is expected, damping does not behave in a viscous manner as it is often the higher notes with the longest sustain. If damping was proportional to velocity than higher notes would be damped out quickly relative to lower notes. This provides insight to the methods of modelling the damping that may be required.

4 CAD MODEL

4.1 Introduction

Effective and efficient methods for creating a CAD model of the instruments being studied are needed. Currently no such methodology exists and the complex nature of the geometry present makes this a difficult task. Furthermore, the geometry created needs to be customisable so that key geometric variables can be altered and the effects of these changes analysed. Ideally, a model that meets these requirements and that is easily used by other investigators would be developed.

4.2 Development of Methodology

Initial efforts on modelling the handpan in CAD programs utilised CREO parametric software (the only CAD package available to students) by default. This proved an uphill battle and was abandoned after significant efforts demonstrated that the process was not going to provide suitable outcomes. Primarily, CREO did not allow for effective creation of geometry or an efficient method of later customisations. This is also the reason why a 3D scan of the instrument, providing a data point field, was not used as the method of modelling.

Investigation of other methods of modelling showed that SolidWorks has a deform feature which allows for suitable generation of geometry. Using this feature, a rough blank of the handpan can be created and additional features formed using dies.

An attempt was made to create the hand pan as a single piece. This proved rather difficult and made changing geometric features very difficult. Thus an improved method that utilised a ‘cake slice’ system as adopted. Figure 9 shows a view of the handpan from above and overlays the note and the way to partition the instrument into slices.

This cake slice method means that a default note blank can be created and then the geometry altered to meet requirements. Further work was conducted to make the blank a highly customisable set up that contained all required features and functions within SolidWorks. A detailed methodology and set of instructions regarding the creation of the CAD model is contained within Appendix .

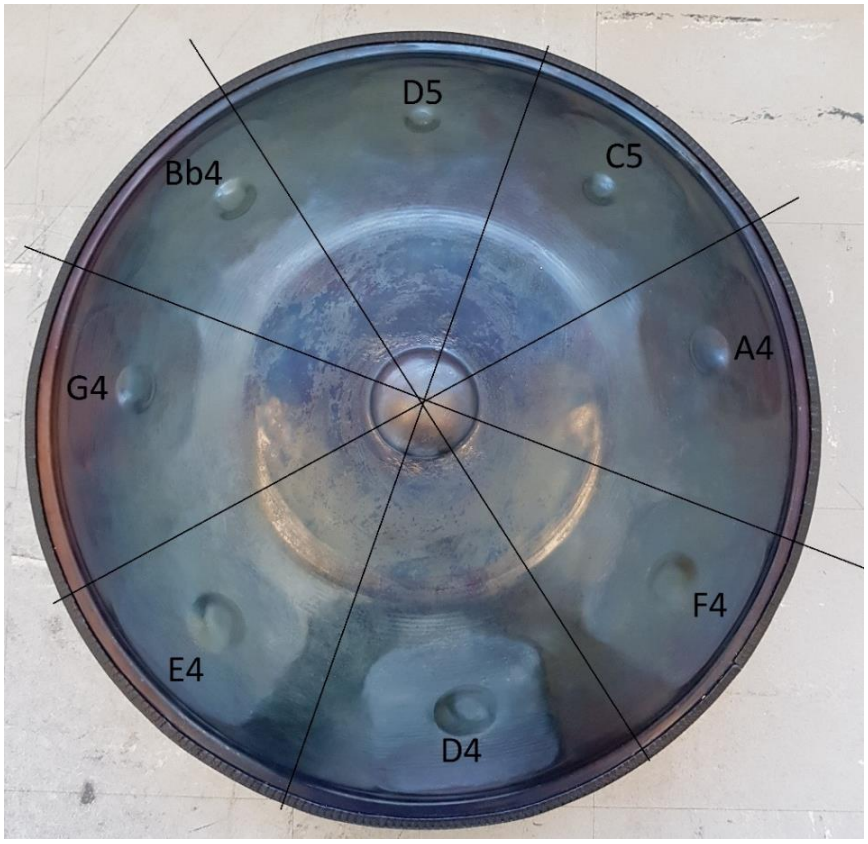

Figure 9: Cake Slice View

4.3 Outcomes

An example of a single slice note is shown in Figure 10. Between notes only the panel section of the notes changes but as they all have similar features, this note is customisable in its key geometries. An example of the completed assembly is shown in Figure 11. This compares very well to the actual instrument in Figure 9.

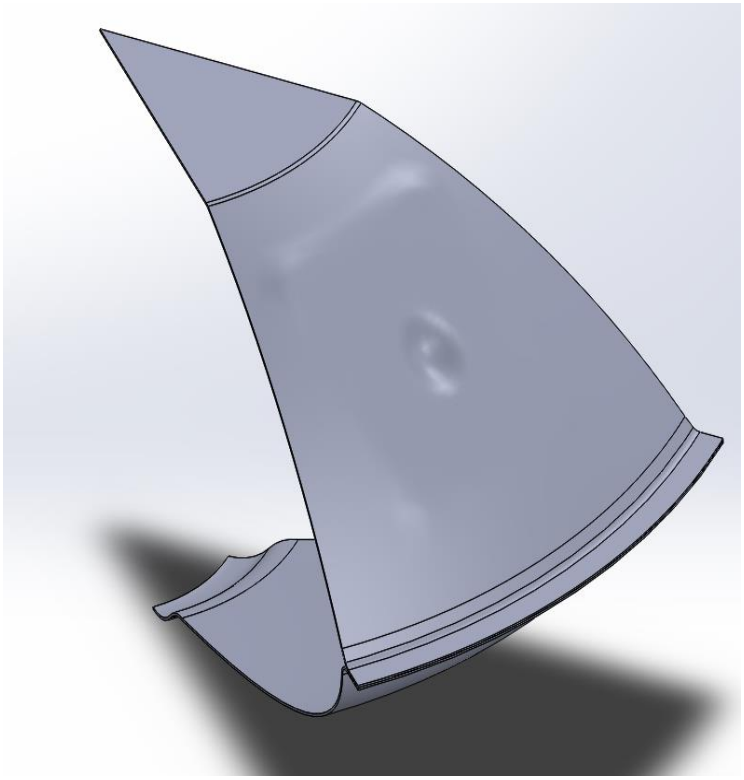

Figure 10: D4 Note Cake Slice – Isometric View

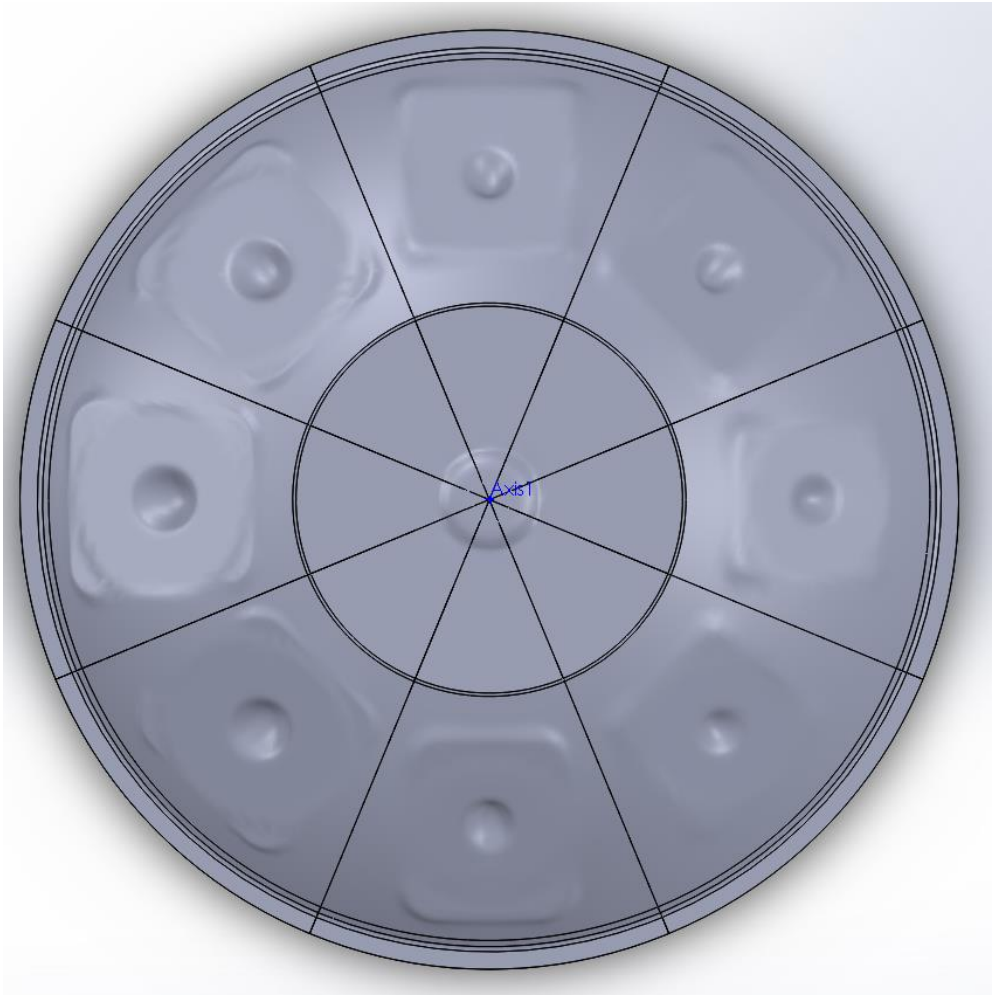

Figure 11: Completed CAD Model - Top View

4.4 Further Work

4.4.1 3D Scan

While a data point field is not suitable for the purpose of analysis it does have value if it is available. This is available at UQ, however, the author was not aware until late in the thesis so work utilising this tool is rudimentary. Figure 12 shows the data point field scan of the Pi Drum instrument. This scan is particularly useful for drawing out geometric information to feed into the existing model.

Figure 12: 3D Scan - Pi Drum

It is also possible to compare CAD models to this data point field to examine their fidelity in modelling geometry. This was not performed as there was insufficient time, however, it would be a very useful tool for CAD model validation and verification.

4.4.2 Other Instruments

Cake slice methods are not as useful when the geometry is not symmetric and equal sized slices cannot be used. However, it can still be useful in the modelling. Slices are no longer able to be equal in size and as reusable. Slices of different sizes need to be used and the methods of creating deformation remain the same but are more time consuming. This is applicable to many handpans, including the further studied Meridian handpan in Figure 13.

Figure 13: Meridian Handpan

4.5 Discussion and Recommendations

Current methodology provides a robust and customisable CAD model. Using 3D scans to create geometrically more accurate and precise models will increase model performance and provide better FE study results. Clearly, the existing CAD model is a good representation of the Pi Drum but 3D scans show that improvement can be made.

Moving forward, the 3D scan should be used to improve existing CAD models. Analytical results show that modal frequency is highly sensitive to geometry. Therefore, increased model accuracy may provide the largest increase in correlation between physical and digital results.

5 THEORETICAL ANALYSIS

5.1 Introduction

Existing analytical plate vibrations theory as presented in 2.1.6 can be used to provide estimates of modal frequencies. All that is required is material properties, assumptions of vibrational mode, and measurements of the physical system. These equations will also provide insight into how certain geometric variables will change modal frequencies.

5.2 Pi Drum Measurements

Important geometric measurements of the Pi Drum and its notes were taken. Measurements for the notes are contained in Table 3. Additionally, material properties and further geometric variables are included in Table 4.

The convention used defines a as the length of the note and b as the width. The same is true of the elliptical dimple.

Table 3: Pi Drum Critical Note Dimensions

Pi Drum Critical Note Dimensions

Note	a (mm)	b (mm)	Dimple a (mm)	Dimple b (mm)
D4	125	105	45	37.5
E4	110	90	35	30
F4	100	90	30	25
G4	115	100	35	30
A4	120	90	35	30
Bb4	125	105	45	37.5
C5	120	105	45	40
D5	100	85	30	25

Table 4: Pi Drum Variables

Pi Drum Variables

Variable	Name	Value	Units
E	Elastic Modulus	207	GPa
ν	Poisson's Ratio	0.3	Unitless
h	Plate thickness	0.95	mm
ρ	Density	7800	$\frac{kg}{m^3}$

Plate thickness was determined by finding the surface area of the CAD model and dividing the mass of the Pi Drum by this figure.

5.2.1 Rectangular Plates

Using 2.1.6.1 and the information in Table 3 and Table 4 estimates of the modal frequencies of the notes can be made by assuming they are rectangular plates and the dimples are not present. This was done for two boundary conditions; all edges simply supported (SS) and all edges fixed (often called clamped). Table 5 contains the results for the actual thickness plate, double thickness plate and the measured value of the fundamental mode from section 3.4. The plot of the data for actual thickness and measured data is shown in Figure 14. All results are in Hz.

Table 5: Analytical Solutions - Rectangular Plate

Pi Drum Analytical Solutions – Rectangular Plate

Note	Measured	SS	Fixed	SS Double	Fixed Double
D4	294.3	359.9	630.5	719.8	1260.9
E4	333	479.5	829.4	958.9	1658.9
F4	351.7	519.8	939.4	1039.7	1878.8
G4	393.2	408.5	727.2	817.1	1454.3

A4	442.4	448.8	742.7	897.5	1485.4
Bb4	467.4	359.9	630.5	719.8	1260.9
C5	524.8	372.6	665.0	745.1	1330.0
D5	589	554.6	977.0	1109.2	1953.9

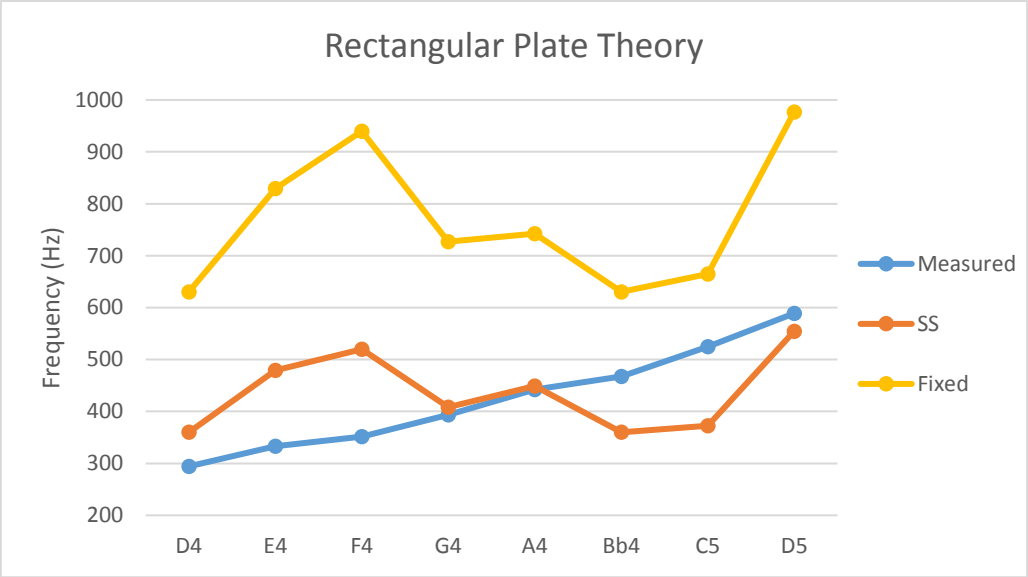

Figure 14: Rectangular Plate Results - Line Graph

5.2.2 Circular Plates

Estimates of the modal frequencies of the notes can be made by assuming they are circular plates and the dimples are not present. The width of the plate was taken as the diameter of the plate. This was done for two boundary conditions; edge is simply supported (SS) and edge is fixed. Table 6 contains the results for the actual and double thickness plate. The plot of the actual thickness and measured data is shown in Figure 15. All results are in Hz.

Table 6: Analytical Solutions - Circular Plate

Pi Drum Analytical Solutions – Circular Plate

Note	Measured	SS	Fixed	SS Double	Fixed Double
D4	294.3	425.6	873.6	851.2	1747.3
E4	333	579.3	1189.1	1158.6	2378.2

F4	351.7	579.3	1189.1	1158.6	2378.2
G4	393.2	469.2	963.2	938.5	1926.4
A4	442.4	579.3	1189.1	1158.6	2378.2
Bb4	467.4	425.6	873.6	851.2	1747.3
C5	524.8	425.6	873.6	851.2	1747.3
D5	589	649.5	1333.1	1298.9	2666.3

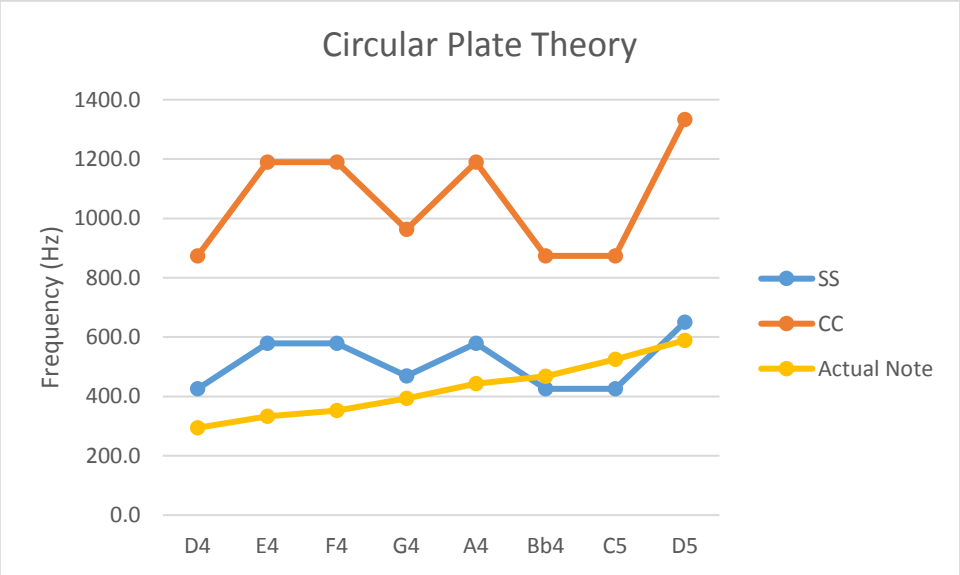

Figure 15: Circular Plate Results

5.2.3 Annular Plates

Estimates of the modal frequencies of the notes can be made by assuming they are annular plates and the dimples are a cut out in the middle of the plate. The dimensions of the annular ring are taken as the average of the dimple *a* and *b* dimensions as inner diameter and the width of the plate as the outer diameter. This was done for two boundary conditions; both edges simply supported (SS) and both edges fixed (CC). Table 7 contains the results for the actual and double thickness plate. The plot of the actual thickness and measured data is shown in Figure 16. All results are in Hz.

Table 7: Analytical Solutions - Annular Plate

Pi Drum Analytical Solutions – Annular Plate

Note	Measured	SS	CC	SS Double	CC Double
D4	294.3	536.7	1178.2	1073.4	2356.3
E4	333	685.9	1475.9	1371.9	2951.9
F4	351.7	594.7	1219.9	1189.4	2439.8
G4	393.2	509.5	1065.4	1019.1	2130.8
A4	442.4	685.9	1475.9	1371.9	2951.9
Bb4	467.4	536.7	1178.2	1073.4	2356.3
C5	524.8	571.9	1279.9	1143.8	2559.7
D5	589	694.7	1445.2	1389.4	2890.5

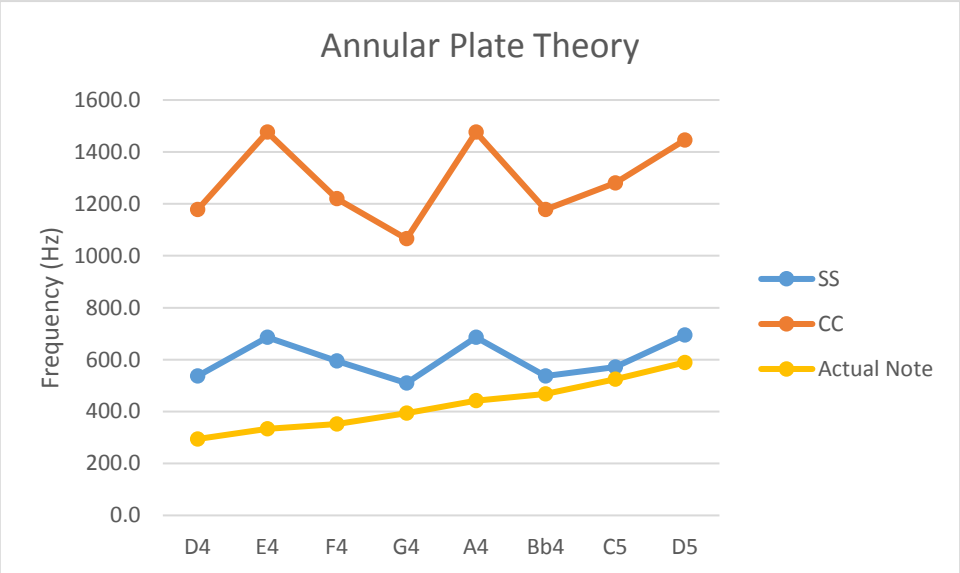

Figure 16: Annular Plate Results

5.3 Discussion

Theoretical results do not seem to provide a good match to actual notes. This can be seen by that fact that all annular plate results are above the actual note as are almost all circular and rectangular results (Figure 14, Figure 15 and Figure 16). Assuming these theoretical results

should be close to the actual note it informs that the simply supported case is always much closer to reality than the fixed case. This is unsurprising as the real note is supported by a membrane of material.

Circular plate theory seems to provide the closest results to real life. If the circular mode shapes shown in Figure 8 are those of real notes, then circular plate theory would provide a mode shape closest to this. This is an interesting point of how the note behaves and warrants further investigation via FEA.

Interestingly, doubling the thickness of a note doubles the frequency of that note. This is a linear relationship, not cubic as it would seem from the equations. Thickness is still, however, a major driver of frequency. The thickness estimate made at the start of this section and used in calculations may not be reliable. It relies on top and bottom shell being equally thick and used a rough measurement of mass. Using geometric data from the 3D scan and mass method may improve the estimate with potential direct measurement methods being preferable. Improved thickness measurements may provide major return in model accuracy.

Importantly, it is the opinion of the author that the dimple in the centre of the note has a strong impact on the note response that is not easily quantifiable nor its change qualitatively simple. This is suspected because notes of almost identical dimensions such as D4 and Bb4 have different notes but their dimple is different in depth. Furthermore, the way in which the note panel is made into the shell of the instrument may affect the boundary conditions. If a note is raised with material perpendicular to the surface of the shell at the edge of the note, this may make the boundary condition shift to a stiffer boundary condition, having a large effect.

6 FEA ANALYSIS

6.1 Introduction

Finite Element Analysis was performed on both the full assembly of the instrument and individual notes. The results of individual notes are much more informative about what is actually occurring in the areas of interest. Previous research has shown that analysis of individual notes is a valid methodology as interactions are not dominant. Modal analysis solves the Eigen equation to find mode shapes and frequencies. Transient analysis solves the complete set of FE equations at each time step and updates values accordingly, such as stiffness matrix based on geometric changes. Both methods are utilised. In both cases solid shell elements were utilised.

6.2 Modal Analysis

6.2.1 Method and Set-Up

To run a simulation follow the steps outlined. For a complete methodology refer to Appendix .

1. Import geometry into ANSYS as a .STEP file and suppress the die used to create the note indentation.
2. In Workbench Mechanical Set the Model and Modal parameters as described in Appendix D. Primarily focus on correct contact region, mesh method, supports and analysis settings.
3. Run the solver and view the results.

6.2.2 Results

Modal analysis produces results files such as that shown in Figure 17. It is useful because the mode shape and corresponding modal frequency can be viewed. Table 8 contains the first modal frequency for all notes in Hz and the measured frequency from the actual Pi Drum handpan.

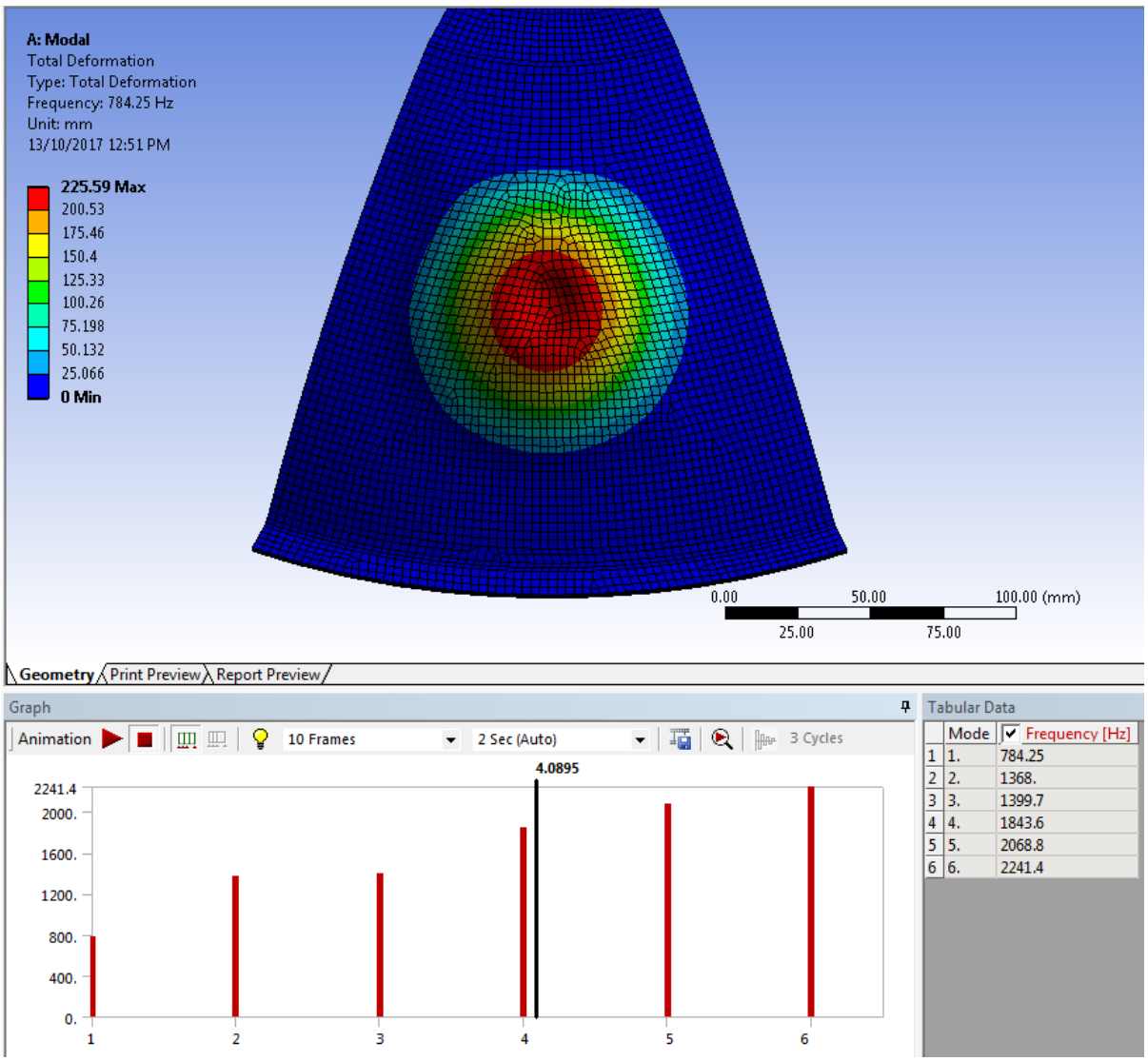

Figure 17: Example Modal Result

Table 8: Modal Analysis Frequencies

Pi Drum FEA – Modal Results

Note	Modal	Measured
D4	617.9	294.3
E4	654.9	333
F4	776.7	351.7
G4	661.1	393.2
A4	781.2	442.4
Bb4	615.6	467.4

C5	627.6	524.8
D5	784.2	589

6.3 Transient Analysis

6.3.1 Method and Set Up

Transient analyses do not provide results in the same manner as modal. It is not possible to directly draw a frequency from the program. Thus a time history for a node or group of nodes needs to be extracted from the target note and then passed through an FFT. While the overall setup in ANSYS is almost identical there are some extra steps outlined in Appendix D.

Some key points regarding the analysis are:

1. A time step in the analysis of $2.5*10^{-5}$ seconds,
2. A total number of time increments of 2048 (2^{11}),
3. A triangular impulse peaking at 20N applied over 40 time steps (0.001 seconds),
4. Load applied just above the dimple on each note,
5. Time history taken on a node just below the dimple on each note.

6.3.2 Results

Excel was used to analyse the time series data of a node on the desired note. Figure 18 shows the FFT of the A4 note performed in excel. Table 9 contains the data for all notes transient and modal analysis as well as measured note frequency. Figure 19 shows these data graphically. Appendix D (Figure 80 to Figure 87) shows the FFT for all notes presented.

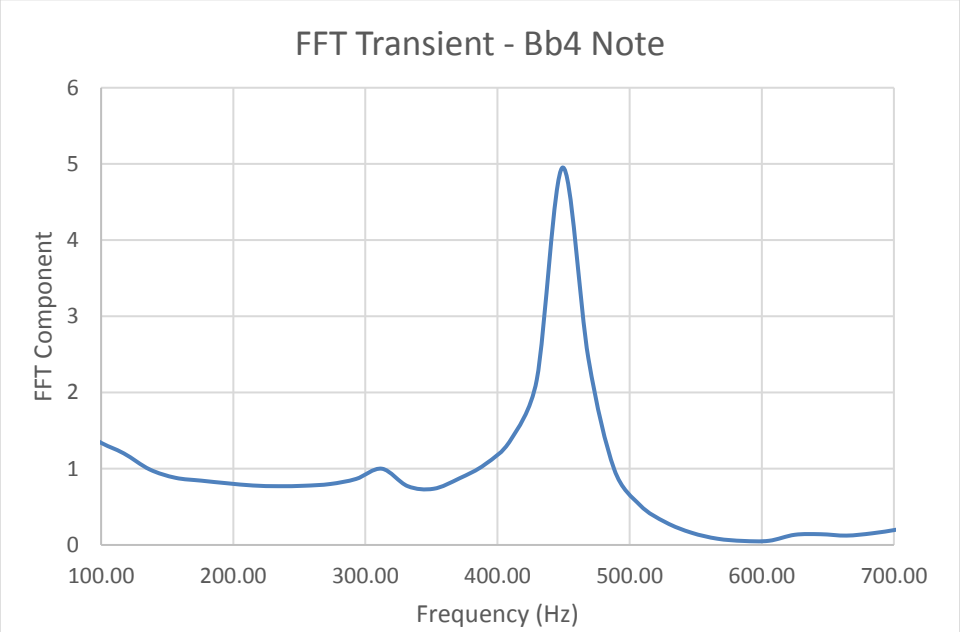

Figure 18: FFT of A4 Note

Table 9: Transient, Modal and Measured Frequencies

Pi Drum FEA – Transient Results

Note	Transient	Measured	Modal
D4	312.5	294.3	617.9
E4	293	333	654.9
F4	390	351.7	776.7
G4	507	393.2	661.1
A4	469	442.4	781.2
Bb4	449	467.4	615.6
C5	469	524.8	627.6
D5	586	589	784.2

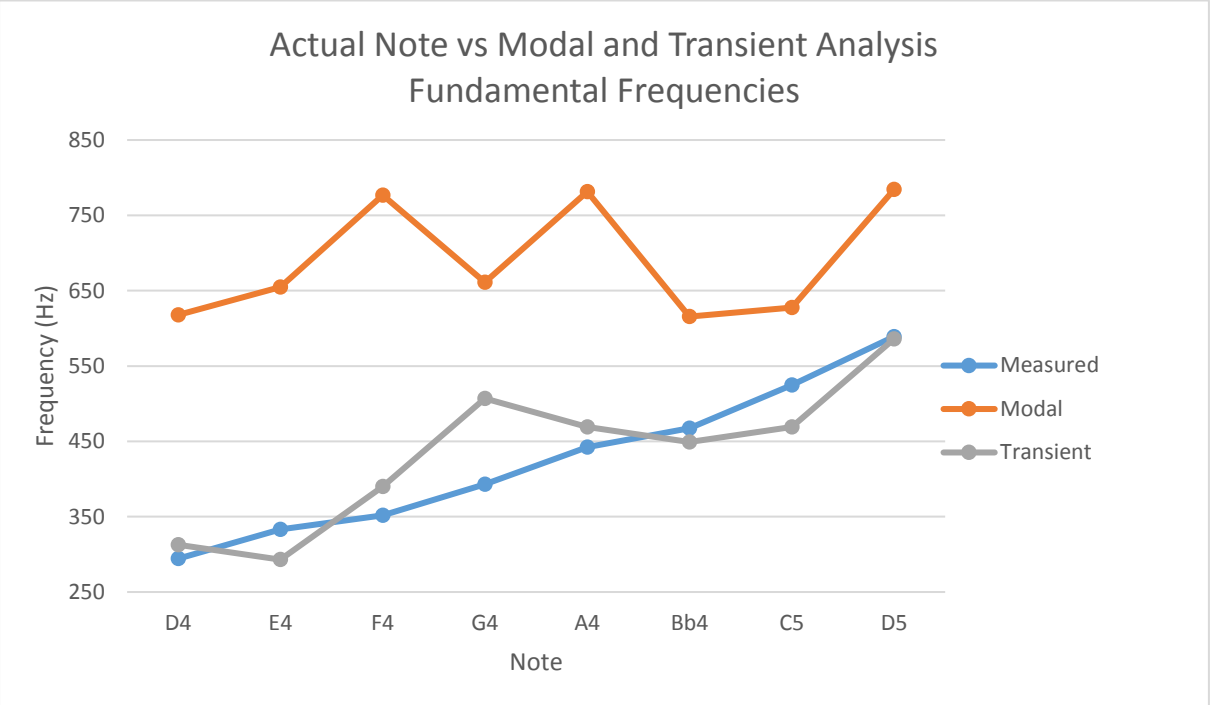

Figure 19: Transient, Modal and Measured Results Line Graph

6.4 Discussion

Transient analysis of the notes provides a great increase in result quality when compared to the actual instrument. This suggests that non-linear effects need to be taken into account to get accurate results. While they are a significant improvement over modal they still leave a large amount to be desired.

Interestingly, the modal results show little fluctuation for all notes. Importantly the mode shape acquired from the modal analysis aligns with what is expected from previous work on hanpdans. It seems to behave as an almost circular plate in its shape. This is a good indicator that the model has validity.

The author is unsure if the transient results provide sufficient accuracy. Perhaps geometric effects are so significant that current geometry is not accurate enough. This is likely a leading cause of the discrepancy between transient and physical results.

7 GEOMETRIC EFFECTS

7.1 Introduction

Note D5 on the Pi Drum shows the greatest correlation between the FEA model and physical instrument. As such, this note will be used to investigate geometric effects on modal response. Some simple geometric changes are used including: doubling the thickness of the material, removing the dimple, raising the note up so it has stiffer edges and altering the aspect ratio of the note. These effects should provide a baseline for what effects are most significant.

7.2 Method

A CAD model of the D5 note was modified to have the following geometric changes:

- No Dimple,
- Double plate thickness,
- A raised note,
- Double the aspect ratio (AR) with and without a dimple,
- Half the AR with and without a dimple and,
- Normal note dimensions.

These geometric changes were then analysed via modal and transient analysis respectively.

For all notes the effect of removing the dimple, doubling the thickness and raising the note was analysed via modal analysis. For consistency these were only compared with other modal results and the more detailed analysis of the D5 note was compared within itself.

7.3 Results

7.3.1 All Notes Modal

Table 10 contains the modal analysis results of all notes under three geometric changes. Figure 20 shows these same data plotted as line graphs to highlight general trends of geometric changes.

Table 10: All Notes Geometric Effects

Differing Geometric Effects – Modal Analysis – All Notes

Note	Measured	Modal	No Dimple	Raised Note	Thicker
D4	294.3	617.9	552.5	1079.2	1043
E4	333	654.9	598.2	827.8	1133.9
F4	351.7	776.7	718.7	995.2	1295.3
G4	393.2	661.1	608	825.9	1141
A4	442.4	781.2	749.3	1068.5	1275.3
Bb4	467.4	615.6	548.2	1086.4	1040.1
C5	524.8	627.6	558.5	824.3	1056.8
D5	589	784.2	723.4	1041.1	1303.2

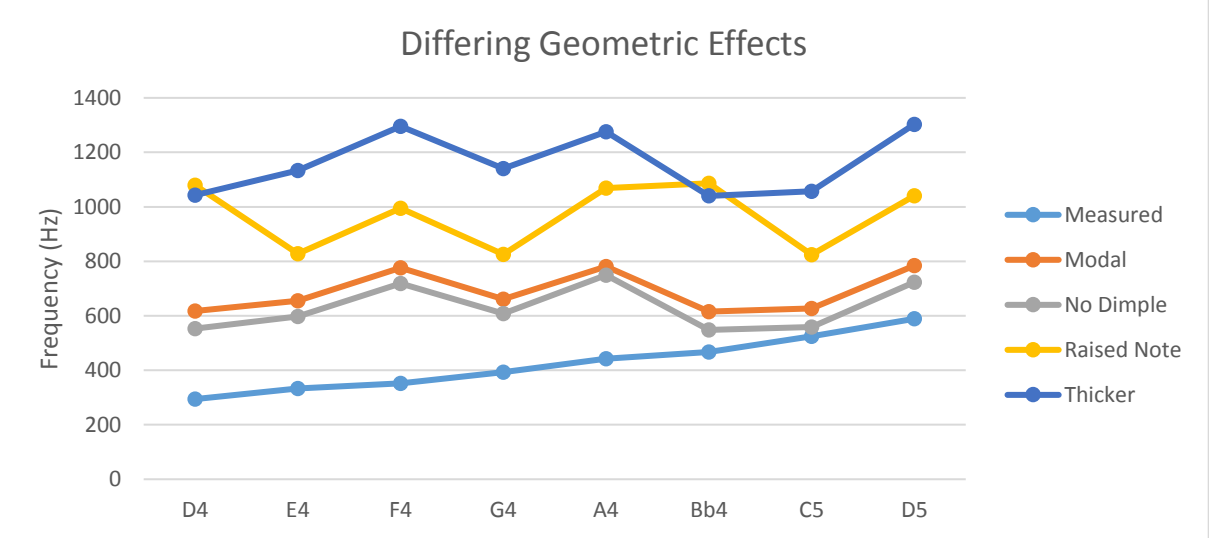

Figure 20: Differing Geometric Effects - Modal Analysis

7.3.2 D5 Note Analysis

All geometric effects were analysed for the D5 note and the data for modal and transient analyses are presented in Table 11 and Figure 21, with FFTs of notes in Appendix E.

Table 11: D5 Note - Modal and Transient Analysis

D5 Note Modal and Transient Analysis

Type	Modal	Transient
No Dimple	552.5	527.3
Measured	589	589
Normal	617.9	586
Double Thickness	1043	937.5
Raised	1079.2	918
Double AR No Dimple	1295.1	1015.6
Double AR	1457.2	1035.2
Half AR	1920.7	1035.2
Half AR No Dimple	2390.7	1113.3

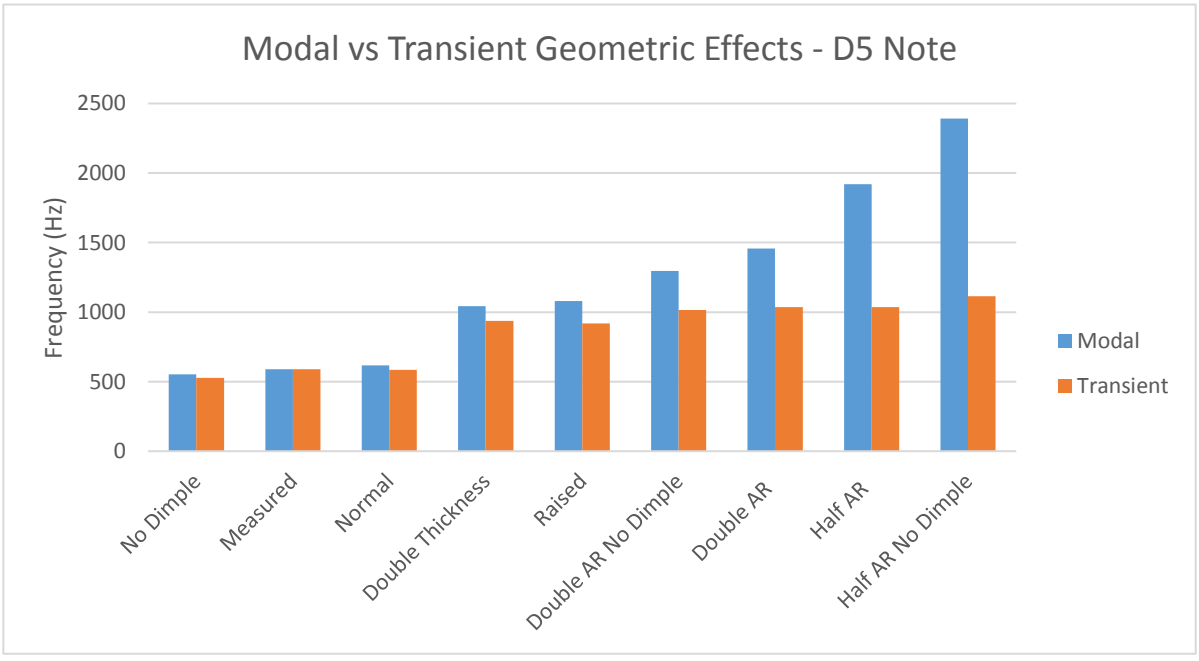

Figure 21: D5 Note - Modal vs Transient Geometric Effects

7.4 Discussion

Geometric changes have been studied in a broad but shallow manner. Changes examined can provide an idea of general trends for certain changes but no detailed insight. Figure 20 provides useful trend comparison for each change studied. Removing the dimple has a measurable and significant change of a 50 Hz reduction in modal frequency compared to the normal note. It follows the same trend pattern too. Very interestingly doubling the thickness of the note does not quite double the modal frequency.

Raising the note to make the boundary condition stiffer has an erratic effect on modal frequency but always increases it by a minimum of 30%. This erratic change is too be expected as differing sized notes have differing amounts of raised material leading into the note and thus varying stiffness's along the edges of the notes.

In all modal analyses the FEA result is above the actual note of the instrument. In some cases it is by only a small amount (C5 note) and in others it is decided pronounced (F4 note). This is an interesting point and warrants further investigation.

Modal and transient analyses provide a point of further interest. In all examined notes the transient analysis shows a lower frequency that the modal. This was expected but it becomes particularly pronounced at the effects that create higher frequencies. Differences between modal and transient results are limited for the normal note but a twofold difference is present in the Half AR notes. This is another interesting point and warrants further investigation.

8 DISCUSSION

Physical testing was a less rigorous process than had been envisaged. Using a human finger without a standardised strike imparts some uncertainty into the results. However, the alternative of using a striker produced high pitched responses and in reality a human finger is used while playing the instrument. Also, using the anechoic chamber created sharper results than would be otherwise attainable. Results show very low levels of error compared to expected notes with both the Pi Drum and Meridian which indicates the method is not fundamentally flawed, assuming the instruments were well tuned to begin with. Thus, baseline testing resulting can be deemed both precise and accurate. Some key differences between the instruments provide much insight into possible further investigation.

Existing CAD modelling procedures are both expandable to other instruments and useful for examining geometric changes. However, as shown by Figure 12 there is a method for achieving greater accuracy and precision. The organic nature of the shapes in these instruments makes the CAD modelling process the most challenging part of any project with these instruments. Balancing a customisable model and exactness of geometry is a headwind to progress. Using an augmented 3D scan information and current modelling techniques method will result in superior models.

Theoretical analysis provides a baseline for expected frequencies but seems to be vastly different from measured modal frequencies. One possible source of some of this error is imprecision in measurements taken of the geometry. Primarily, the thickness calculation, which strongly influences theoretical analysis, was a simple calculation. The method of weighing and finding surface to calculate thickness may not be sufficiently accurate. Furthermore, the equations used are highly sensitive to geometry (including thickness) and boundary conditions. Estimating the boundary conditions therefore has a large effect. Following this, the organic

nature of geometry means measurement errors will be significant and this can also have a large impact on the theoretical results.

Based on Figure 7 and Figure 8 it can be assumed that circular plate type modal vibrations are occurring in the note region of the instrument. This aligns with circular plate theory providing the closest correlation between theory and practicality. Further FEA confirmed that the plate seemed to be vibrating in an almost circular mode as shown in Figure 17. The modal values attained from FEA followed the trend of theoretical calculations in being far above physically observed frequencies. This suggests that non-linearities in the system are significant, geometric sensitivities are very high or both.

Transient analyses provided more realistic results when compared to modal but where still often significantly different from observed results. Again, sensitivity to geometry likely had an effect. Some notes aligned transient and reality quite well, such as the D5 note. This could be due to chance that its geometry was better aligned but more likely attributable to chance.

Dimples in the centre of the note provide an interesting phenomena. They lower the observed frequency in both transient and modal analyses. Reasons for this drop could be it affecting boundary conditions or making the plate behave with greater stiffness in the middle. The drop in frequency the dimples cause is consistent across all notes analysed.

Raising the note creates a stiffer edge, approximating a more fixed edge condition. This, as expected, increased the frequency of the note. Because of the inconsistent nature of raising the edges (different sized notes have different amounts of raised edge, for example) the change caused is also inconsistent. Figure 20 shows this is in contrast with other simple geometric changes, which still follow the same profile between notes at different frequencies.

9 CONCLUSIONS AND RECOMMENDATIONS

9.1 Conclusions

While a specific, highly repeatable, method for physical testing of handpans was not developed, the method generated and used provided consistent and realistic results. True scientific repeatability was not achieved for the method but error minimisation was still realized and the use of an anechoic chamber and high fidelity microphone gave clean, consistent data. Further experimentation on the instruments need not deviate from existing methods, if it is required at all.

Physical testing provided a confirmation of the interaction between notes the instrument experiences. However, it also showed that these interactions do not affect model frequencies. Furthermore, comparing results from both instruments highlighted the increased damping present in the Pi Drum. This damping was likely caused by two things; the joint of the two shells and structural damping within the steel. This is a candidate for further investigation and increased modelling attention.

CAD modelling procedures were developed entirely from scratch for this project. Existing methodology is very useful for its customisable nature but could be improved by augmenting it with accurate 3D scan information. Current models are not accurate enough to capture the geometry sufficiently and need to be improved for results that correlate more precisely with physical systems. This may be the single largest improvement that can be made to the digital modelling process.

Theoretical analysis of the notes provided interesting insight into the behaviour of the system. Thickness calculations were not particularly robust and may have had a significant impact on results attained. In combination with the mode shapes from FEA the analytical results suggest the notes vibrate in a circular plate manner. This is a point of interest and may be informative

for further work. This analysis showed that the frequencies present are highly dependent on and sensitive too geometry. Using more accurate geometric information from the 3D scan may help improve the correlation between theoretical and physical results.

Modal frequencies attained from FEA analysis of the notes suggest that non-linearities are significant. This is in agreement with existing literature too. Overall trends of modal analysis provided some insight into system behaviour but did not provide predictive capability as the results were far off physical outcomes, in some cases by over 200%. Transient analysis showed that non-linear solving of the system provided much more accurate results but still had large improvements to be made. Thus, non-linearities are a driving factor and need to be considered.

All geometric changes when analysed via modal and transient had the same trend movement and followed what would be expected. This is good for model validation purposes and helped provide insight into what can affect the note present. Particularly the raised edge notes had large increases in frequency and this may be a useful method of controlling frequencies present, along with the dimple.

A superficial examination of geometric effects of the handpan is presented in this dissertation. Once modelling methods and models are improved a far deeper exploration of geometric effects should be undertaken. This investigation is a thesis in its own right.

9.2 Recommendations

Recommendations for further or improved work follow:

- CAD model accuracy improvements. This should be done using the existing models and improved data from the 3D scan. Particularly, note die geometry in the SolidWorks model can be greatly improved and thus provide a closer representation to real life. The dimple, which is suspected to have a significant effect, can also be improved using this enhanced geometric data.

- Improve the thickness estimate by measuring directly if possible. Otherwise, use 3D scan information and a more accurate mass measurement to improve the result. It may be the case that top and bottom halves of the instrument are not of equal thickness.
- With improved geometry perform modal analysis on individual notes once again and observe the amount of improvement in results. Also, run a full instrument model FEA and observe for fundamental frequencies there. This process may be highly informative.
- Perform theoretical analysis of notes once again with improved geometric information. Once again, this may be highly informative as improved inputs may show that theoretical analysis, in some form, is useful for design purposes.
- With improved models, examine geometric changes in greater detail. For example, do not only look at two changes in AR, make a refined grid so the response to AR can be plotted for a note. Examine differing dimple geometries, not just their removal.
- Improve the modelling of damping in the system when performing FEA. Focus especially on the rim joint of the two shells.
- Create a CAD model of the Meridian handpan and analyse this. Its slightly more consistent geometry and reduced damping may mean it is more conducive to modelling and provide greater insight (i.e. less noise in the analysis to worry about).

Further direction for investigation will be found when performing these recommendations.

10 REFERENCES

Achong, A. (1996). "The steelpan as a system of non-linear mode-localized oscillators, I: Theory, simulations, experiments and bifurcations." Journal of Sound and Vibration **197**(4): 471-487.

Achong, A. (1996). "Vibrational analysis of mass loaded plates and shallow shells by the receptance method with application to the steelpan." Journal of sound and vibration **191**(2): 207-217.

Achong, A. and K. Sinanan-Singh (1997). "The steelpan as a system of non-linear mode-localized oscillators, part II: coupled sub-systems, simulations and experiments." Journal of sound and vibration **203**(4): 547-561.

Adams, V. and A. Askenazi (1999). Building Better Products with Finite Element Analysis, OnWord Press.

Alon, E. (2015). Analysis and Synthesis of the Handpan Sound, University of York.

Alon, E. and D. T. Murphy (2015). "ANALYSIS AND RESYNTHESIS OF THE HANDPAN SOUND."

Gay, D. A. (2008). "Finite element modelling of steelpan acoustics." Journal of the Acoustical Society of America **123**(5): 3799-3799.

Google (2017). Handpan Manufacturers. Mountain View, Google.

Han, W. and M. Petyt (1997). "Geometrically nonlinear vibration analysis of thin, rectangular plates using the hierarchical finite element method—I: The fundamental mode of isotropic plates." Computers & Structures **63**(2): 295-308.

ICT, N. (2017). "Free Vibration of a Cantilever Beam (Continuous System)." Retrieved 9th of September, 2017, from http://iitg.vlab.co.in/?sub=62&brch=175&sim=1080&cnt=1.

Leissa, A. W. (1969). Vibration of plates, OHIO STATE UNIV COLUMBUS.

Leissa, A. W. (1973). "The free vibration of rectangular plates." Journal of Sound and Vibration **31**(3): 257-293.

Monteil, M., C. Touzé and O. Thomas (2013). "Nonlinear vibrations of steelpans: analysis of mode coupling in view of modal sound synthesis."

Morrison, A. and T. Rossing (2007). "Modes of vibration and sound radiation from the hang." Archives of Acoustics **32**(3): 551-560.

Paniverse. (2017). "DEEPAN in progress – New generation Pan's." Retrieved 20th of October, 2017, from https://i1.wp.com/paniverse.org/wp-content/uploads/2016/06/20160618_165758-e1466491305592.jpg.

Rao, S. S. (2011). Mechanical vibrations, Prentice Hall Upper Saddle River.

Rohner, F. and S. Schärer (2007). History, Development and Tuning of the HANG. International Symposium on Musical Acoustics (ISMA 2007).

Rossing, T., A. Morrison, U. Hansen, F. Rohner and S. Schärer (2007). Acoustics of the Hang: A hand-played steel instrument. International Symposium on Musical Acoustics (ISMA 2007).

Shi, D., X. Shi, W. L. Li, Q. Wang and J. Han (2014). "Vibration Analysis of Annular Sector Plates under Different Boundary Conditions." Shock and Vibration **2014**: 11.

Software, M. (2011). Dynamic Analysis User's Guide: MSC Nastran 2012, MacNeal-Schwendler Corporation.

11 APPENDICES

11.1 Appendix A

11.1.1 Analytical Rectangular Plate Solution Coefficients

TABLE 4.2.—*Frequency Coefficients for Equation (4.17) and Different Mode Shapes; $\nu=0.25$*

Boundary conditions	Deflection function or mode shape	N	K
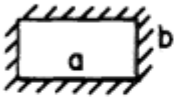	$\left(\cos\frac{2\pi x}{a}-1\right)\left(\cos\frac{2\pi y}{b}-1\right)$	2.25	$12+8\left(\frac{a}{b}\right)^2+12\left(\frac{a}{b}\right)^4$
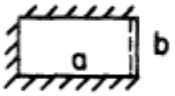	$\left(\cos\frac{3\pi x}{2a}-\cos\frac{\pi x}{2a}\right)\left(\cos\frac{2\pi y}{b}-1\right)$	1.50	$3.85+5\left(\frac{a}{b}\right)^2+8\left(\frac{a}{b}\right)^4$
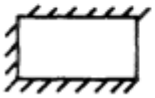	$\left(1-\cos\frac{\pi x}{2a}\right)\left(\cos\frac{2\pi y}{b}-1\right)$	.340	$0.0468+0.340\left(\frac{a}{b}\right)^2+1.814\left(\frac{a}{b}\right)^4$
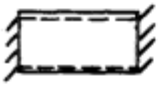	$\left(\cos\frac{2\pi x}{a}-1\right)\sin\frac{\pi y}{b}$	.75	$4+2\left(\frac{a}{b}\right)^2+0.75\left(\frac{a}{b}\right)^4$
	$\left(\cos\frac{2\pi x}{a}-1\right)\frac{y}{b}$	.50	$2.67+0.304\left(\frac{a}{b}\right)^2$
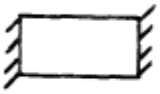	$\cos\frac{2\pi x}{a}-1$	1.50	8
	$\left(\cos\frac{3\pi x}{2a}-\cos\frac{\pi x}{2a}\right)\left(\cos\frac{3\pi y}{2b}-\cos\frac{\pi y}{2b}\right)$	1.00	$2.56+3.12\left(\frac{a}{b}\right)^2+2.56\left(\frac{a}{b}\right)^4$
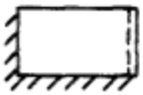	$\left(\cos\frac{3\pi x}{2a}-\cos\frac{\pi x}{2a}\right)\left(1-\cos\frac{\pi y}{2b}\right)$	.227	$0.581+0.213\left(\frac{a}{b}\right)^2+0.031\left(\frac{a}{b}\right)^4$

Figure 22: Rectangular Plate Boundary Condition Constants

Boundary conditions	Deflection function or mode shape	N	K
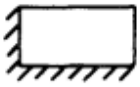	$\left(1-\cos\frac{\pi x}{2a}\right)\left(1-\cos\frac{\pi y}{2b}\right)$	0.0514	$0.0071+0.024\left(\frac{a}{b}\right)^2+0.0071\left(\frac{a}{b}\right)^4$
	$\left(\cos\frac{3\pi x}{2a}-\cos\frac{\pi x}{2a}\right)\sin\frac{\pi y}{b}$	.50	$1.28+1.25\left(\frac{a}{b}\right)^2+0.50\left(\frac{a}{b}\right)^4$
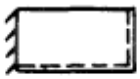	$\left(\cos\frac{3\pi x}{2a}-\cos\frac{\pi x}{2a}\right)\frac{y}{b}$	.333	$0.853+0.190\left(\frac{a}{b}\right)^2$
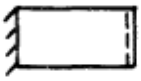	$\cos\frac{3\pi x}{2a}-\cos\frac{\pi x}{2a}$	1.00	2.56
	$\left(1-\cos\frac{\pi x}{2a}\right)\frac{\pi^2}{b^2}\sin\frac{\pi y}{b}$	.1134	$0.0156+0.0852\left(\frac{a}{b}\right)^2+0.1134\left(\frac{a}{b}\right)^4$
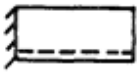	$\left(1-\cos\frac{\pi x}{2a}\right)\frac{y}{b}$	.0756	$0.0104+0.0190\left(\frac{a}{b}\right)^2$
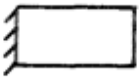	$1-\cos\frac{\pi x}{2a}$	.2268	0.0313
	$\sin\frac{\pi x}{a}\sin\frac{\pi y}{b}$	.25	$0.25+0.50\left(\frac{a}{b}\right)^2+0.25\left(\frac{a}{b}\right)^4$
	$\left(\sin\frac{\pi x}{a}\right)\frac{y}{b}$	.1667	$0.1667+0.0760\left(\frac{a}{b}\right)^2$
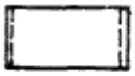	$\sin\frac{\pi x}{a}$	.50	0.50

Figure 23: Rectangular Plate Boundary Condition Constants Continued

11.1.2 Analytical Circular Plate Solution Coefficients

TABLE 2.1.—*Values of* $\lambda^2=\omega a^2\sqrt{\rho/D}$ *for a Clamped Circular Plate*

s	λ² for values of n of—														
	0	1	2	3	4	5	6	7	8	9	10	11	12	13	14
0	10.2158	21.26	34.88	51.04	69.6659	90.7390	114.2126	140.0561	168.2445	198.7561	231.5732	266.6790	304.0601	343.7038	385.5996
1	39.771	60.82	84.58	111.01	140.1079	171.8029	206.0706	242.8782	282.1977	324.0036	368.2734				
2	89.104	120.08	153.81	190.30	229.5186	271.4283	316.0015	363.2097							
3	158.183	199.06	242.71	289.17	338.4113	390.3896									
4	247.005	297.77	351.38	407.72											
5	355.568	416.20	479.65	545.97											
6	483.872	554.37	627.75	703.95											
7	631.914	712.30	795.52	881.67											
8	799.702	889.95	983.07	1079.0											
9	987.216	1087.4	1190.4	1296.2											

Figure 24: Clamped Circular Plate Boundary Condition Constants

TABLE 2.3.—*Values of* $\lambda^2=\omega a^2\sqrt{\rho/D}$ *for a Simply Supported Circular Plate;* $\nu=0.3$

s	λ² for values of n of—		
	0	1	2
0	4.977	13.94	25.65
1	29.76	48.51	70.14
2	74.20	102.80	134.33
3	138.34	176.84	218.24

Figure 25: Simply Supported Circular Plate Boundary Condition Constants

11.1.3 Analytical Annular Plate Solution Coefficients

TABLE 2.18.—*Frequency Parameters* $\omega a^2\sqrt{\rho/D}$ *for a Clamped, Clamped Annular Plate*

n	s	$\omega a^2\sqrt{\rho/D}$ for values of b/a of—				
		0.1	0.3	0.5	0.7	0.9
0	0	27.3	45.2	89.2	248	2237
1	0	28.4	46.6	90.2	249	2238
2	0	36.7	51.0	93.3	251	------
3	0	51.2	60.0	99.0	256	2243
0	1	75.3	125	246	686	6167
1	1	78.6	127	248	686	6167
2	1	90.5	134	253	689	------
3	1	112	145	259	694	6174

Figure 26: Clamped Annular Plate Boundary Condition Constants

TABLE 2.25.—*Values of* $\lambda^2=\omega a^2\sqrt{\rho/D}$ *for an Annular Plate Simply Supported on Both Edges;* $\nu=1/3$

n	λ^2 for values of b/a of—						
	0.1	0.2	0.3	0.4	0.5	0.6	0.7
0	14.44	17.39	21.31	28.25	40.01	62.09	110.67
1	16.77	19.19	----------	30.00	----------	62.41	----------
2	25.97	27.55	----------	36.14	----------	68.41	----------

Figure 27: Simply Supported Annular Plate Boundary Condition Constants

11.2 Appendix B

11.2.1 Matlab Code for Audio Sample Analysis

```
[x,Fs] = audioread('M A flat s.wav') % open the wav file
% find out sampling rate,etc
% Fs = sample rate
% bits = number of bits per sample

N=length(x)
% N = number of samples

% Now generate a general plot of the frequency spectrum

f=Fs/N.*(0:N-1);
% calculate each frequency component

figure(1)
Y=fft(x,N);
Y=abs(Y(1:N))./(N/2);
plot(f,Y)
xlabel('Frequency (Hz)')
ylabel('Relative Power')
title('FFT of Meridian - A flat s')
axis([0 2000 0 0.02])
savefig('FFT MAflats.fig')
% Plots the Fourier transform of the signal giving the frequency domain

figure(2)
t=[1/Fs:1/Fs:length(x)/Fs];
plot(t,x)
xlabel('Time (s)')
ylabel('Relative Power')
title('Response of Meridian - A flat s')
axis([0 3 -1 1])
savefig('Response MAflats')
% Plots the soundwave that has been recorded

figure(3)
P=20*log10(abs(x))
t=[1/Fs:1/Fs:length(P)/Fs];
plot(t,P)
xlabel('Time (s)')
ylabel('Relative Power (dB)')
title('Decibel Response of Meridian - A flat s')
axis([0 5 -100 1])
savefig('Power Response MAflats.fig')
% Plots the soundwave on a relative intensity decibel scale

figure(4)
spectrogram(x,4096,0,f/25,Fs, 'yaxis');
title('Spectrogram of Meridian - A flat s')
savefig('Spectrogram MAflats.fig')
% Plots the spectrogram of the signal for given spectrogram parameters
```

Figure 28: Audio Sample Analysis Matlab Code

11.2.2 Tables of Observations of Physical Testing

Table 12: FFT, Spectrogram and Power Response Observations - Pi Drum No Stand

Note (Hz)	Other Notes Present (Hz)	Observations
D4	152.5	Many other peaks, very noisy graph. Slight double peak at 884. 884 peak has longest sustain by factor of 2. Also maintains highest intensity. Slight beats present.
E4	297.7 and 154.3	Slight double peak at 335, very clear otherwise, 335 very dominant. 335 clearly the most intense at start but has an equal sustain with 662.
F4	Many	Very noisy with multiple peaks across the spectrum. 1047 is dominant. Poor sustain, not much insight to offer
G4	146.7 and 510.4	Noise but 394 clearly dominant. 510 has longest sustain.
A4	510.4	443 is most dominant followed by 884.7. 443 longest sustain by considerable amount. Clear beats present.
Bb4	152.4, 510.4 and 830	Noisy signal, first and third mode not present. 510 is dominant followed by 152. 830 has longest sustain, noisy and not much to decipher.
C5	151.7, 505.2	Multiple peaks around 525 peak. 1050 dominant then 505 then 525. Similar intensity and sustain at the 500-525 range. Some beats present.
D5	146.8, 1416	Double peak at 588, bit of noise in lower frequencies, 598 very dominant. 595 has longest sustain, beats visible in the 588 peak. Beats developed.

Table 13: FFT, Spectrogram and Power Response Observations - Pi Drum Stand

Note (Hz)	Other Notes Present (Hz)	Observations
D4	148.9	Very clean signal, well defined individual peaks. Slight double peak at 294 with 298. 294 is dominant and has longest sustain by 50%. Slight beats present.
E4	149, 297.6	Clean signal and 662.4 is massively dominant. 662 most dominant and has equal longest sustain with 333.
F4	297.9, 149.3	Clean response, 149 and 351 are dominant. 351 has greatest intensity but 297 has longest sustain. Very weak but long sustain peak at 830.
G4	149.8	Very clean signal, 393 and 786 equally and very dominant. similar intensities and sustains for 393 and 786
A4	150.2	Very clean with 442 massively dominant. 442 sustain massive compared to rest.
Bb4	148.9, 510.6, 1179	Clean signal, 467.4 very dominant, followed by 933. 933 has longest sustain.
C5	1339, 149	Very dominant 524 peak, clean response otherwise. 525 has longest sustain.
D5	149.8	589 very dominant, fairly clear signal. Noisy spectrogram, not very good.

Table 14: FFT, Spectrogram and Power Response Observations - Meridian No Stand

Note (Hz)	Other Notes Present (Hz)	Observations
G3	586.8	586.8 is dominant response and some lower notes creeping in. 586 has longest sustain by 100%, messy lower notes around 194 has high intensity early on.
Ab3	620.8 and 931.4	208 heavily dominant. 600 and 900 longest sustain by 100% and 207 damps out very quickly but has highest intensity.
C4	782.8	263 most dominant with 782 and 524 equal. Higher notes much longer sustain. Slight beats.
Eb4	-	Multiple low power peaks below 622Hz. beats present, 622 longest sustain, 311 highest intensity. Very clear beats.
F4	1046	698 dominant, some lower frequency peaks. 349 and 698 longest sustain, quite a lot happening between 300 and 600, partial beats.
G4	416	Very dominant 391. Slight beats in 391
Bb4	Many, many others	Lots of other notes present in equal magnitude, this is the oddest FFT.
C5	Many, many others	175 has large response. Very busy, beats in 524, also has longest sustain but other notes sustain almost equally. Slight beats.

Table 15: FFT, Spectrogram and Power Response Observations - Meridian Stand

Note (Hz)	Other Notes Present (Hz)	Observations
G3	586.6	586 is equal magnitude to 195.4. 586 has longest sustain by 100%, large amount of notes between 195 and 586. Nice decay
Ab3	620.7	620 is close to e flat 5. 620 has longest sustain by 30% but 207 has highest intensity. Slight beats.
C4	782.8	Linear decrease in power from 262 to 1046. Longest sustain on 700 but 500 700 and 1000 all roughly equal. Messy minor beats.
Eb4	-	Some other low power notes present. 622 has longest sustain. 310 highest intensity. Slight development of beats.
F4	-	Some low power lower frequency notes. 698 is highest intensity and longest sustain, beats in 350. Clear beats.
G4	415	783 dominant followed by 390.8. 783 has highest in intensity and longest sustain.
Bb4	Many others	Again, many other notes present. Beats in 350, 1045 longest, very busy spectrogram.
C5	Multiple others present	Very busy FFT. Beats in 520, also has longest sustain, very busy and cramped.

11.2.3 Pi Drum Spectrograms

11.2.3.1 D4

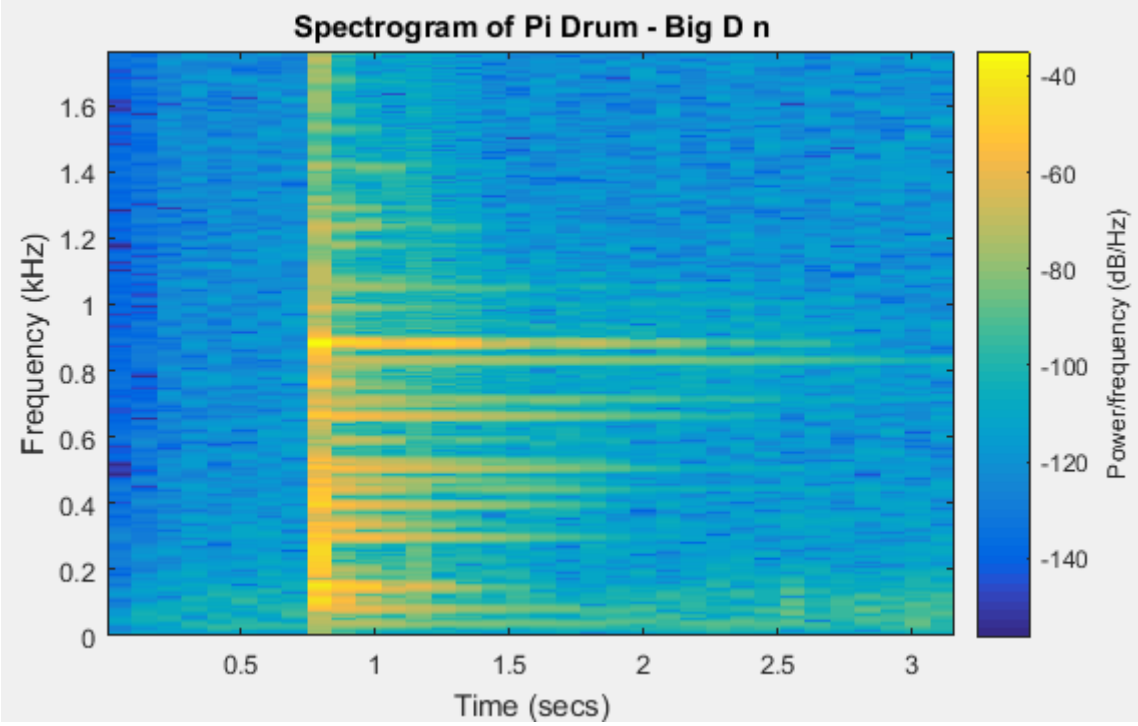

Figure 29: Pi Drum - D4 Spectrogram – No Stand

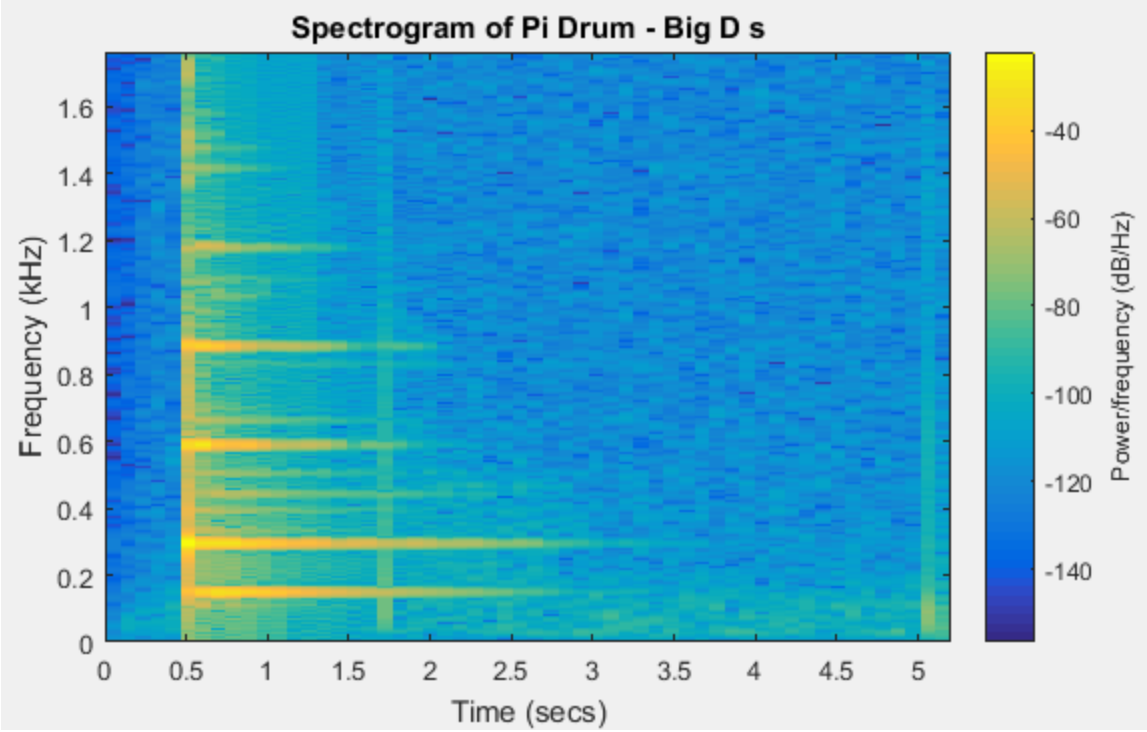

Figure 30: Pi Drum - D4 Spectrogram - Stand

11.2.3.2 E4

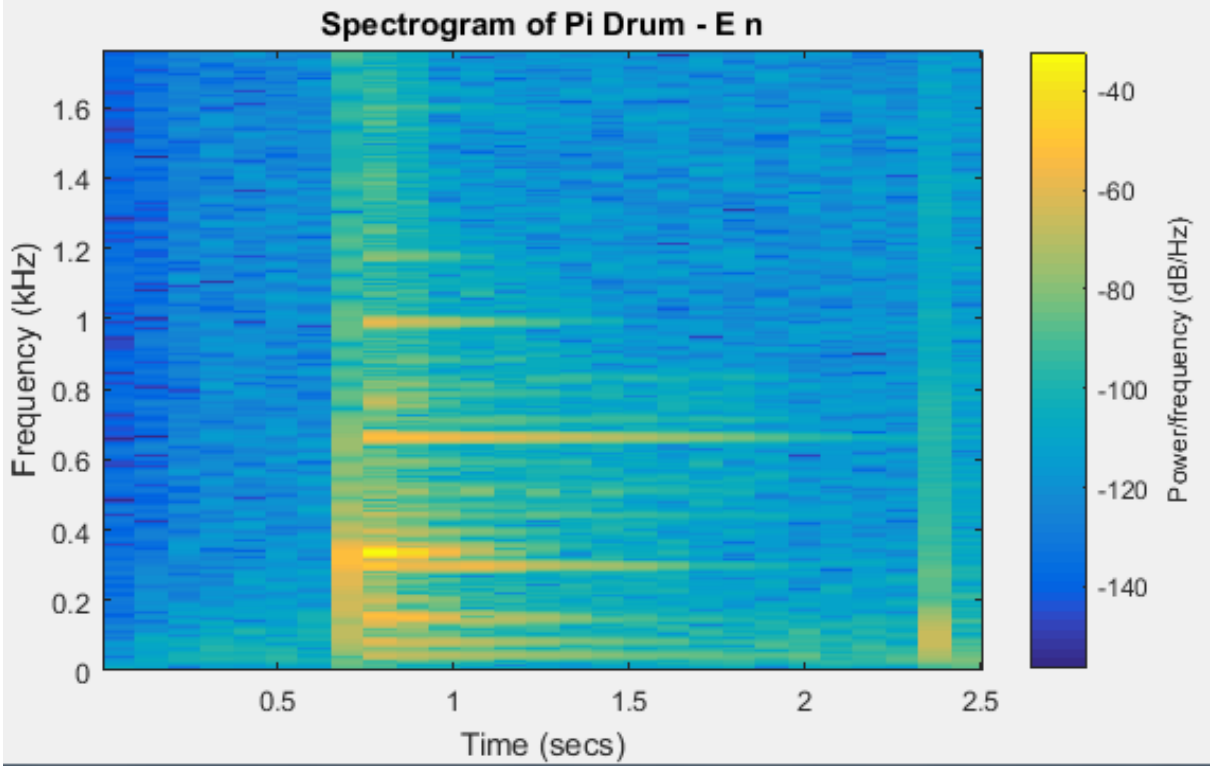

Figure 31: Pi Drum - E4 Spectrogram – No Stand

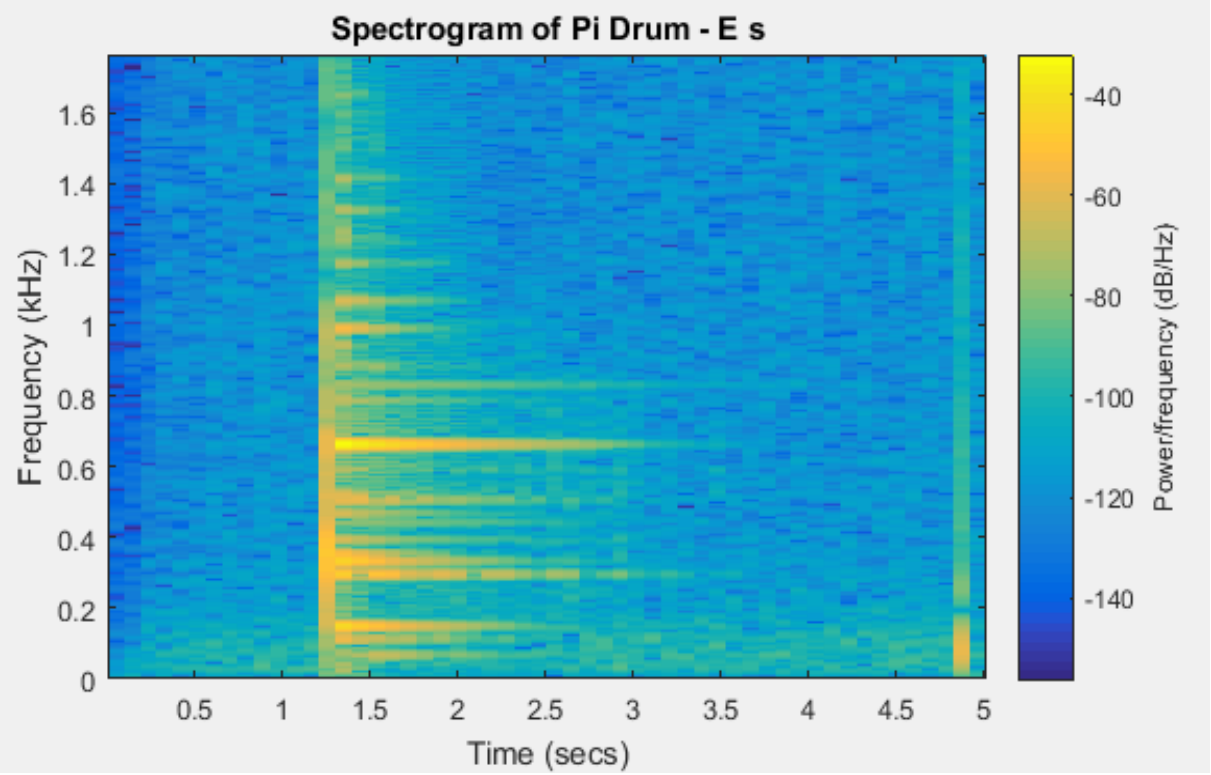

Figure 32: Pi Drum - E4 Spectrogram – Stand

11.2.3.3F4

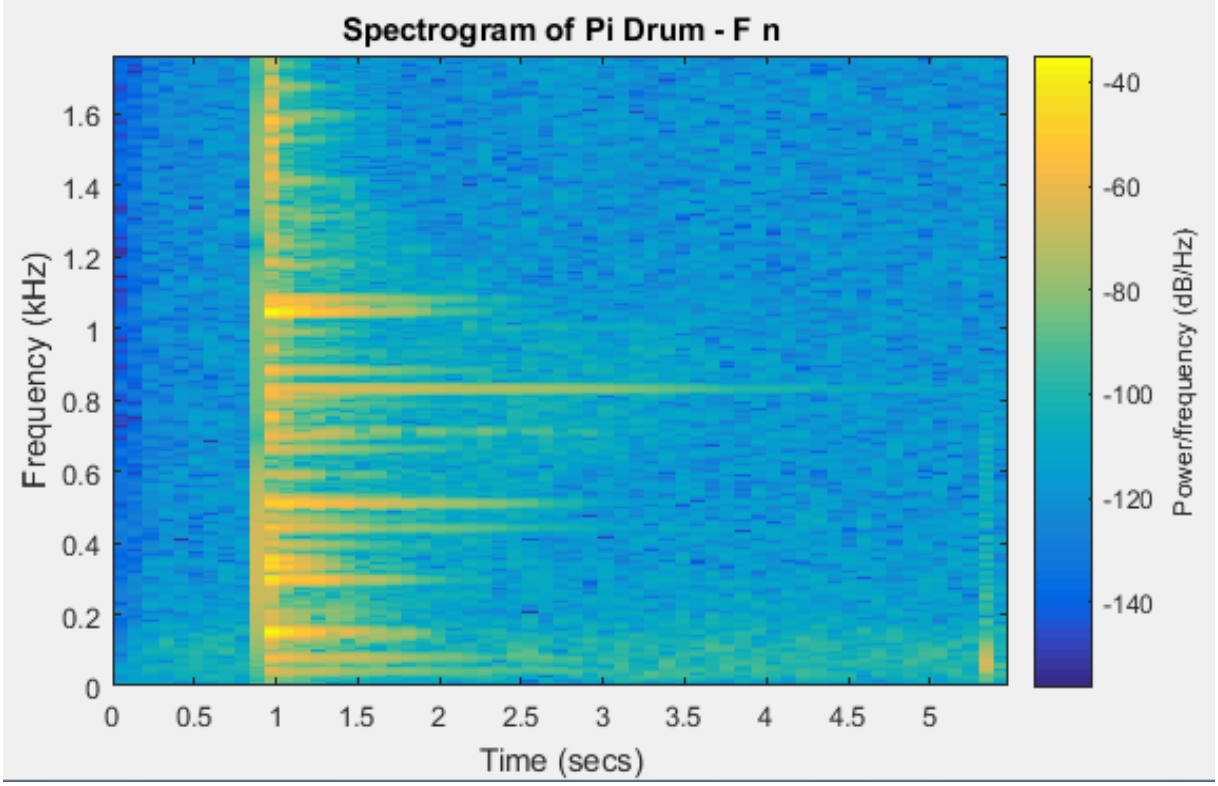

Figure 33: Pi Drum - F4 Spectrogram – No Stand

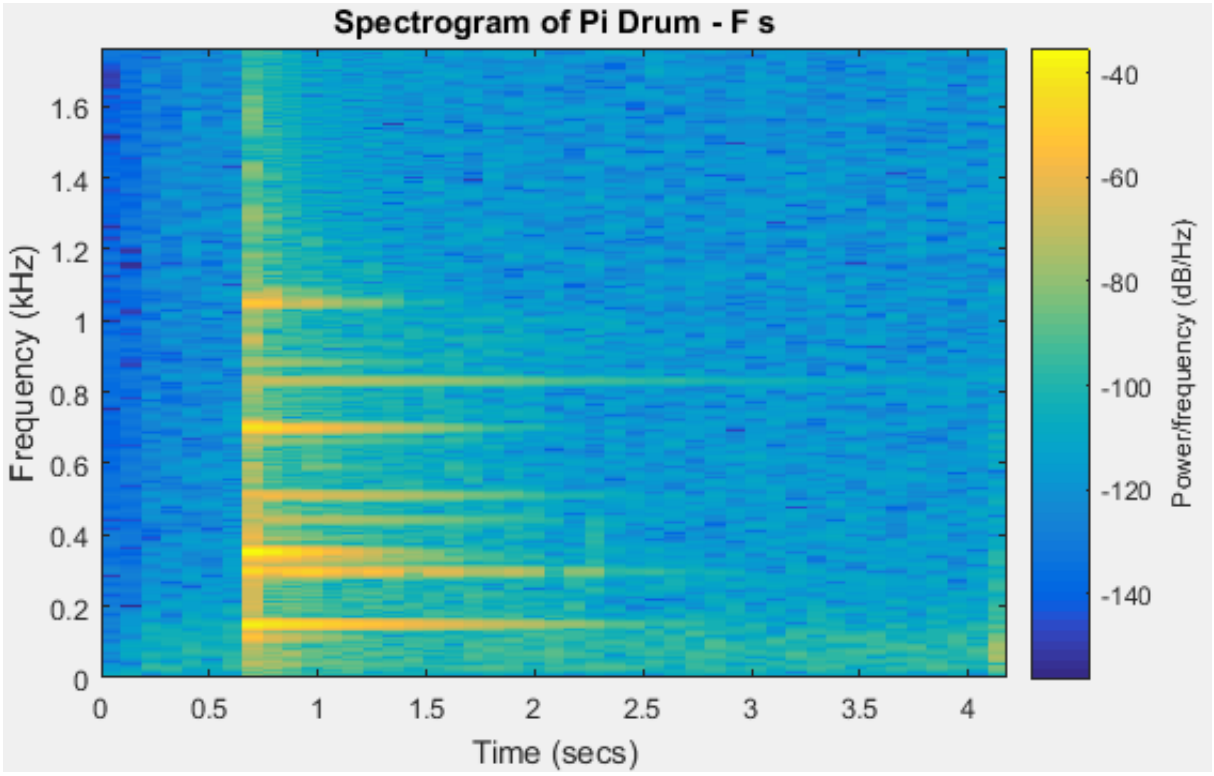

Figure 34: Pi Drum - F4 Spectrogram – Stand

11.2.3.4G4

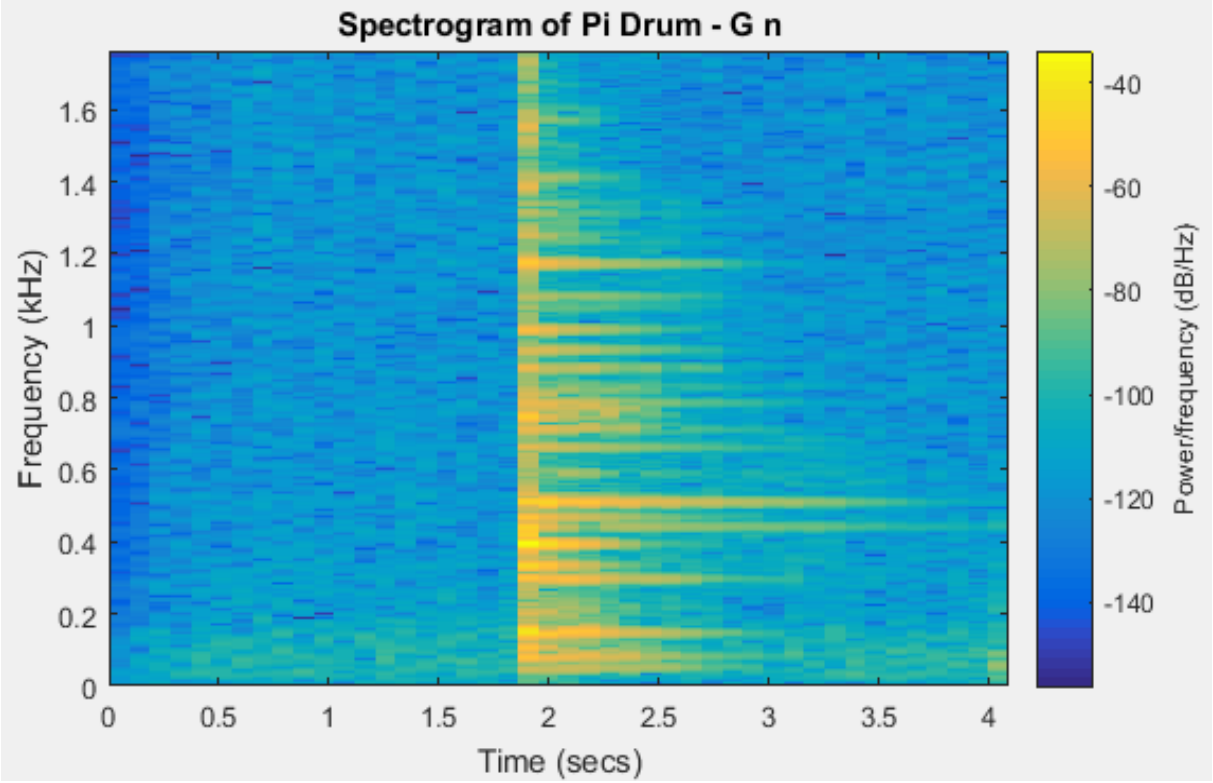

Figure 35: Pi Drum - G4 Spectrogram – No Stand

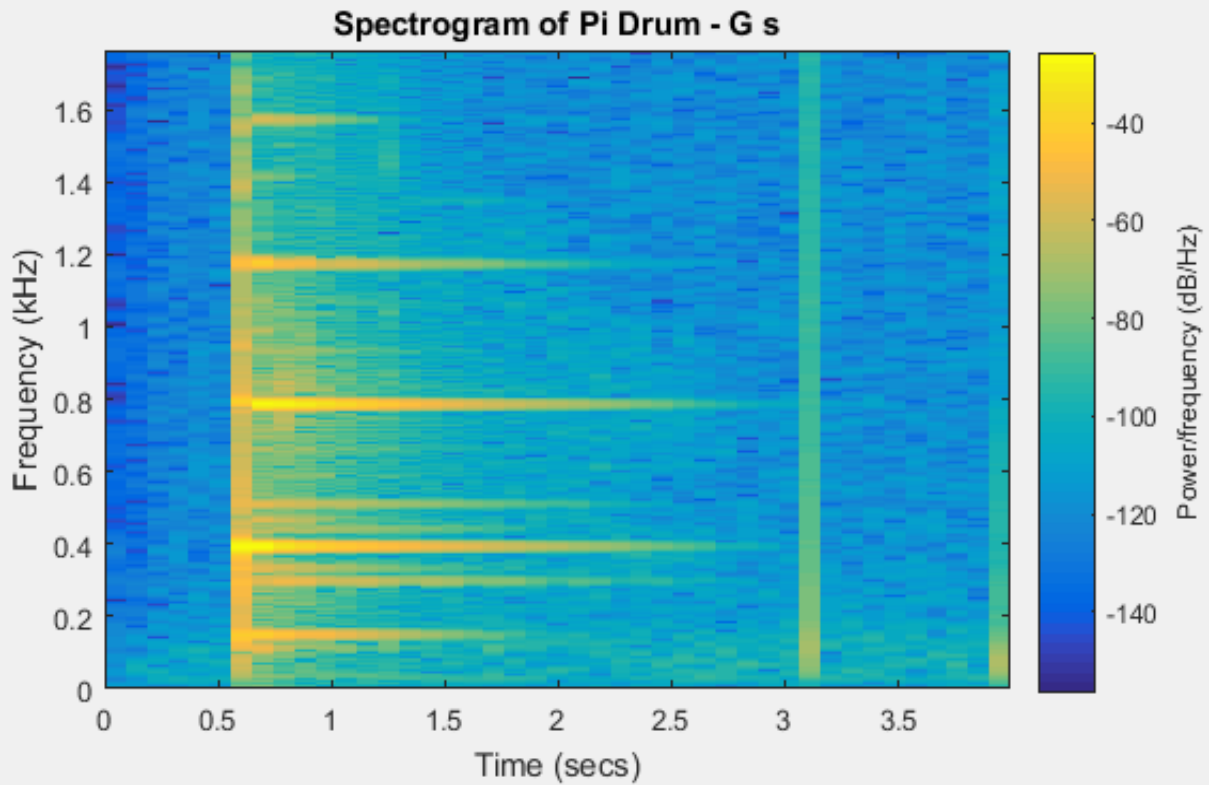

Figure 36: Pi Drum - G4 Spectrogram – Stand

11.2.3.5A4

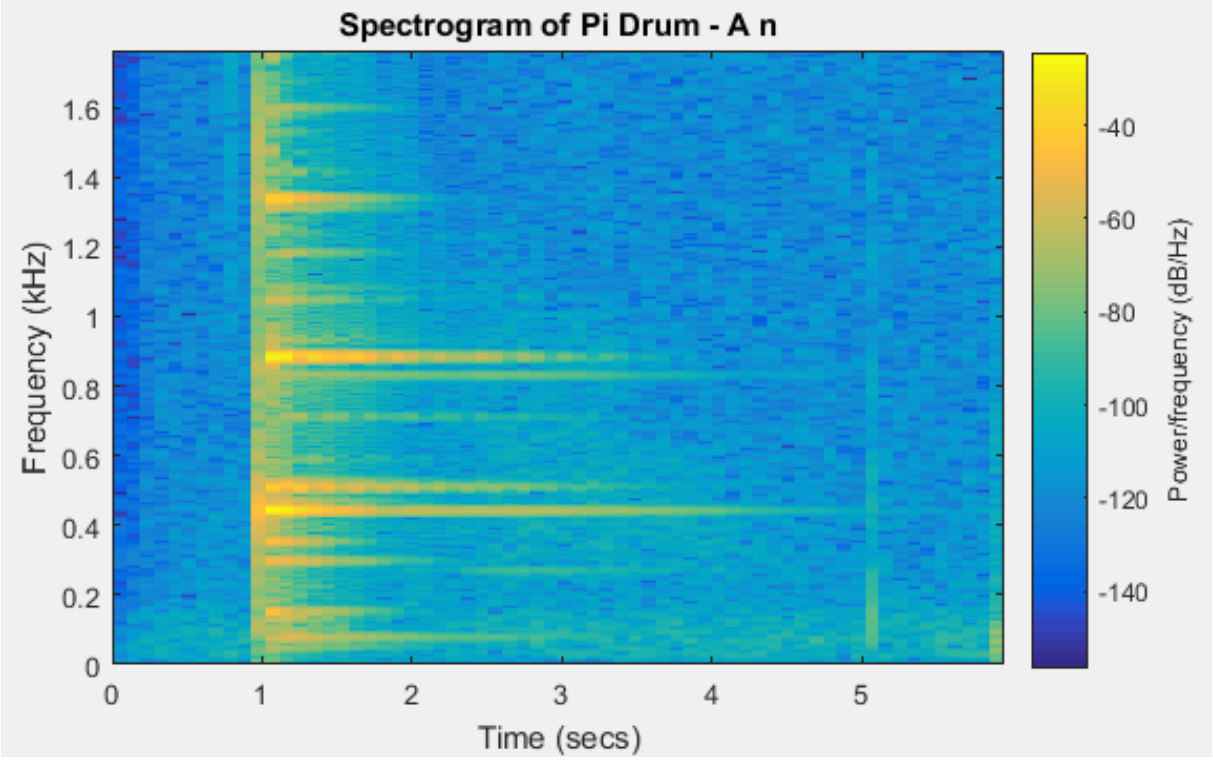

Figure 38: Pi Drum - A4 Spectrogram – No Stand

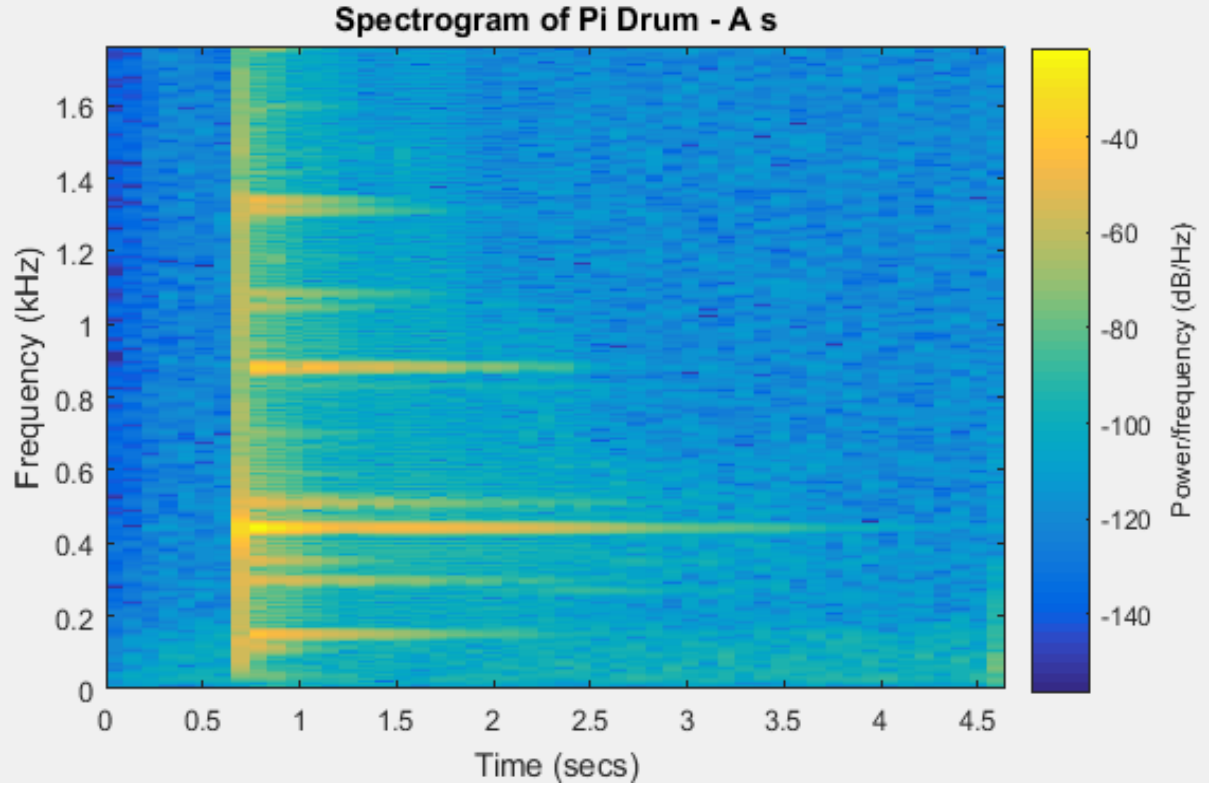

Figure 37: Pi Drum - A4 Spectrogram – Stand

11.2.3.6Bb4

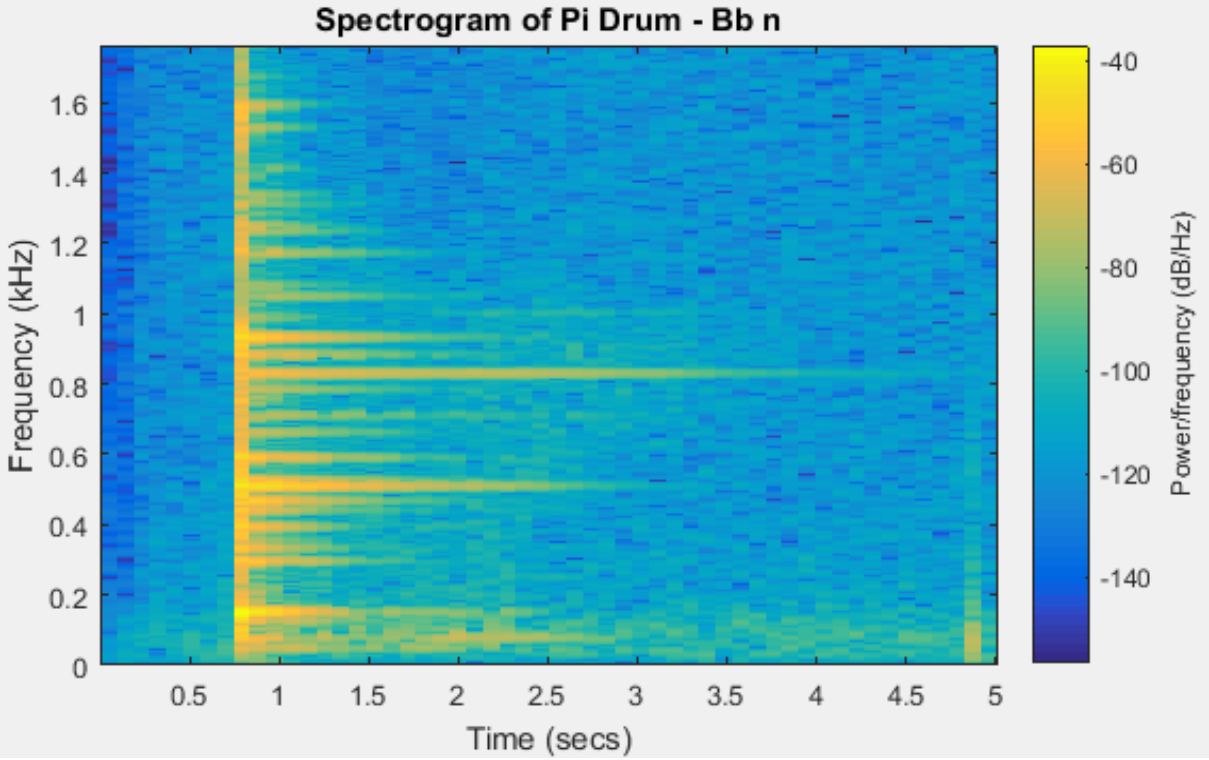

Figure 40: Pi Drum - Bb4 Spectrogram – No Stand

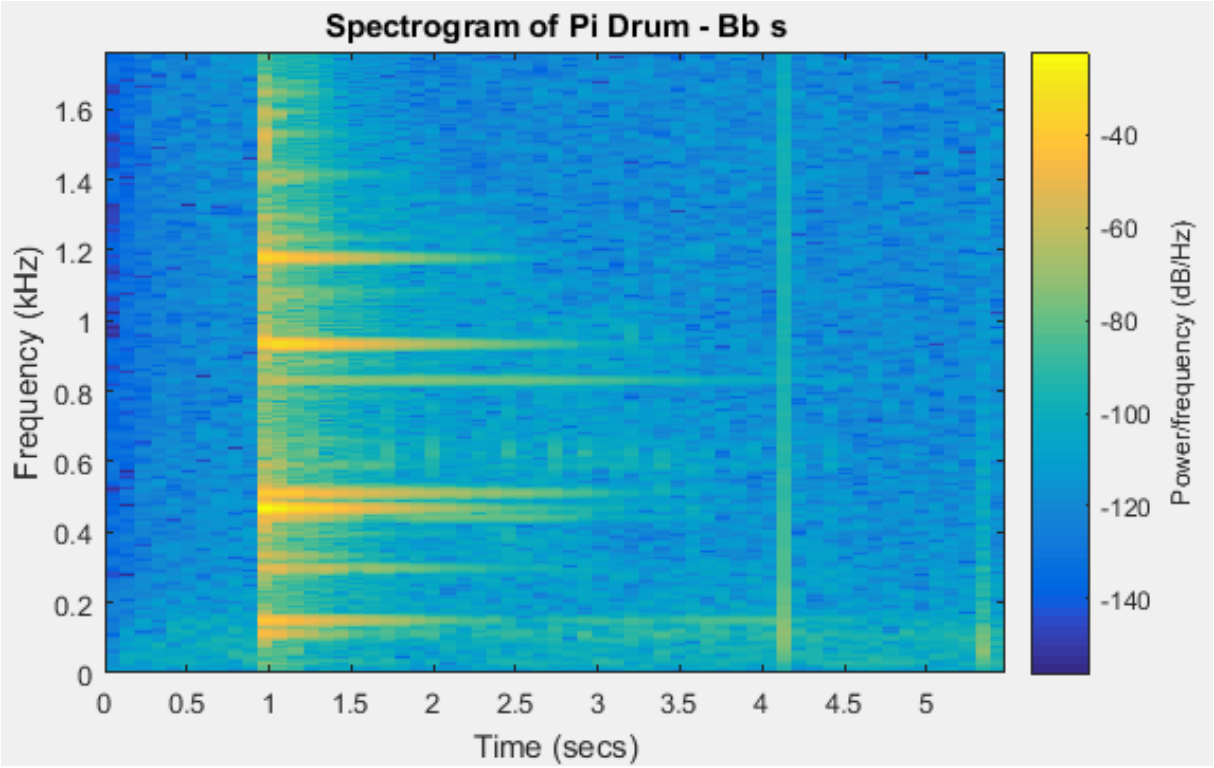

Figure 39: Pi Drum - Bb4 Spectrogram – Stand

11.2.3.7C5

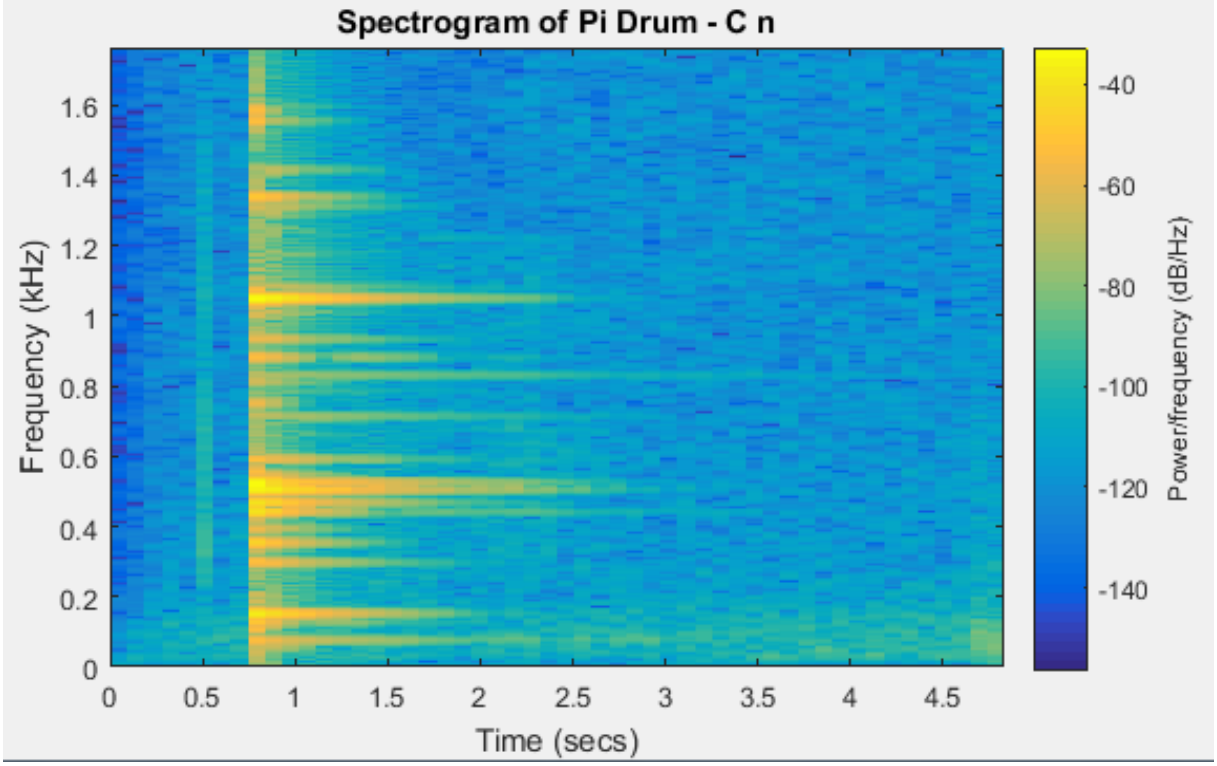

Figure 42: Pi Drum – C5 Spectrogram – No Stand

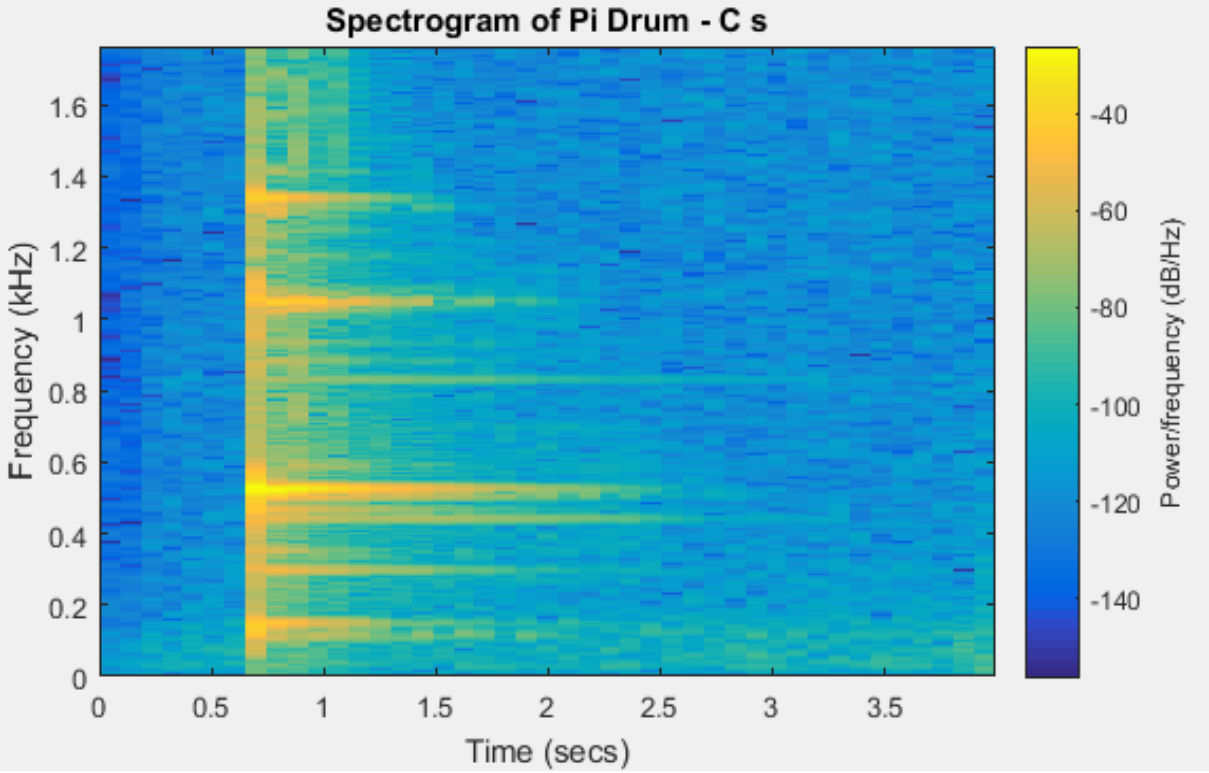

Figure 41: Pi Drum - C5 Spectrogram – Stand

11.2.3.8D5

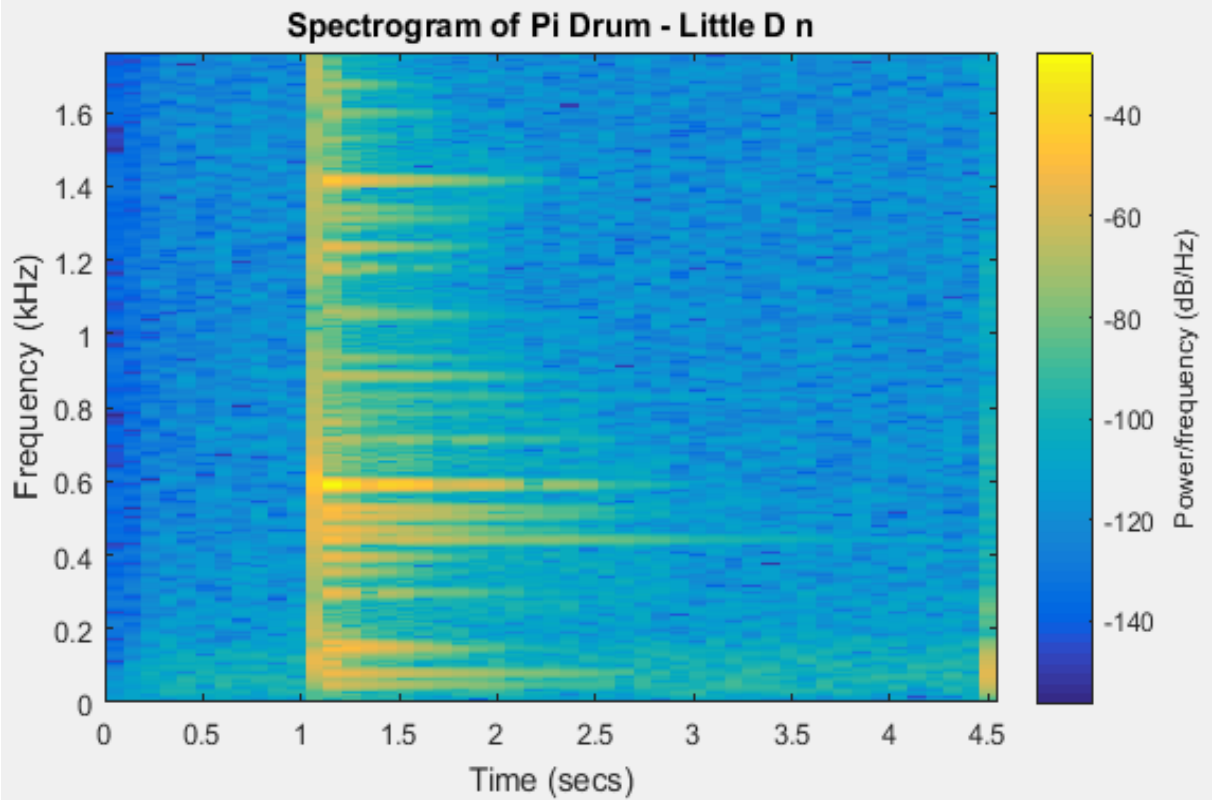

Figure 43: Pi Drum – D5 Spectrogram – No Stand

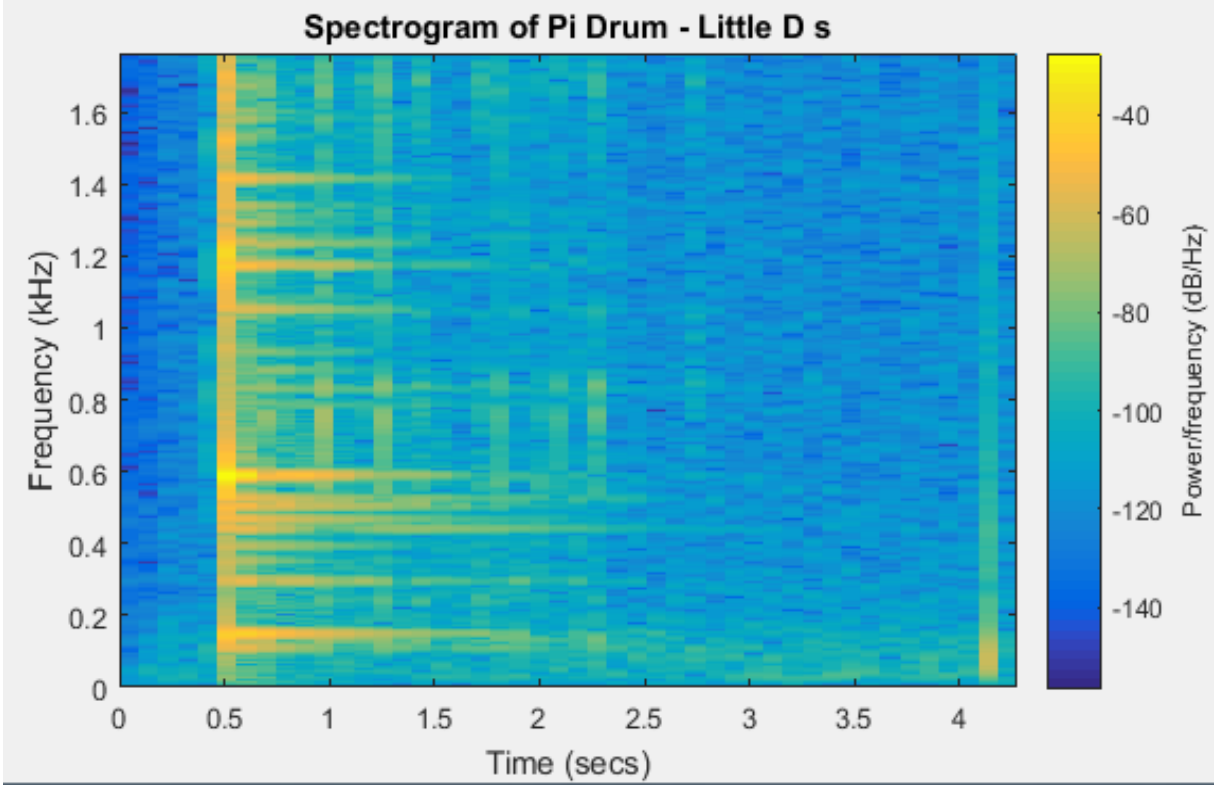

Figure 44: Pi Drum – D5 Spectrogram – Stand

11.2.4 Meridian Spectrograms

11.2.4.1 G3

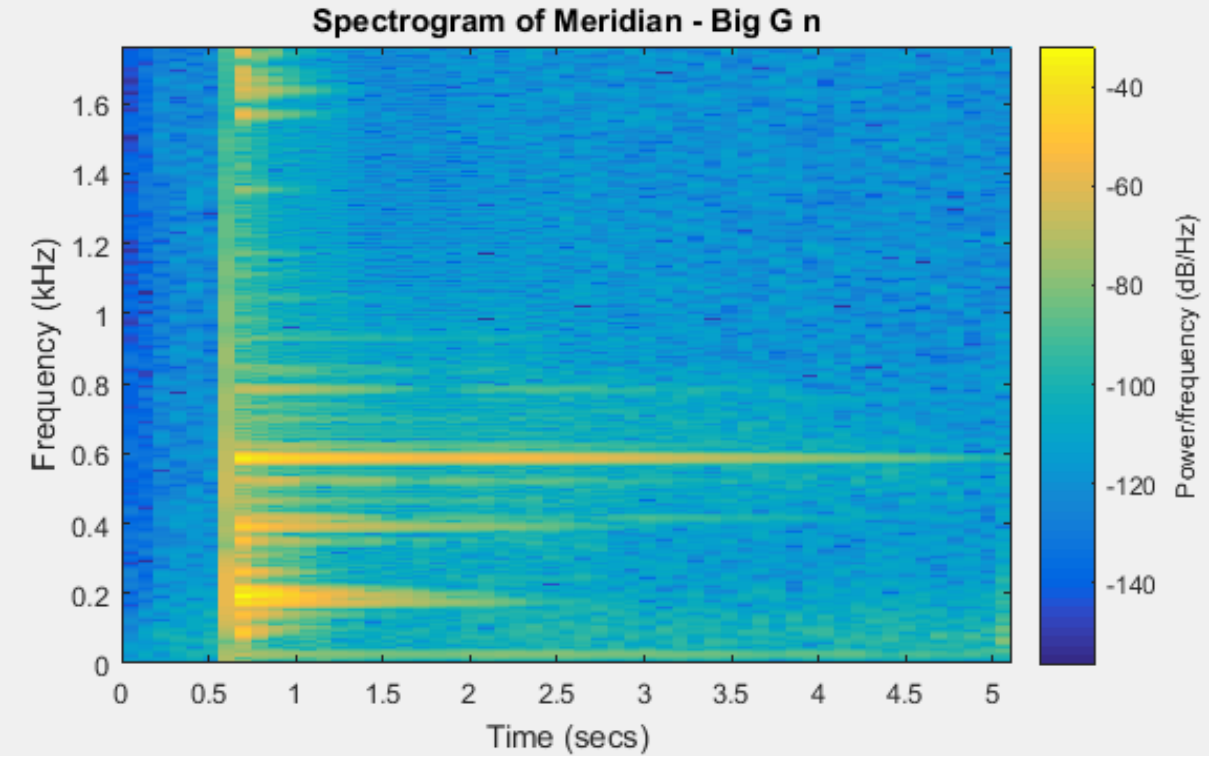

Figure 46: Meridian – G3 Spectrogram – No Stand

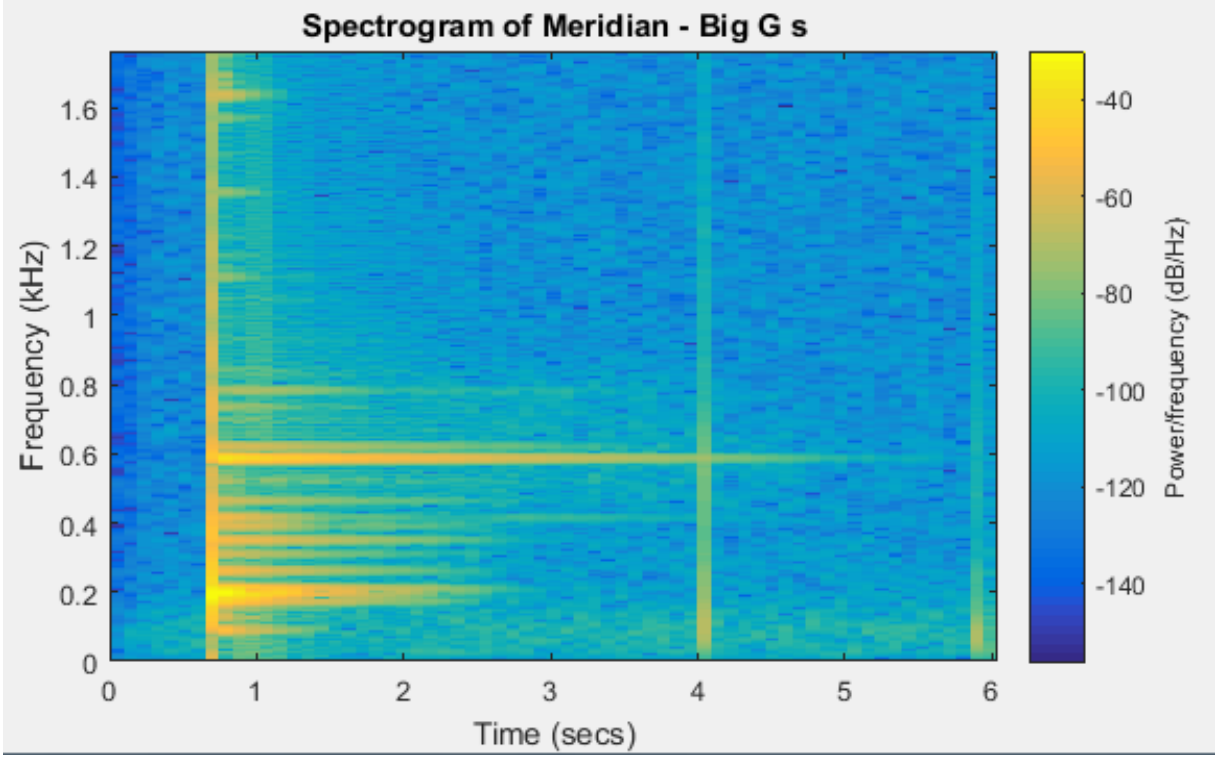

Figure 45: Meridian – G3 Spectrogram – Stand

11.2.4.2Ab3

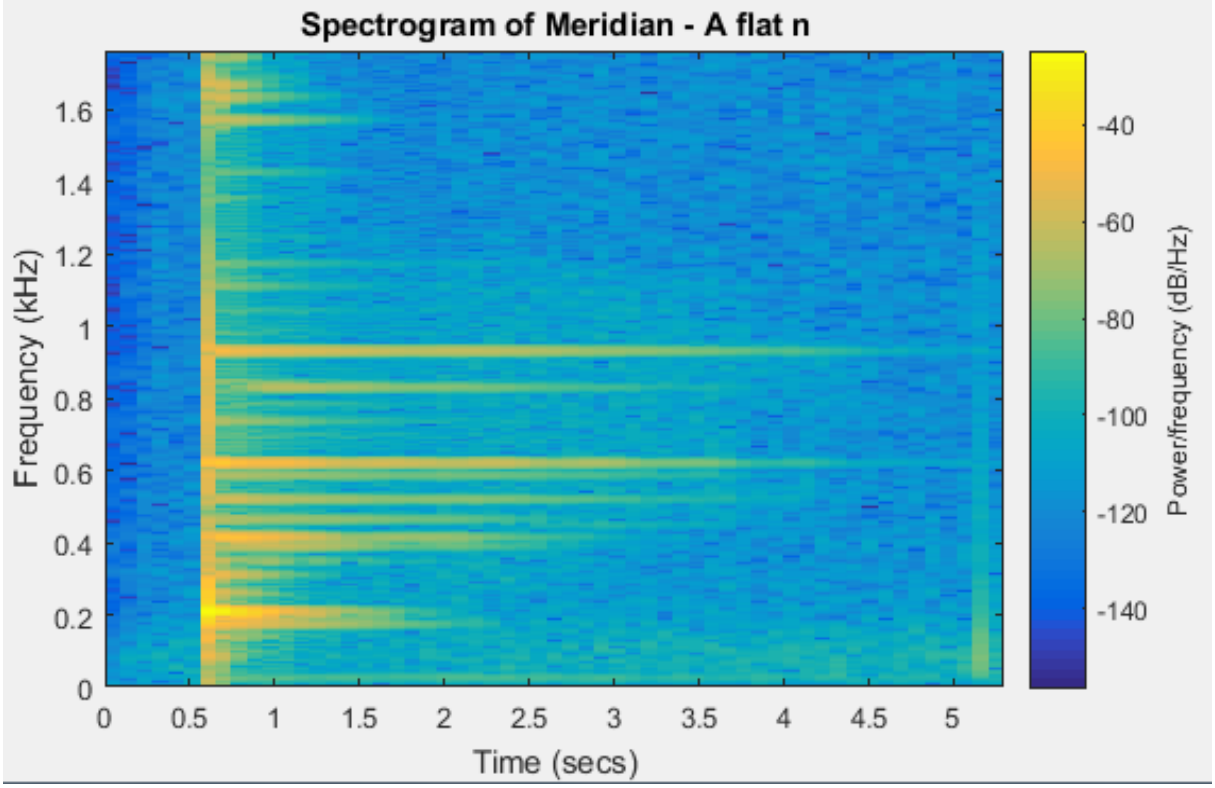

Figure 47: Meridian – Ab3 Spectrogram – No Stand

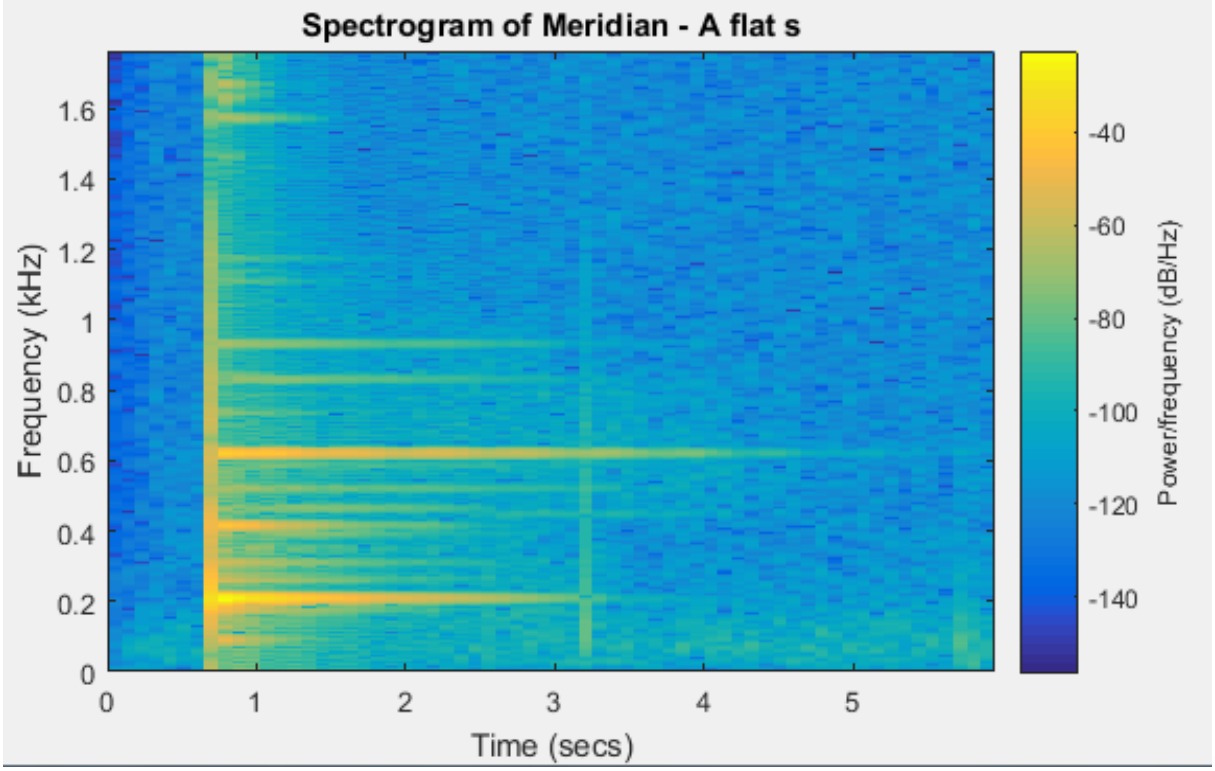

Figure 48: Meridian – Ab3 Spectrogram – Stand

11.2.4.3C4

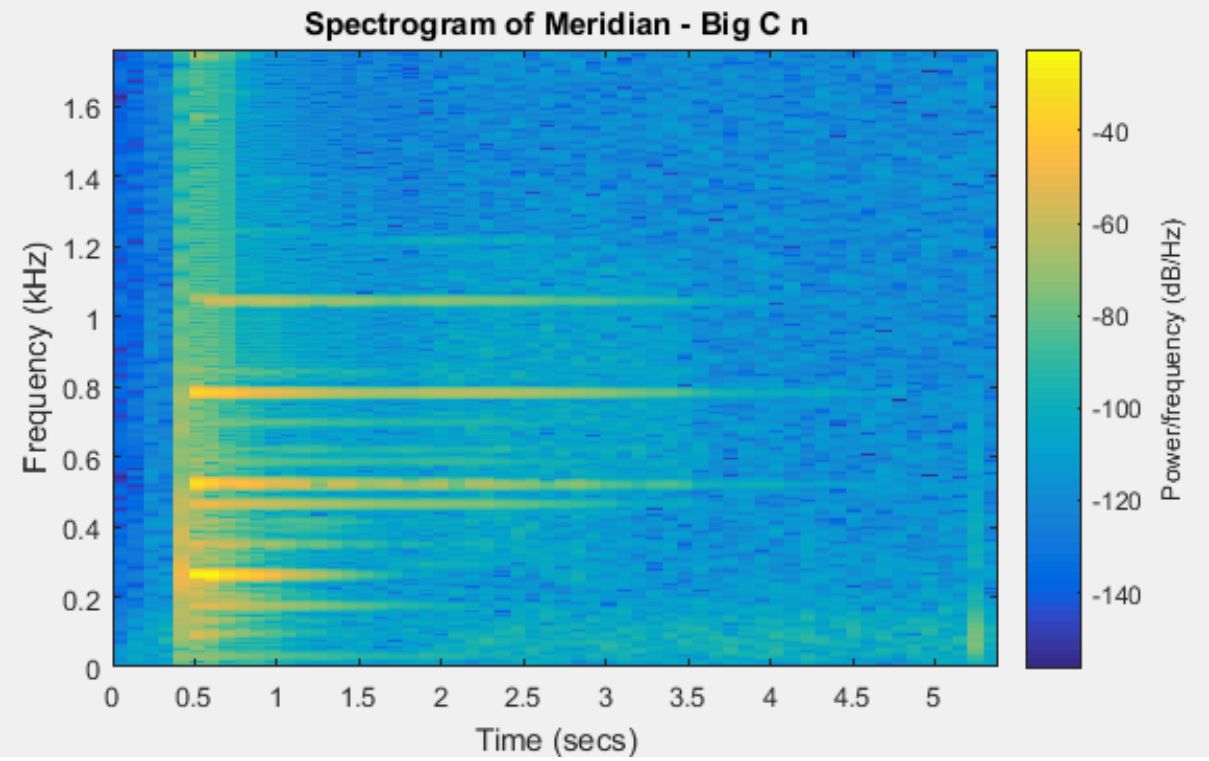

Figure 49: Meridian – C4 Spectrogram – No Stand

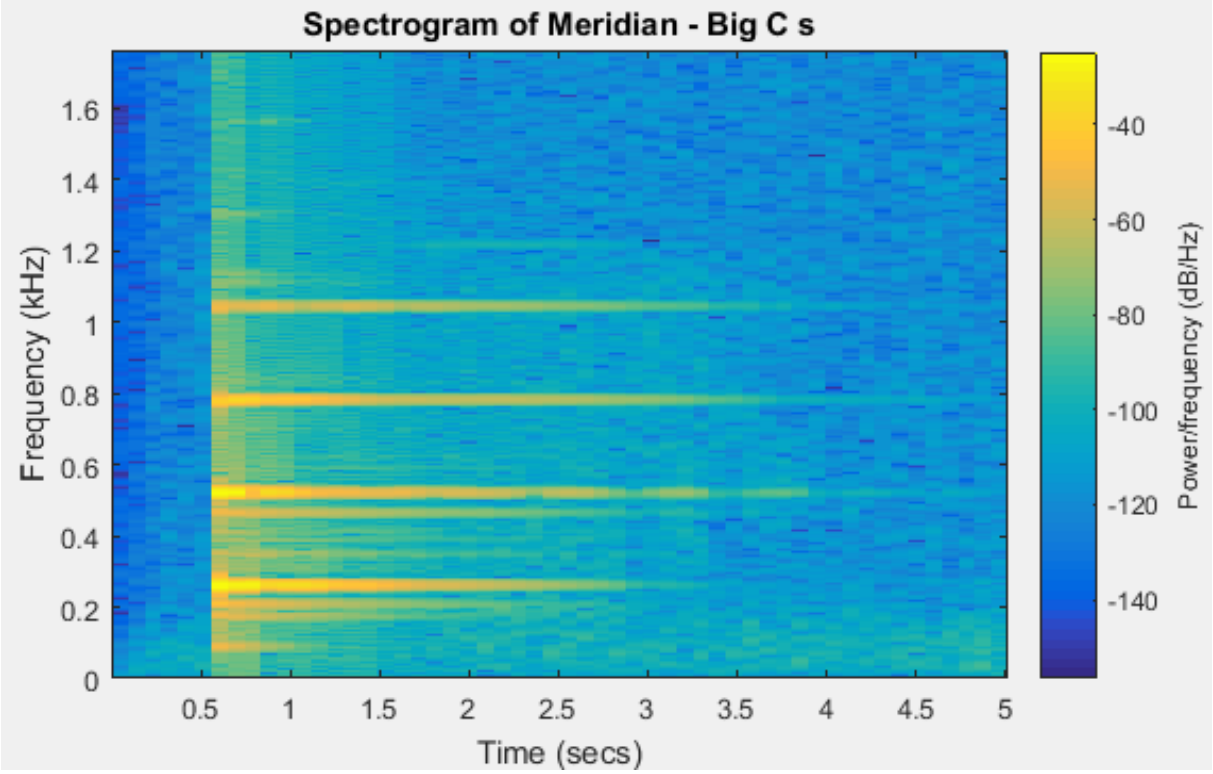

Figure 50: Meridian – C4 Spectrogram – Stand

11.2.4.4Eb4

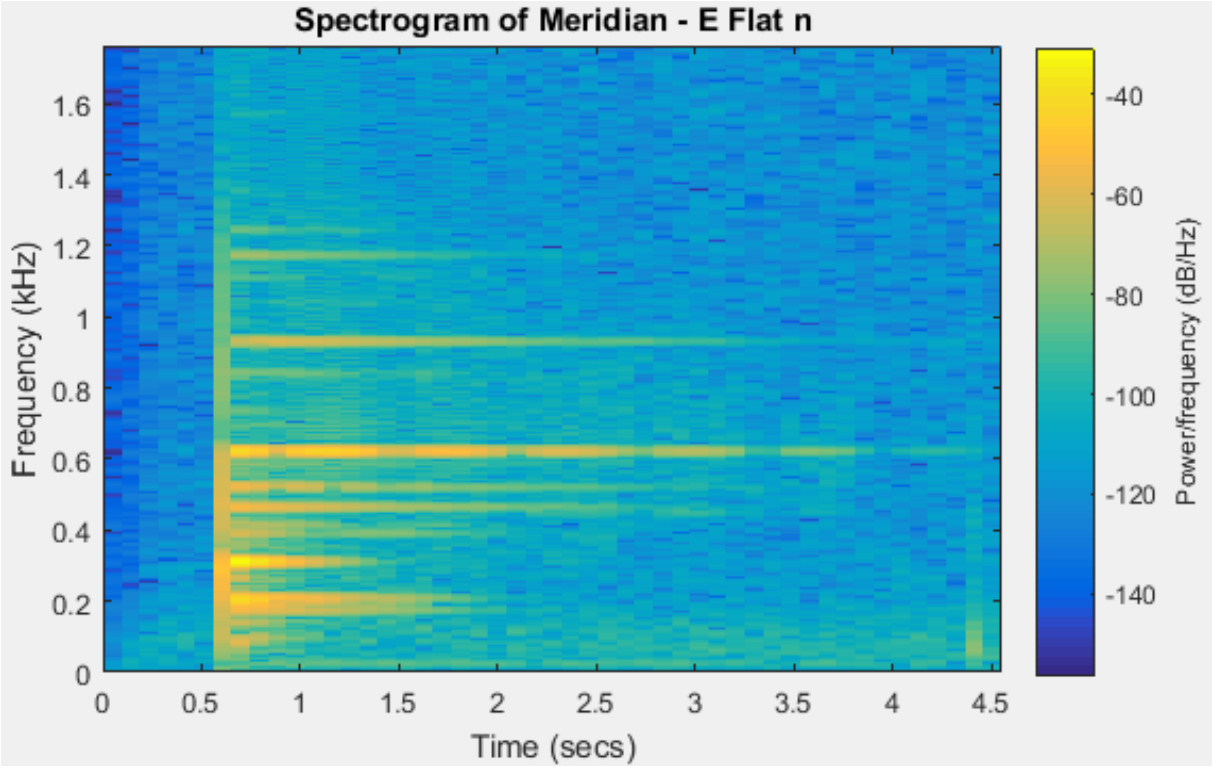

Figure 51: Meridian – Eb4 Spectrogram – No Stand

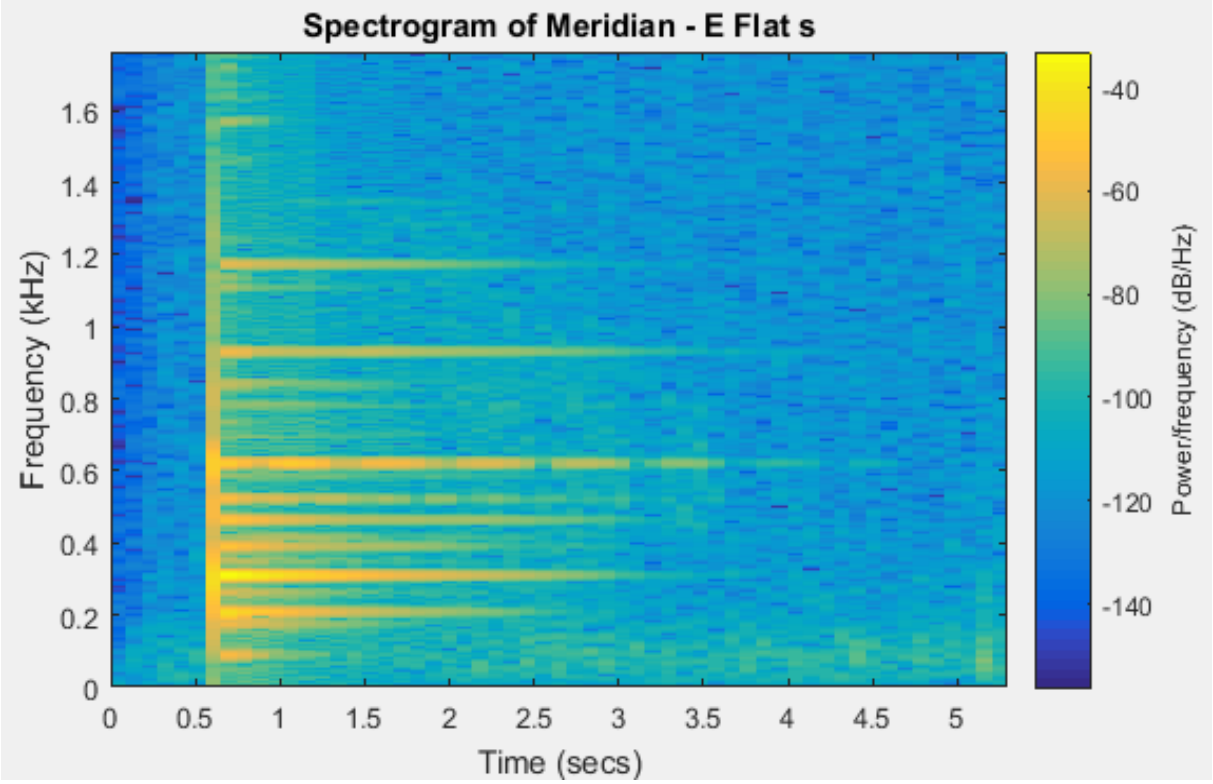

Figure 52: Meridian – Eb4 Spectrogram – No Stand

11.2.4.5F4

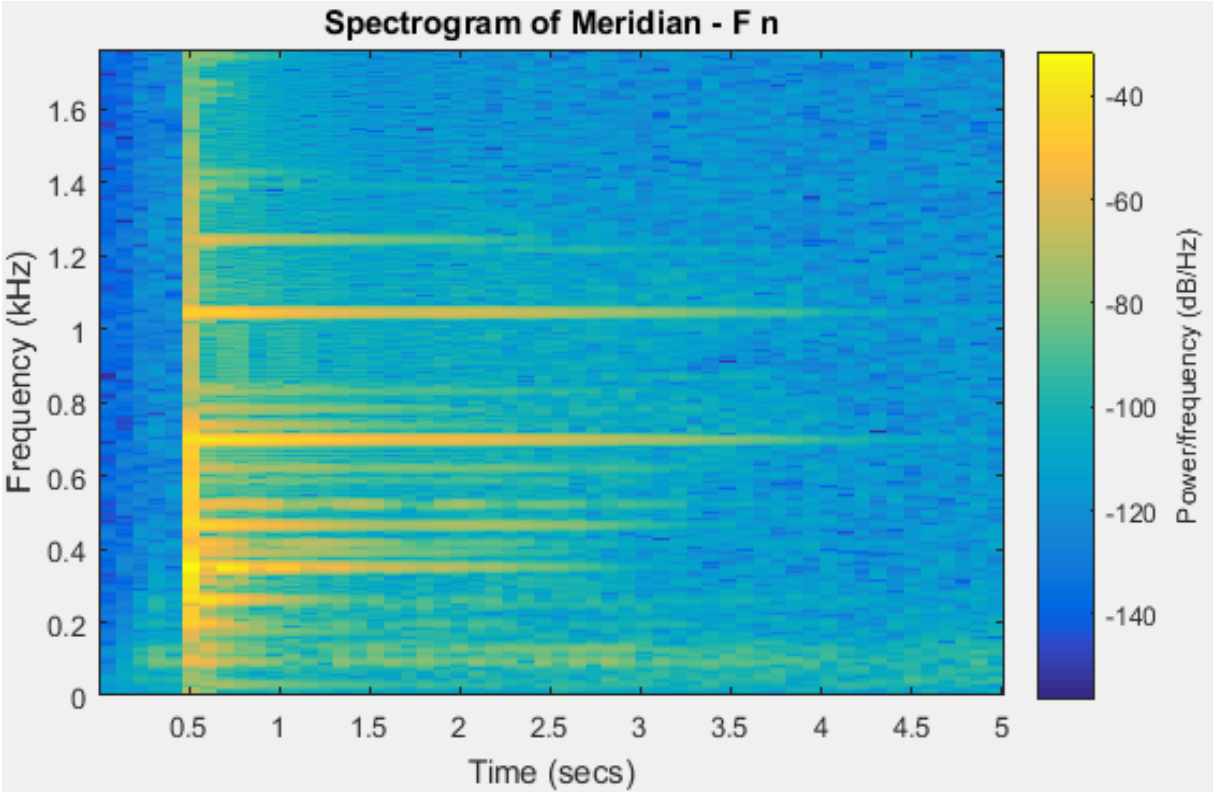

Figure 53: Meridian – F4 Spectrogram – No Stand

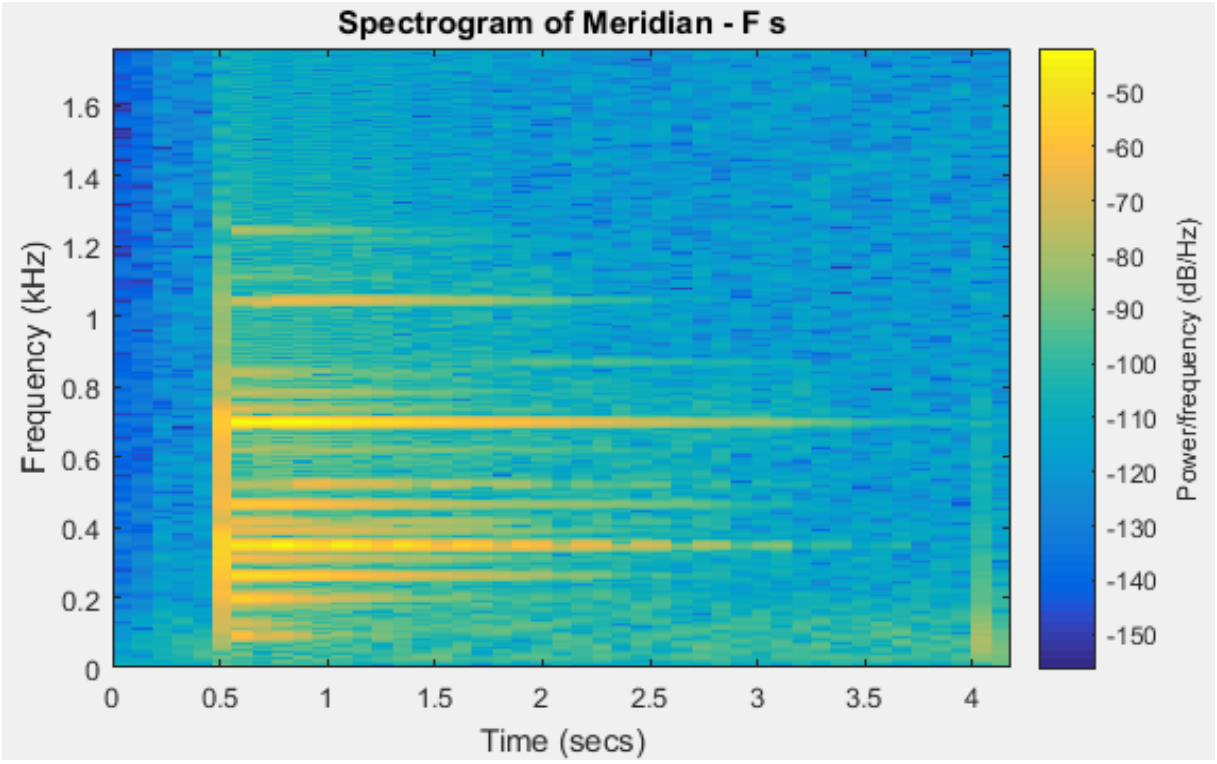

Figure 54: Meridian – F4 Spectrogram – Stand

11.2.4.6G4

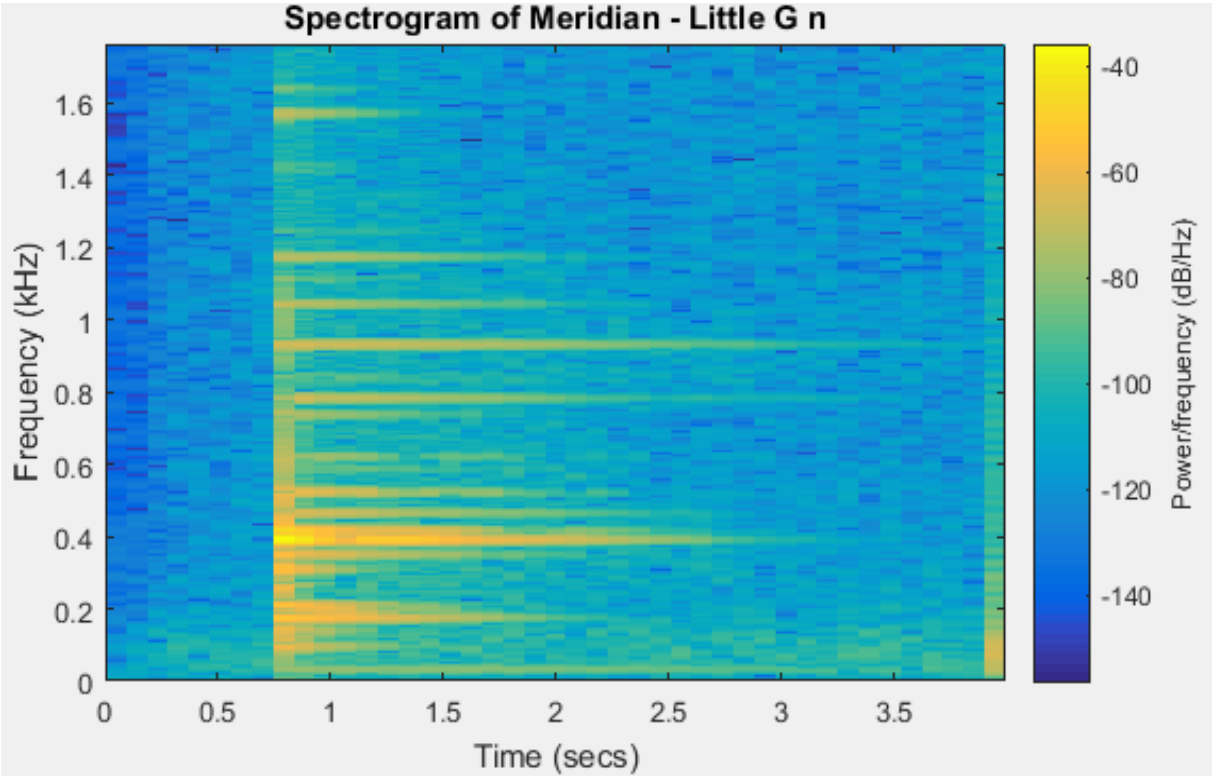

Figure 55: Meridian – G4 Spectrogram – No Stand

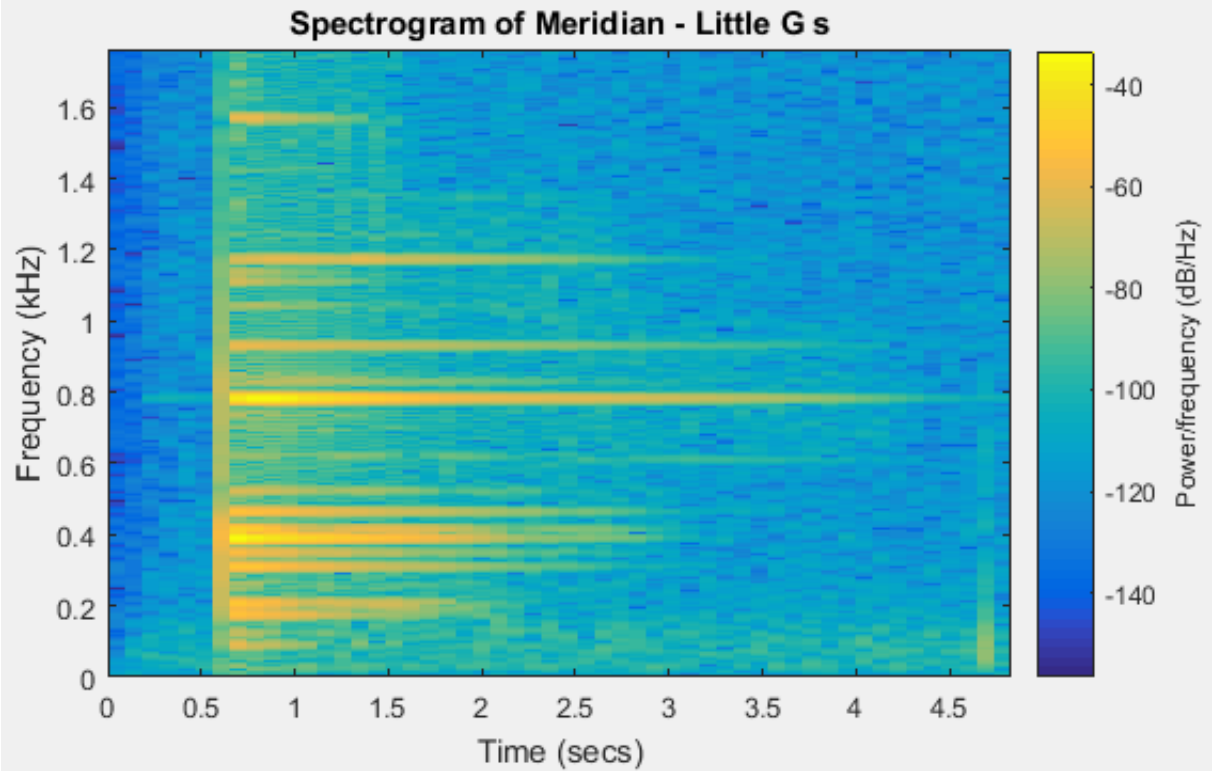

Figure 56: Meridian – G4 Spectrogram – Stand

11.2.4.7Bb4

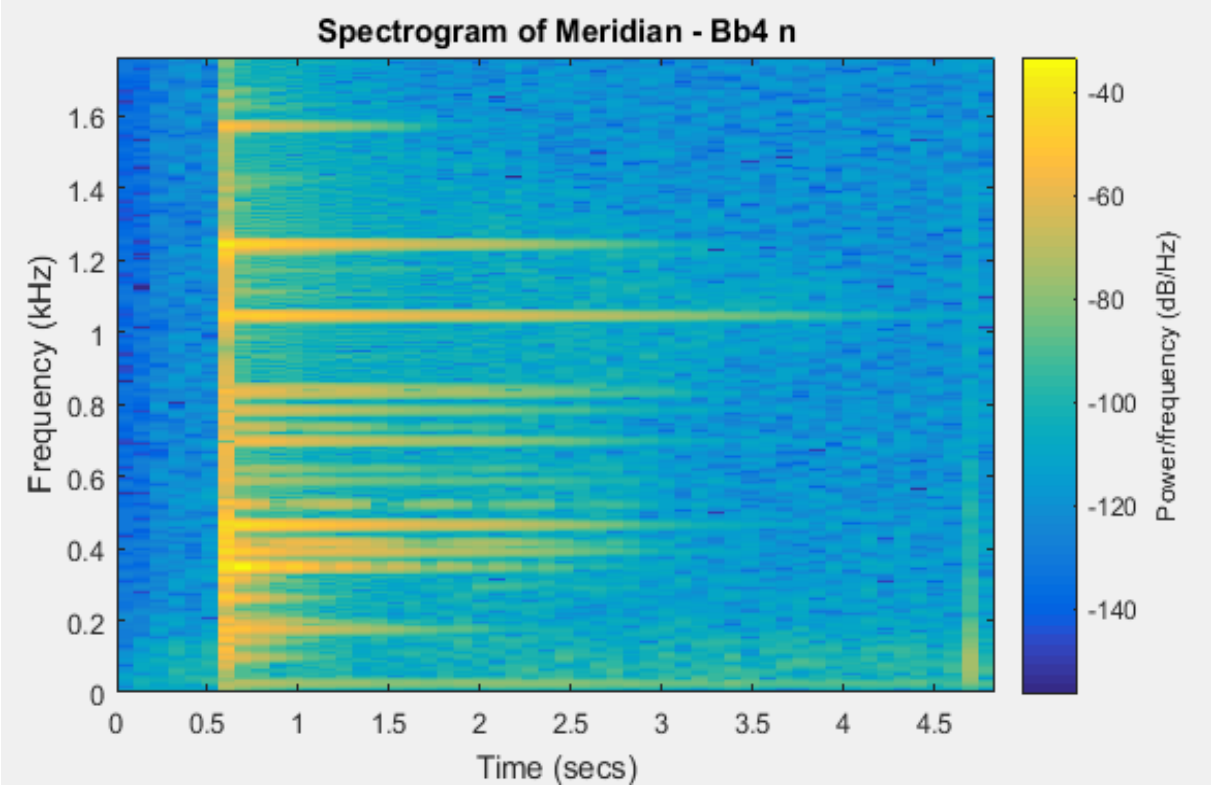

Figure 57: Meridian – Bb4 Spectrogram – No Stand

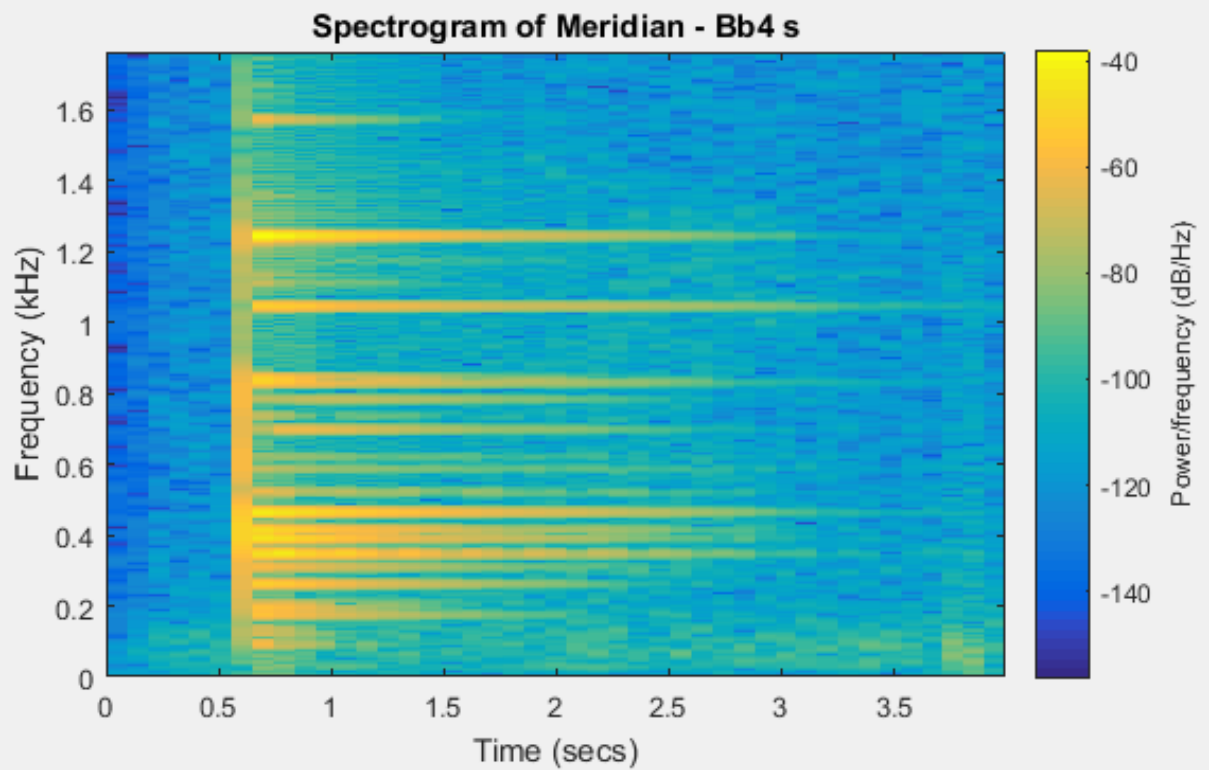

Figure 58: Meridian – Bb4 Spectrogram – Stand

11.2.4.8C5

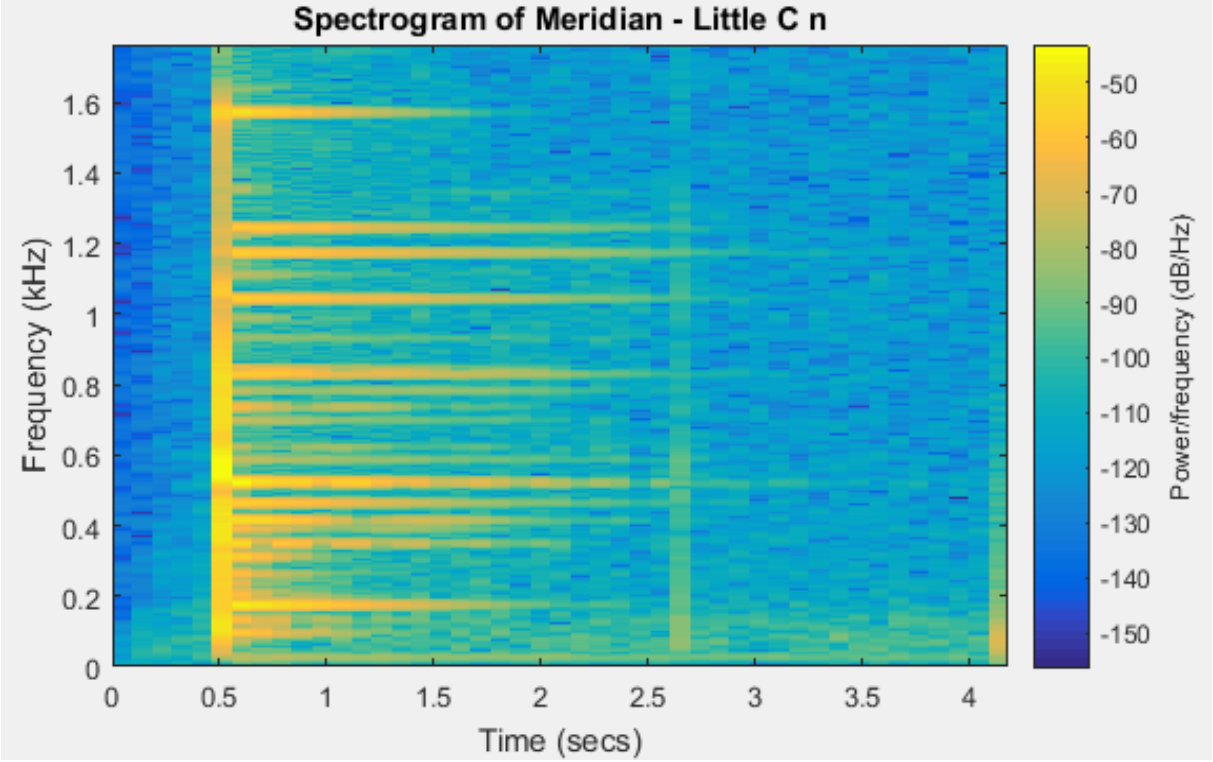

Figure 59: Meridian – C5 Spectrogram – No Stand

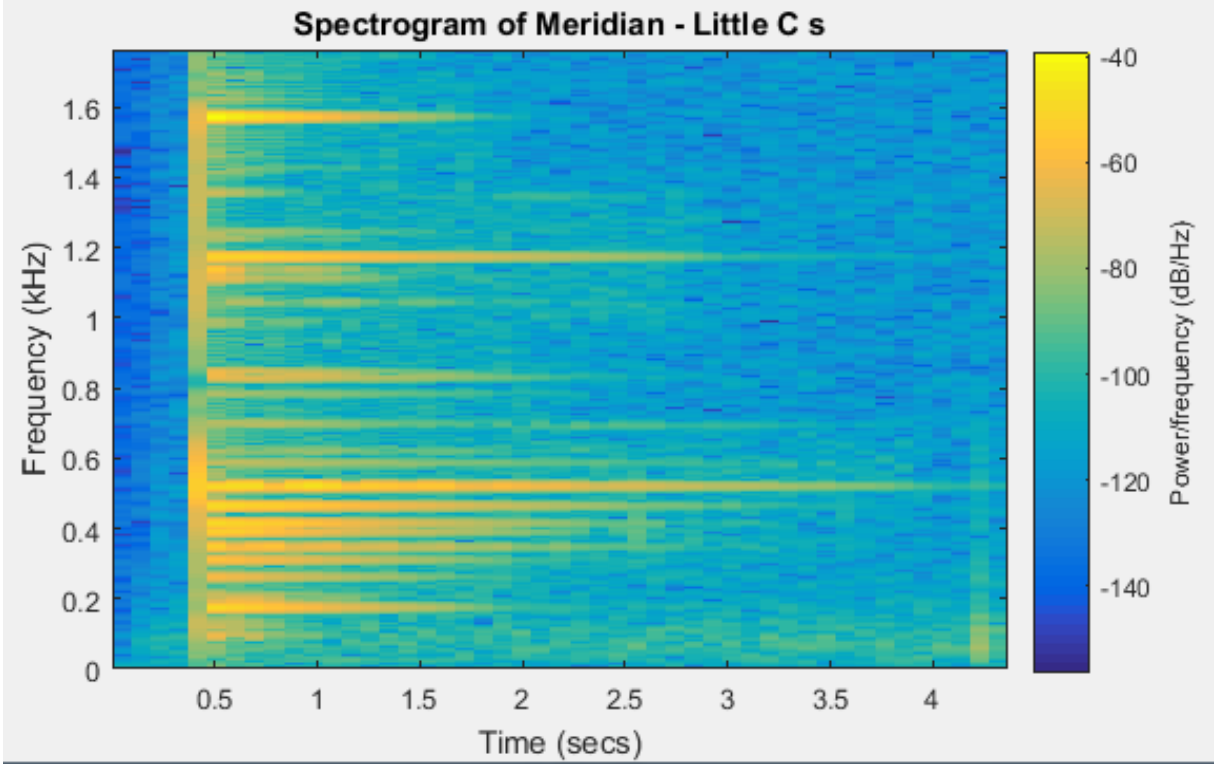

Figure 60: Meridian – C5 Spectrogram – Stand

11.3 Appendix C

Modelling methods described here were used to create the CAD model of the Pi Drum instrument used in the report. This method works for instruments that can be divided equally into parts that contain a single note and has high relevance to all other handpan designs.

1. Divide instrument into equal sections with one note in each section. If equal sections cannot contain a single note, make the divisions unequal. If equal sized sections can be used the following describes how to create an easily customised note. This is the same as Figure 11.
2. Create a sketch of the profile of one half of the instrument if cut through an axis of symmetry. Do this in two parts; a sketch of the top and bottom shells of the instrument (Figure 61 and Figure 62).

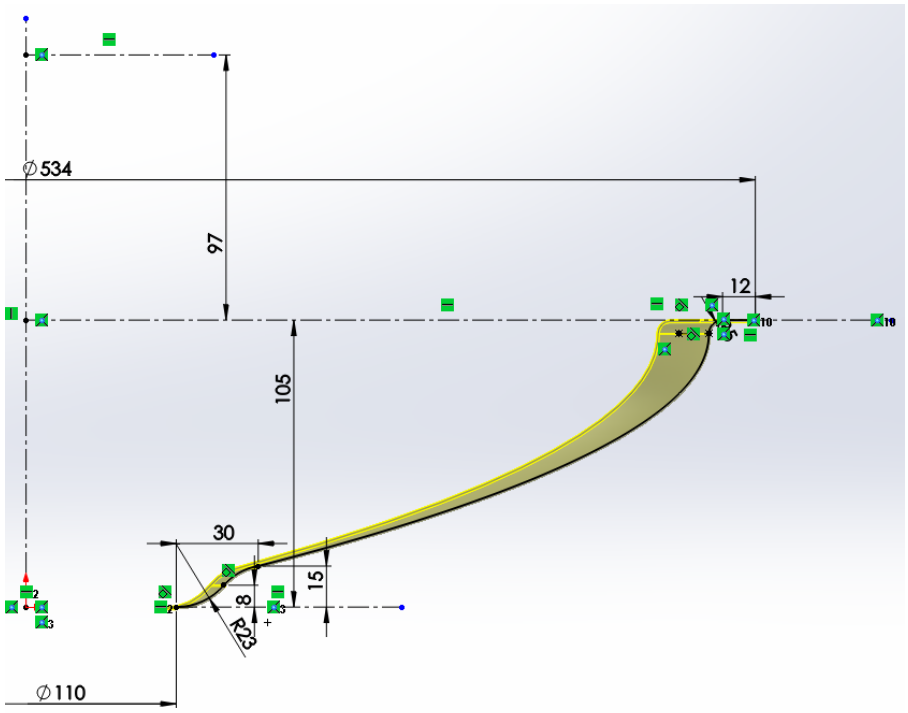

Figure 61: Shell Sketch Bottom

3. Extrude the sketches in equal amounts from the plane they lie on.

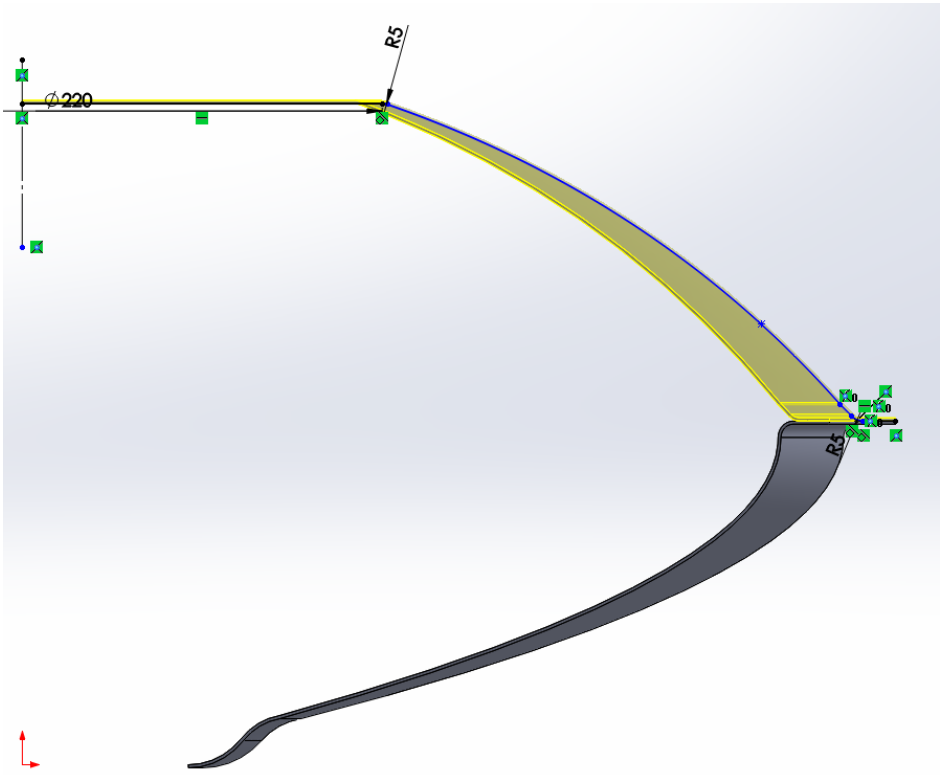

Figure 62: Shell Sketch Top

4. Create a die/boss in the shape of the note you want (Figure 64).

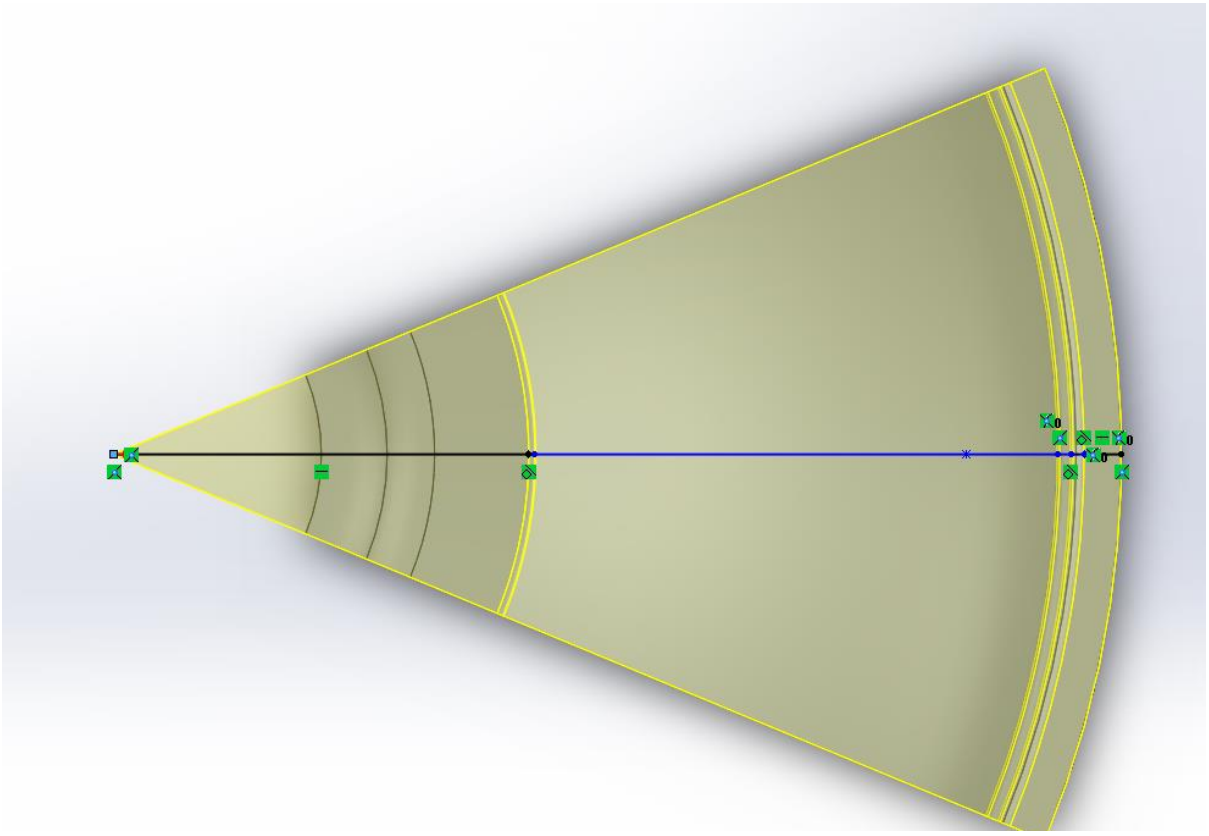

Figure 63: Two Way Revolve

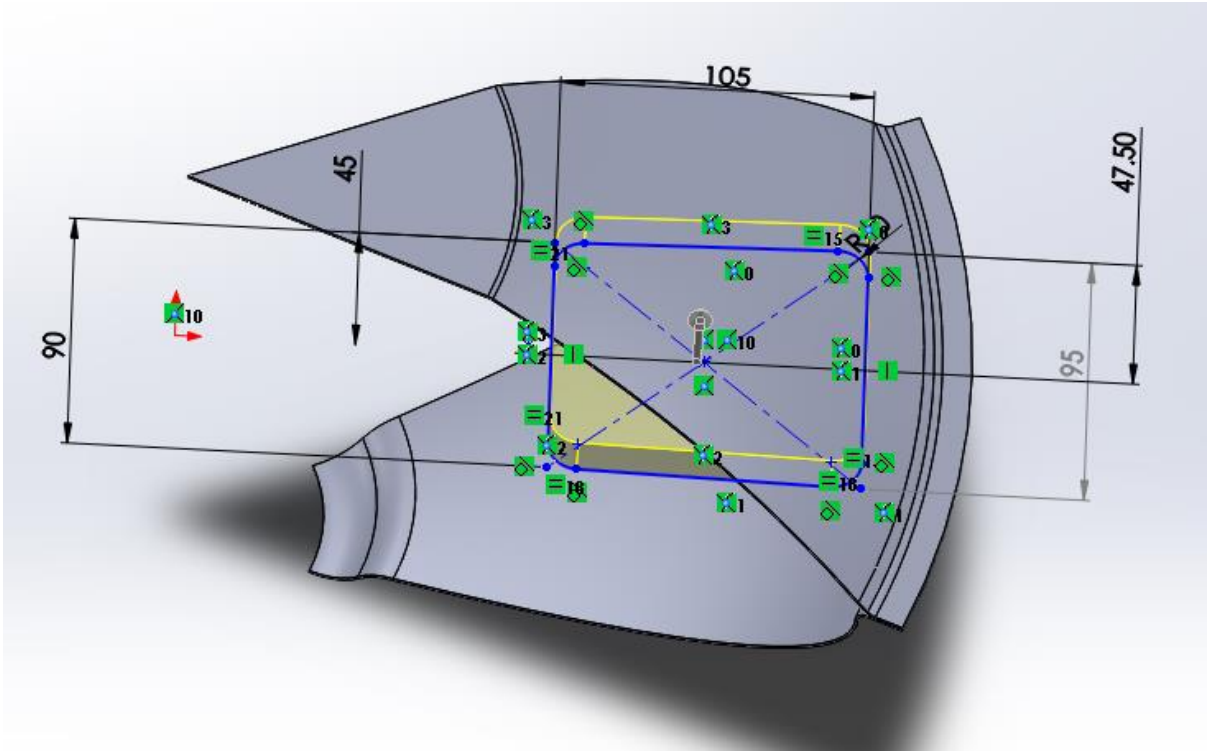

Figure 64: Die

5. Use the deform feature and the die/boss to push from the inside of the note out to create the edges and corners of the note (Figure 65).

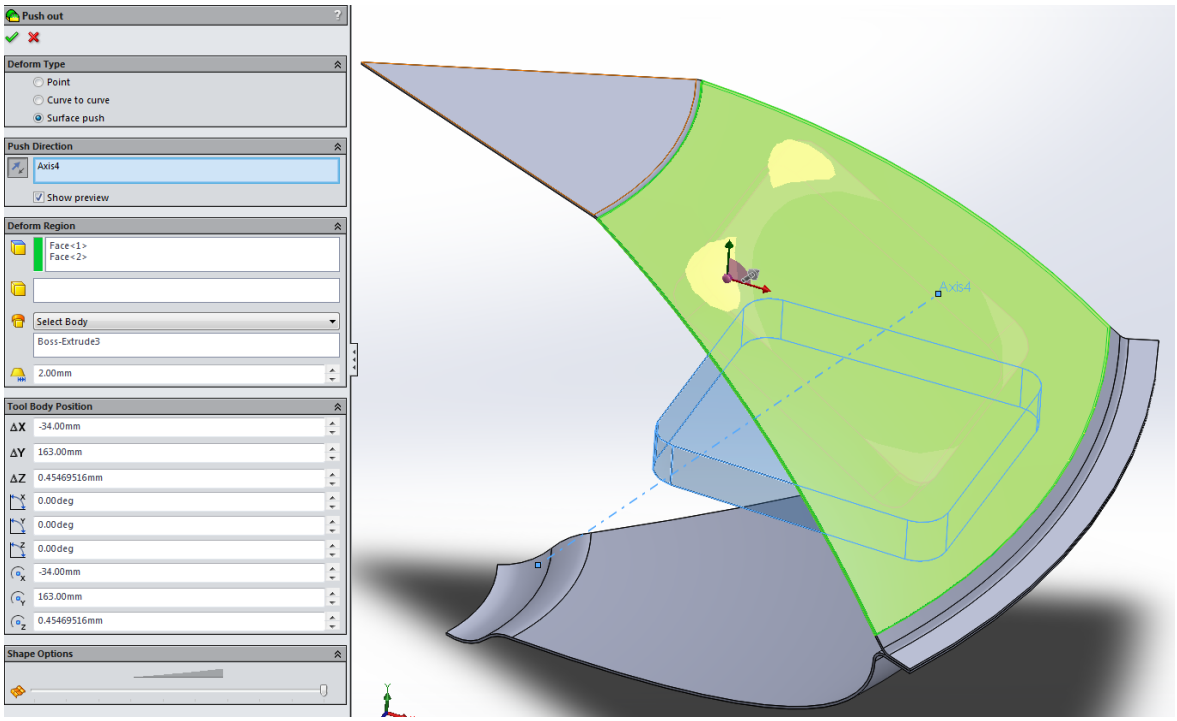

Figure 65: Die Push

6. Use the deform feature to push the remaining curved surface on the note from the outside in using a created rectangle within the feature (Figure 66).

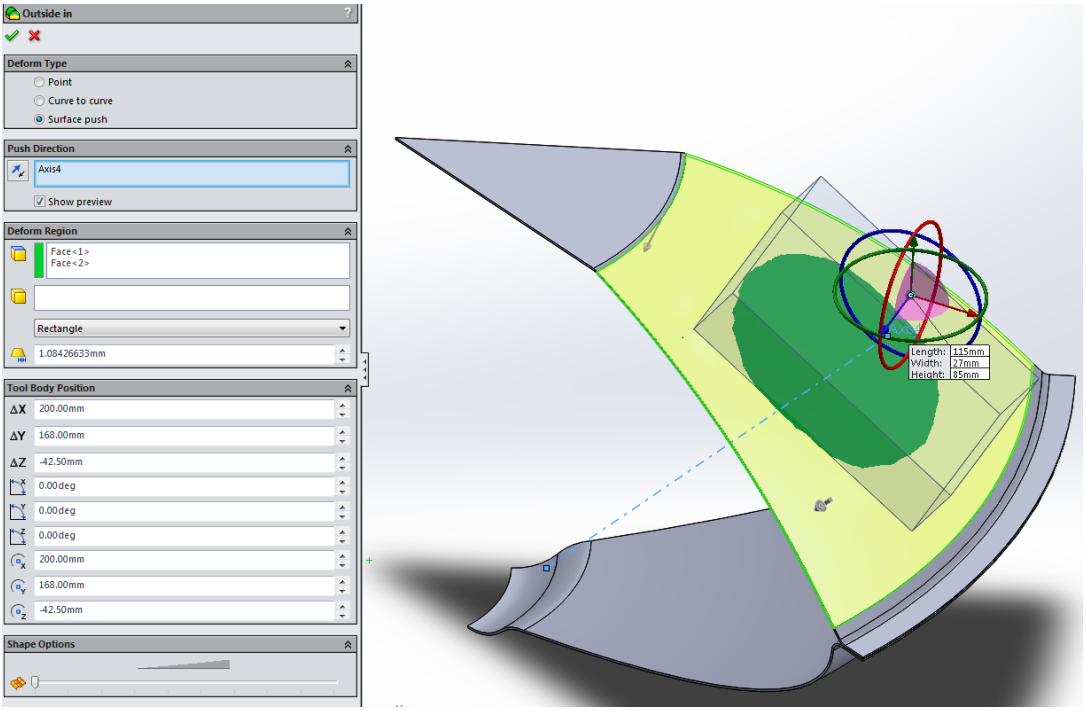

Figure 66: Flattening Die

7. Use the deform feature to create the indent on the note surface. This is done by creating an ellipsoid and pushing it into the note (Figure 67).
8. Create a set of construction lines that follow the edges on the slice in a plane perpendicular to the axis is symmetry at the slice tip (Figure 68).
9. Create all notes needed by changing dimensions in steps 4-7.
10. Assemble notes in order. This step can be challenging as solid works does not like closing a circle. The purpose of the construction lines created on the edge earlier is to provide a datum for assembly. The author used the axis of symmetry at the tip of the notes and the construction line to fully constrain the assembly. This only works if the construction lines are in the same plane, which they will be if the note created is edited using only steps 4-7.

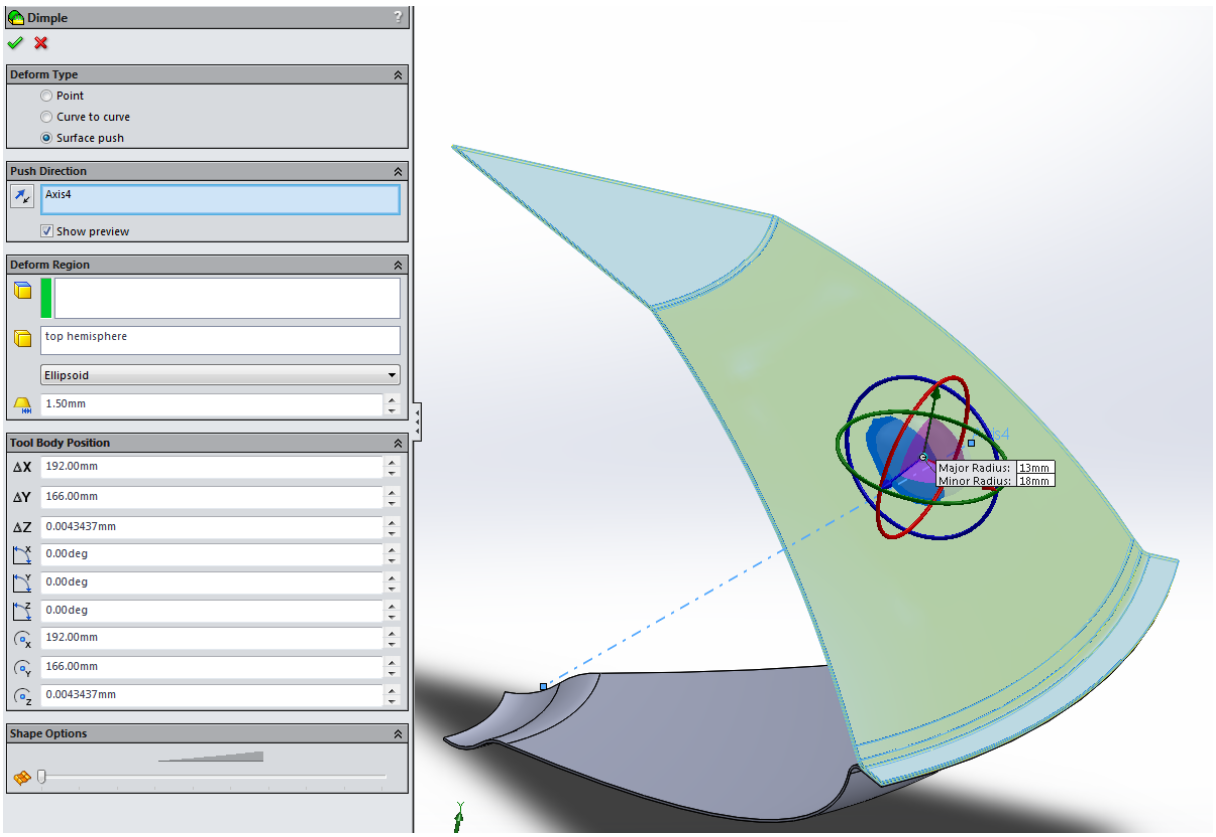

Figure 67: Dimple Indent

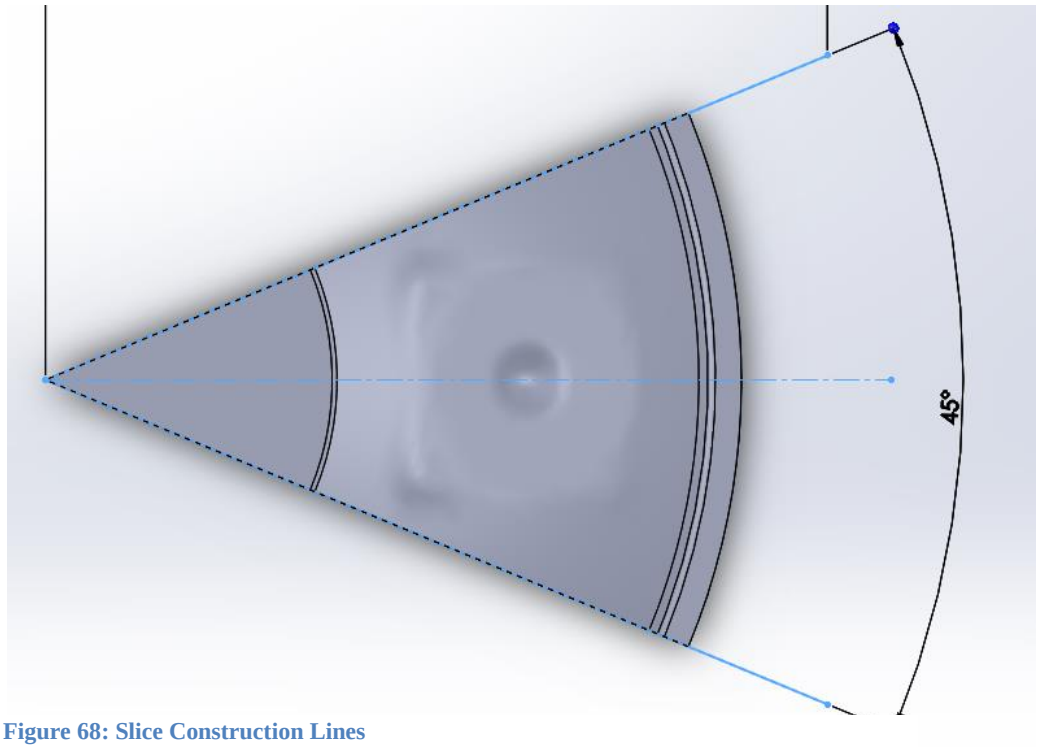

Figure 68: Slice Construction Lines

A brief note. When using the deform feature make sure that faces on both sides of the material you wish to deform are selected. If they are not, the program will deform only one face and add or remove material in the space between the other face, which won't be moved. ANSYS cannot create a shell element on a geometry with sharp changes from a curve to a flat surface. This means you must create appropriate transitions in the geometry when making the sketch of the profile.

11.4 Appendix D

11.4.1 Modal Analysis Method

1. Import geometry into ANSYS as a .STEP file and suppress any body that is not part of the instrument shell.
2. Open Workbench Mechanical and you should have the view shown in Figure 69. Not all of the items shown will be present as they have to be inserted. The correct contact region and mesh body sizing and sweep method need to be inserted.

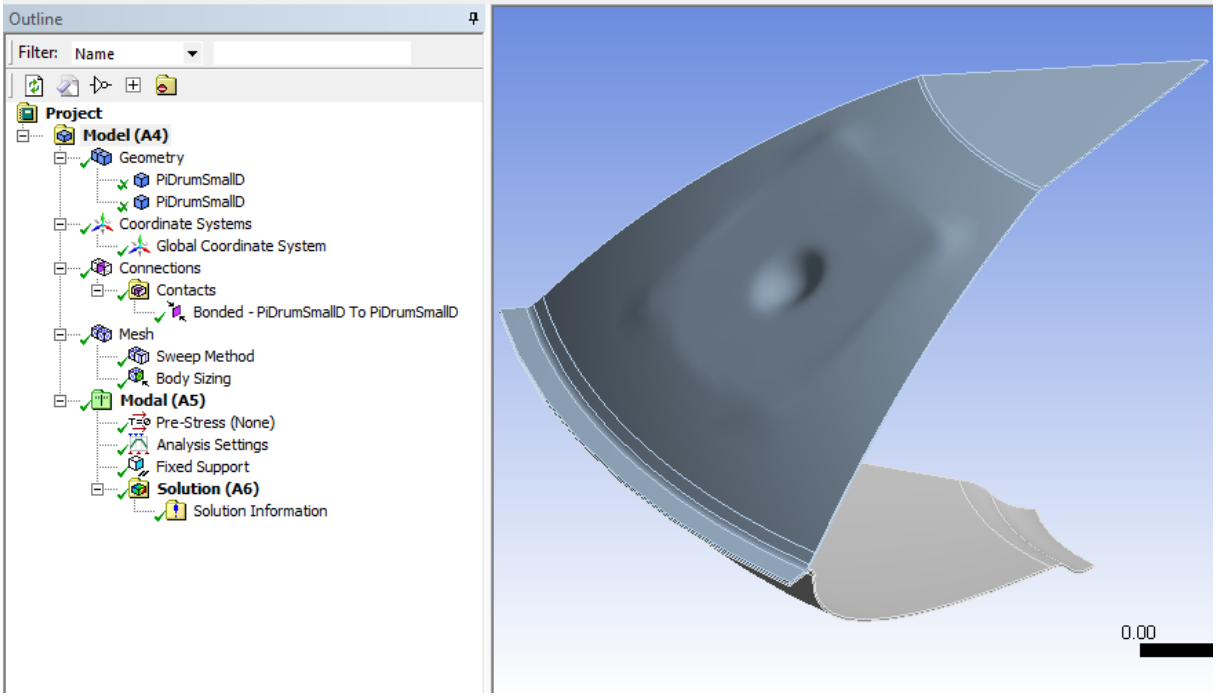

Figure 69: Modal Project Tree Overview

3. The contact region needs to be defined as the contact of the two sections of flat plate on the edge of the two halves of the shell. Figure 71 shows the set up.
4. The geometry sweep method needs to create solid shell elements and the settings needed to achieve this are shown in Figure 70.

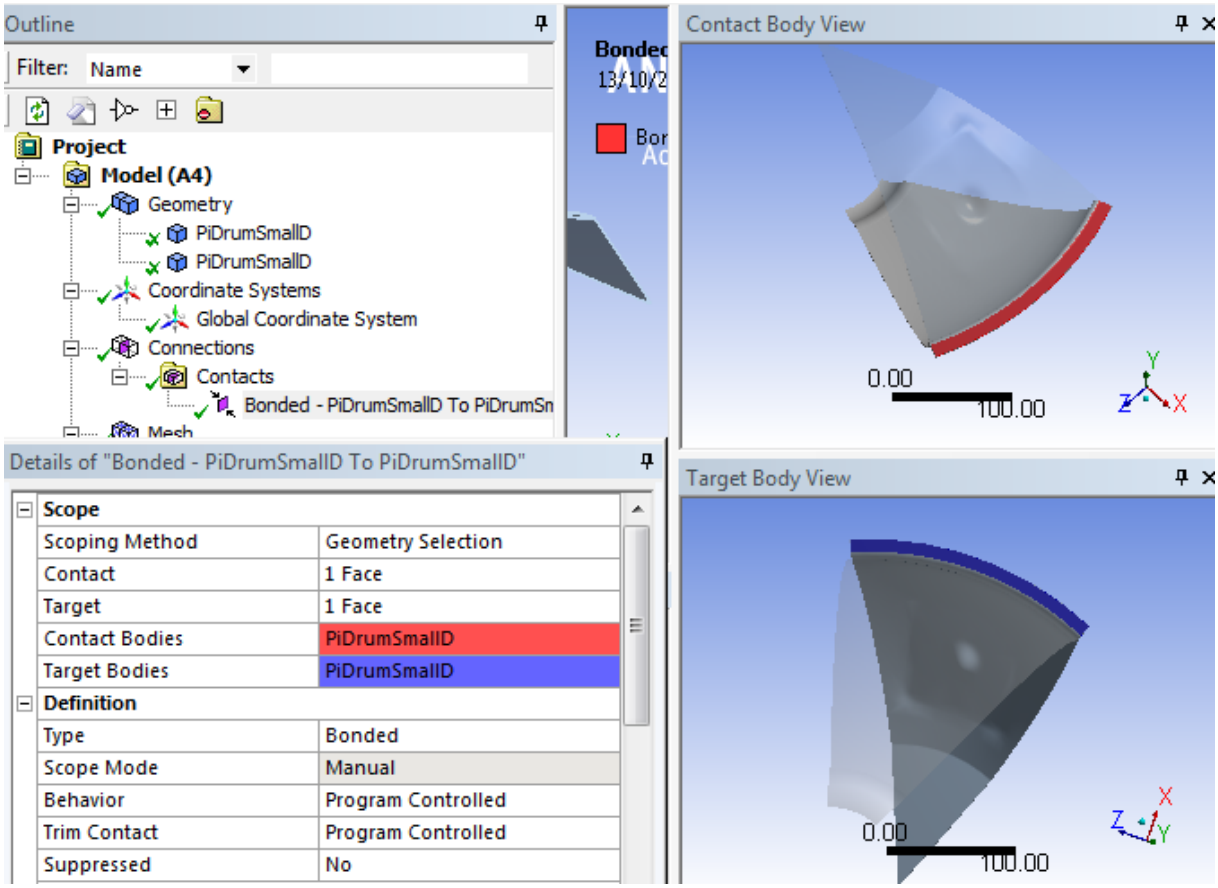

Figure 71: FEA Contact Region Definition

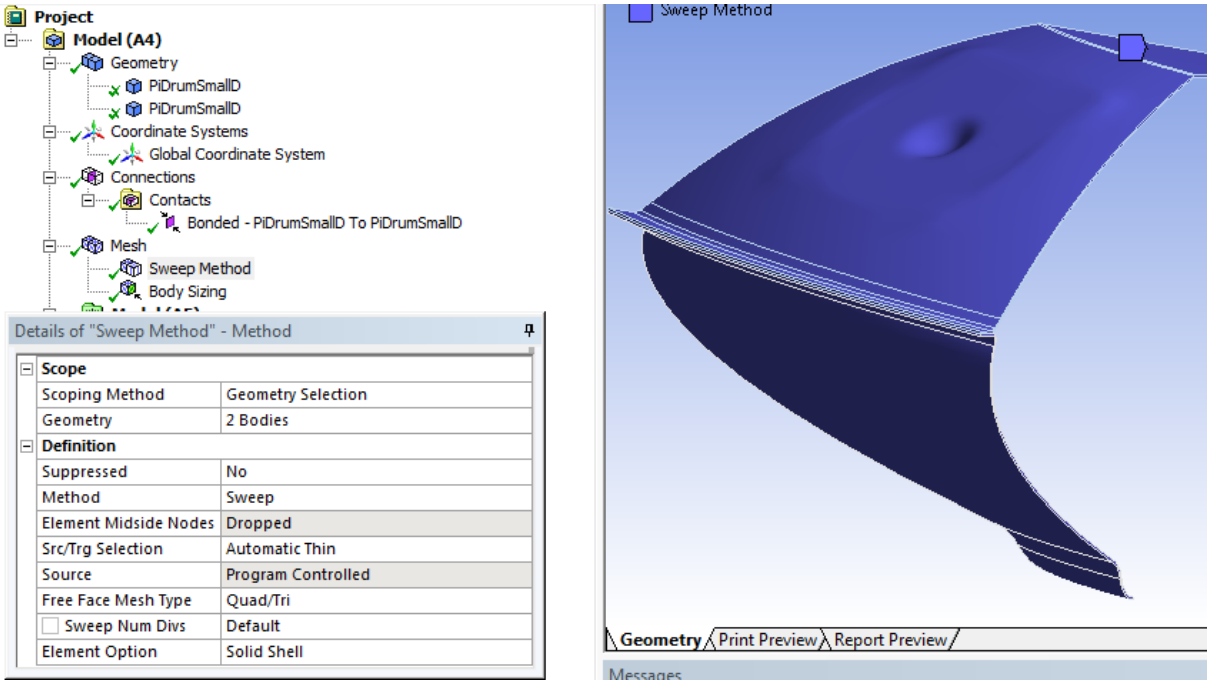

Figure 70: Mesh Sweep Method for Solid Shell Elements

5. Refine the mesh on the body with the note as shown in Figure 72

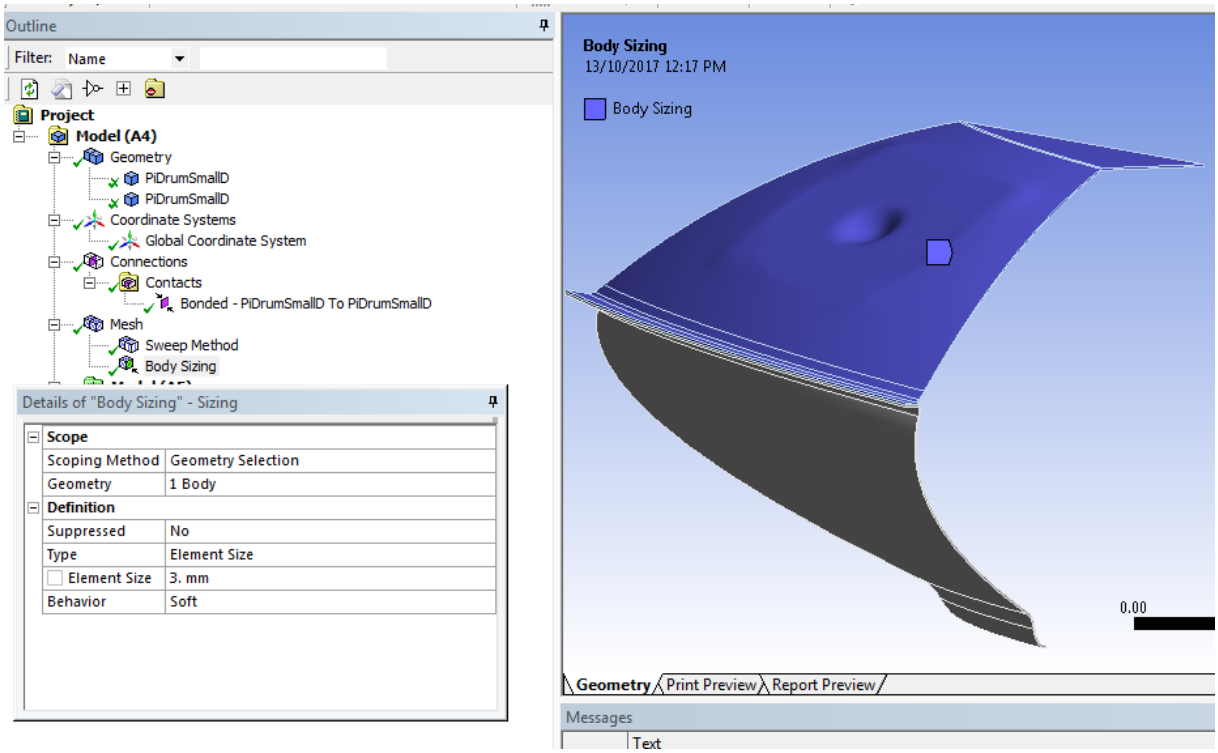

Figure 72: Mesh Refinement

6. Add a fixed support to the surface shown in Figure 73 as well as the edges where the note would be contacting the rest of the instrument (two of these are also shown).

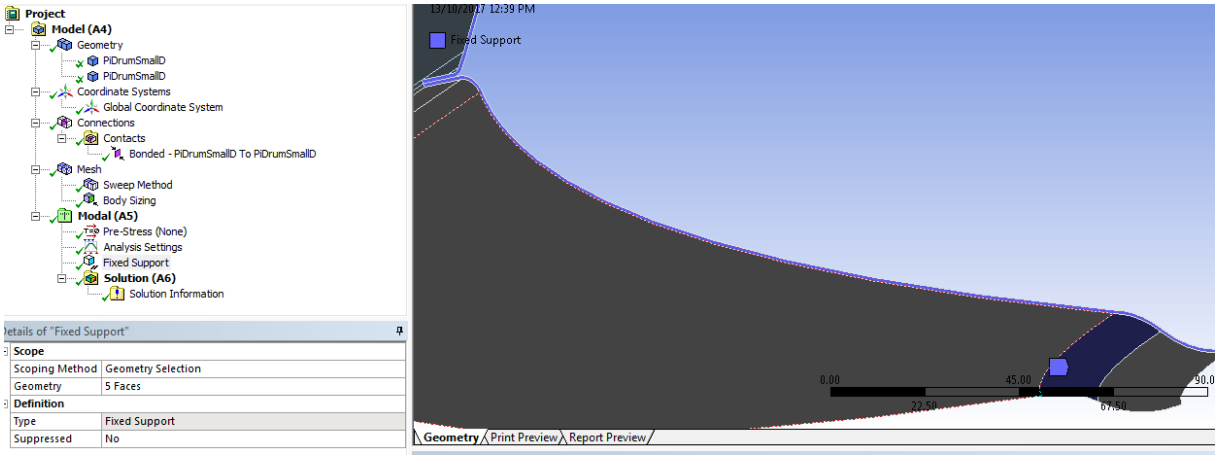

Figure 73: Support for FEA

7. Change Analysis settings to match Figure 74.

8. Results can be viewed by inserting total deformation to see the mode shape and selecting the desired mode. Figure 75 shows this.

Details of "Analysis Settings"

Options	
Max Modes to Find	6
Limit Search to Range	No
Solver Controls	
Damped	Yes
Solver Type	Program Controlled
Rotordynamics Controls	
Coriolis Effect	Off
Campbell Diagram	Off
Output Controls	
Stress	No
Strain	No
Nodal Forces	No
Calculate Reactions	No
General Miscellaneous	No

Figure 74: Analysis Settings

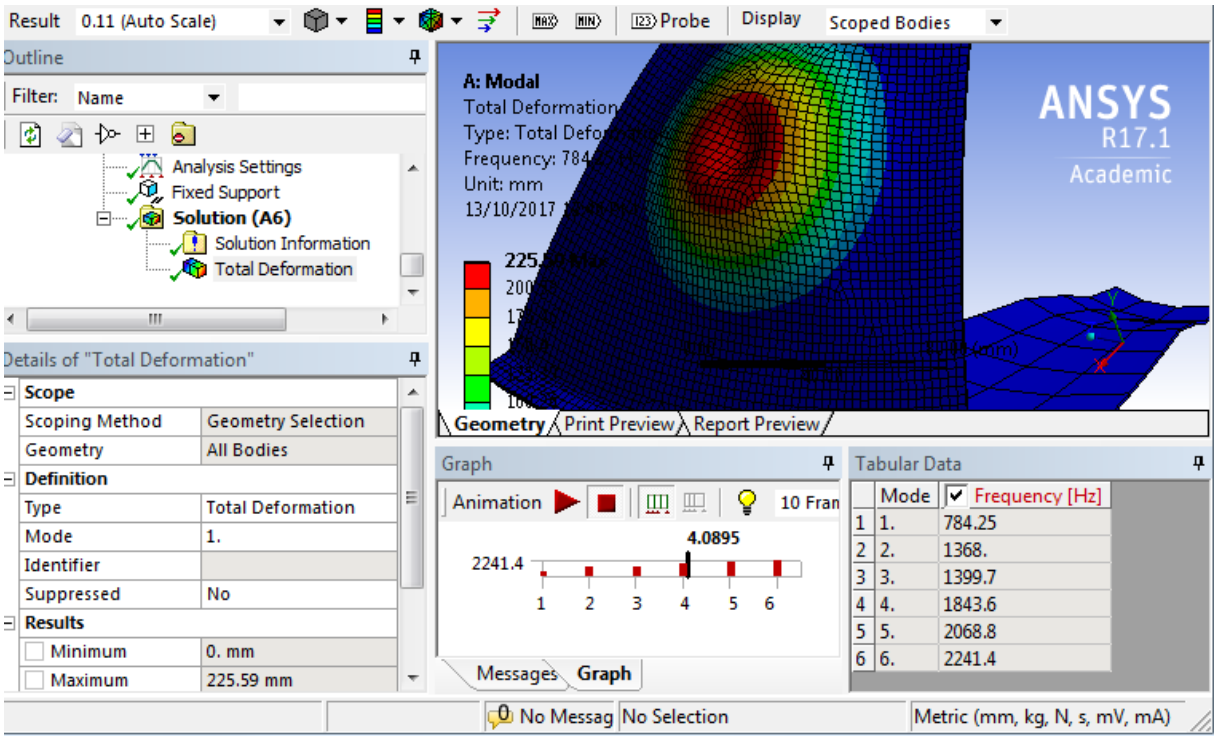

Figure 75: FEA Modal Results

11.4.2 Transient Analysis Method

Transient Analysis Methodology is as follows:

1. Follow the Modal Analysis method from steps 1-6.
2. Create two named selections as shown in Figure 76. Do this by enabling Node select and selecting then then inserting the name. The mesh must have been gated to be able to select a node.

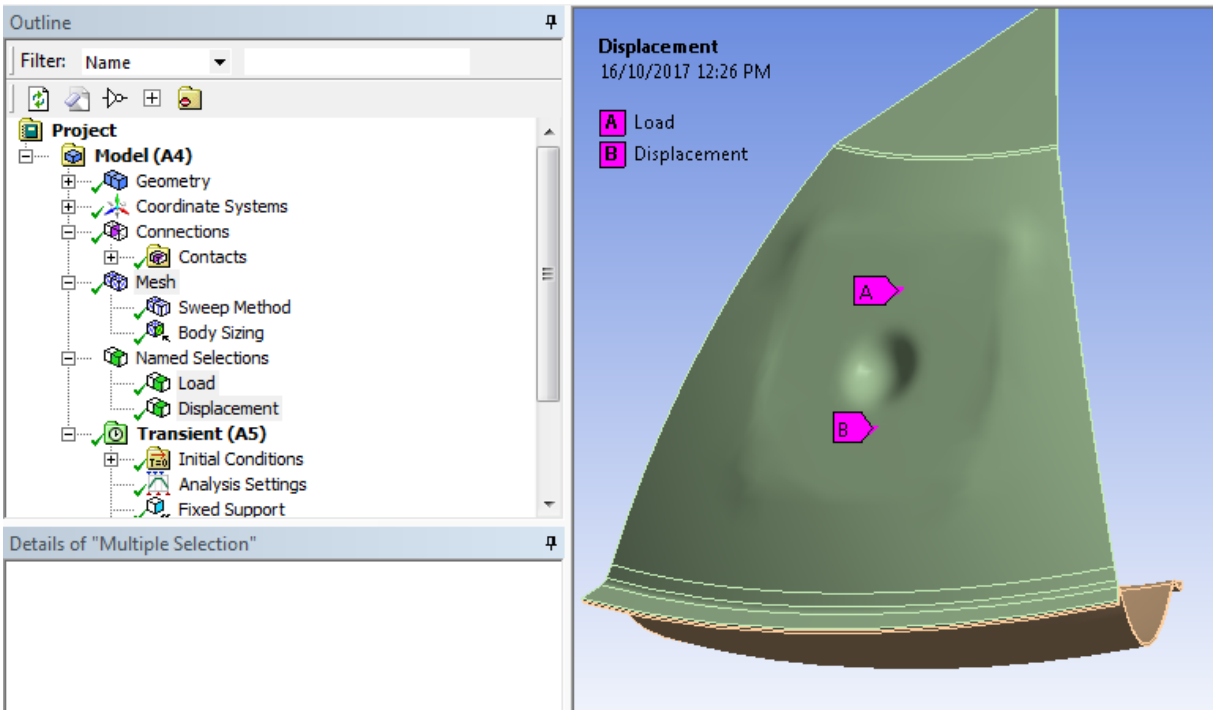

Figure 76: Named Selections

3. Set up the analysis settings as described in 6.3.1 and shown in Figure 78.
4. Apply a nodal force to the point called Load (just above the dimple) with the settings shown in Figure 77.
5. Solve the model (this often takes multiple hours).
6. Extract the time history for the node named Displacement by inserting a deformation result in solution. Scope it as a named selection and then select Displacement.

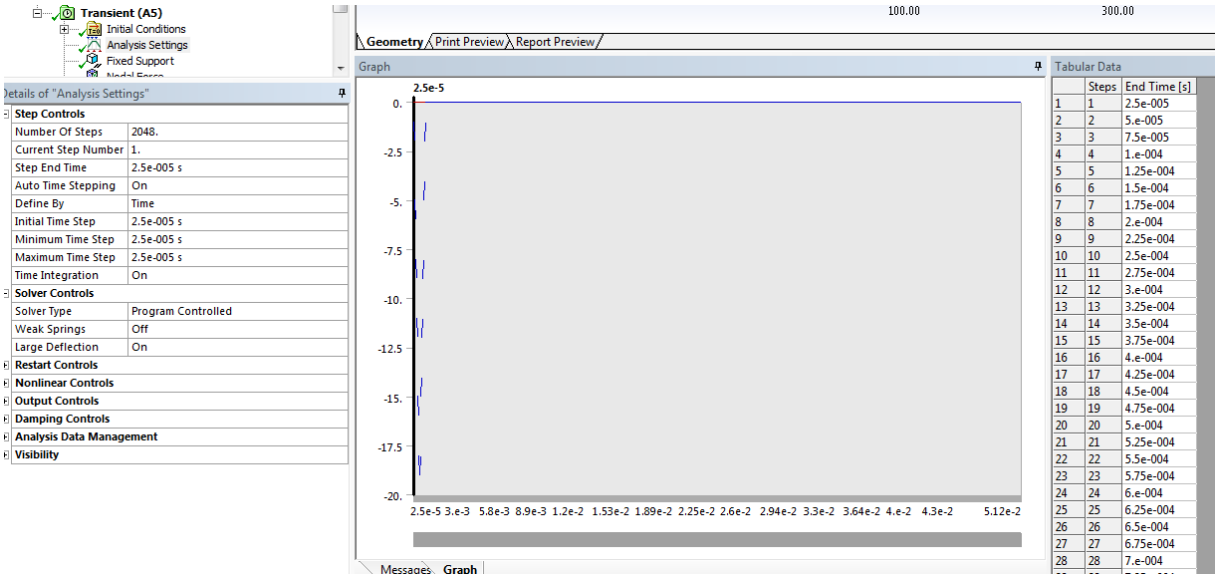

Figure 78: Transient Analysis Settings

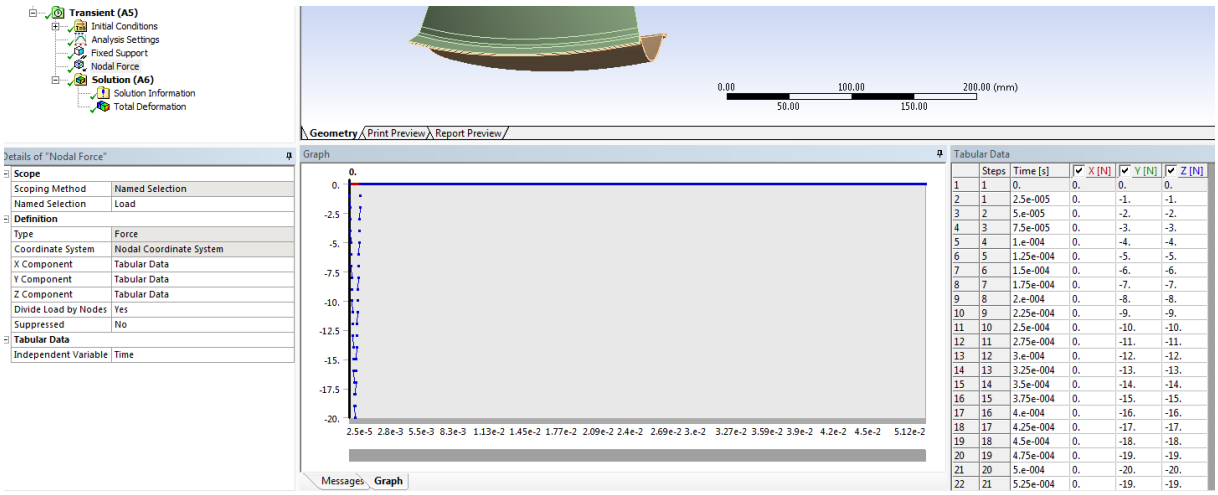

Figure 77: Nodal Force

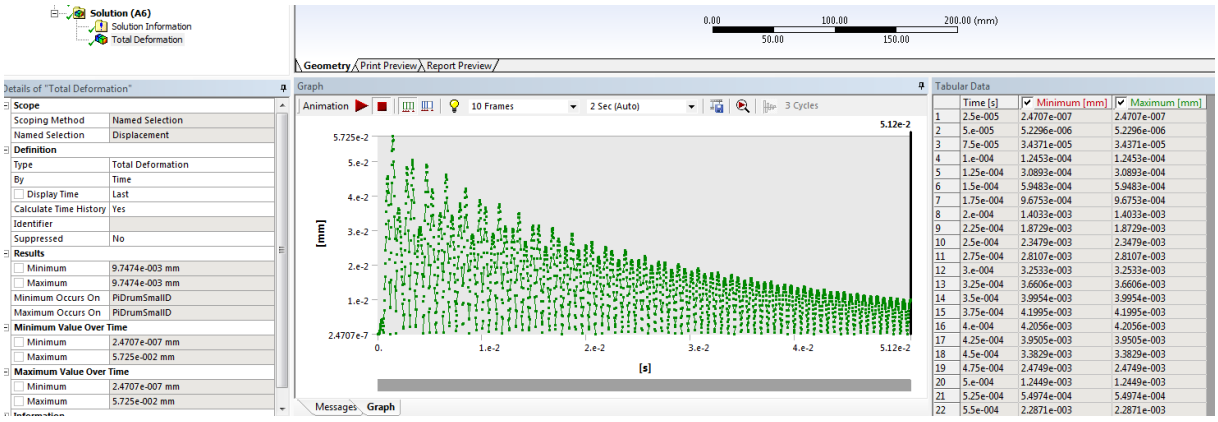

Figure 79: Nodal Displacement Time History

7. Export the time history displacement data and run it through and FFT to determine spectral response.
8. Perform steps 1-7 for all notes and desired geometric changes.

11.4.3 Transient Analysis FFTs

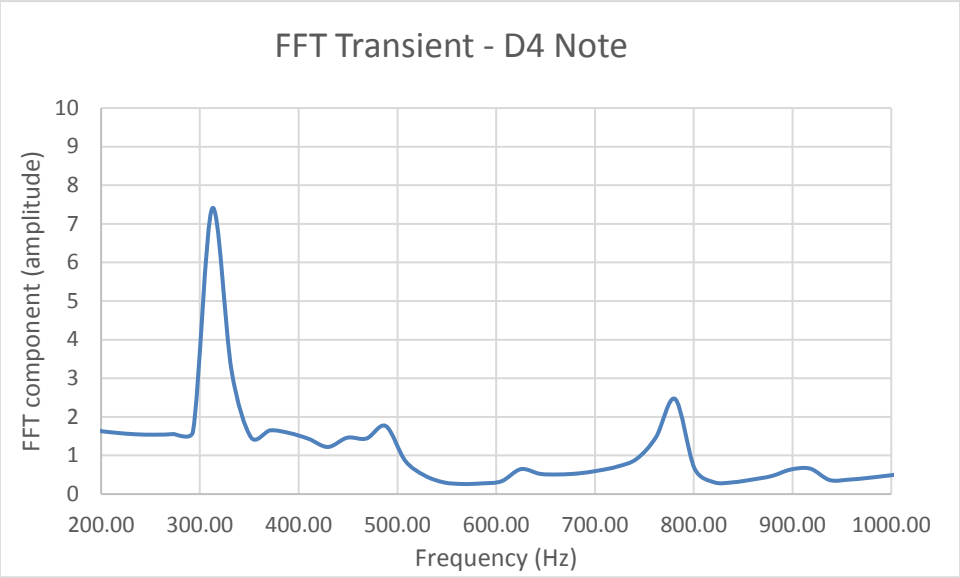

Figure 80: FFT of Transient Analysis Time History - D4

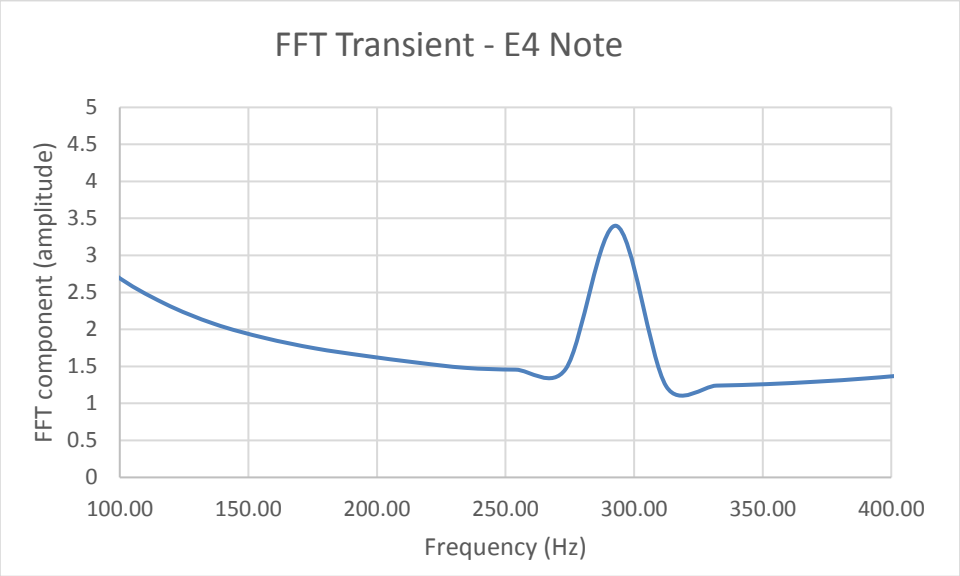

Figure 81: FFT of Transient Analysis Time History - E4

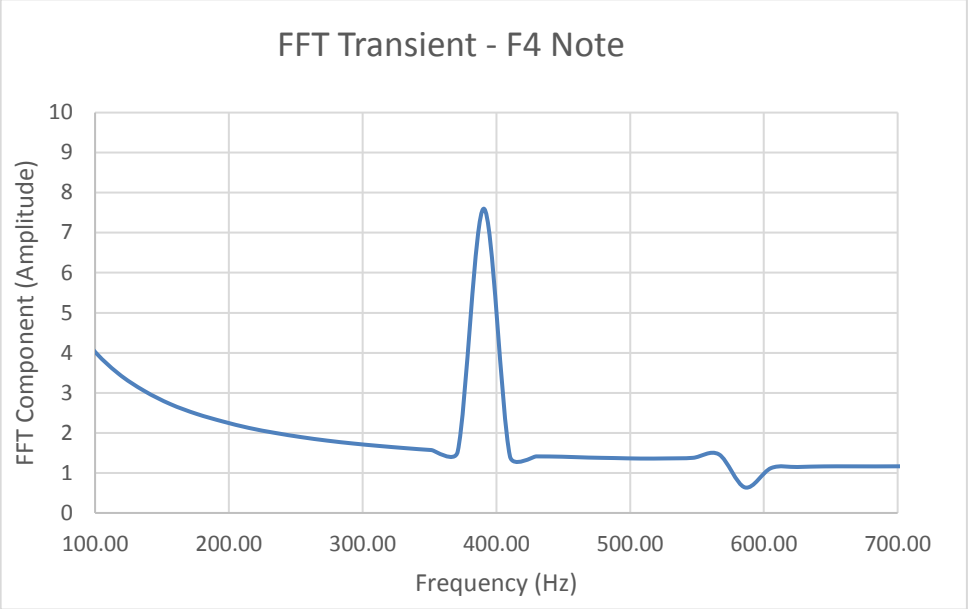

Figure 82: FFT of Transient Analysis Time History - F4

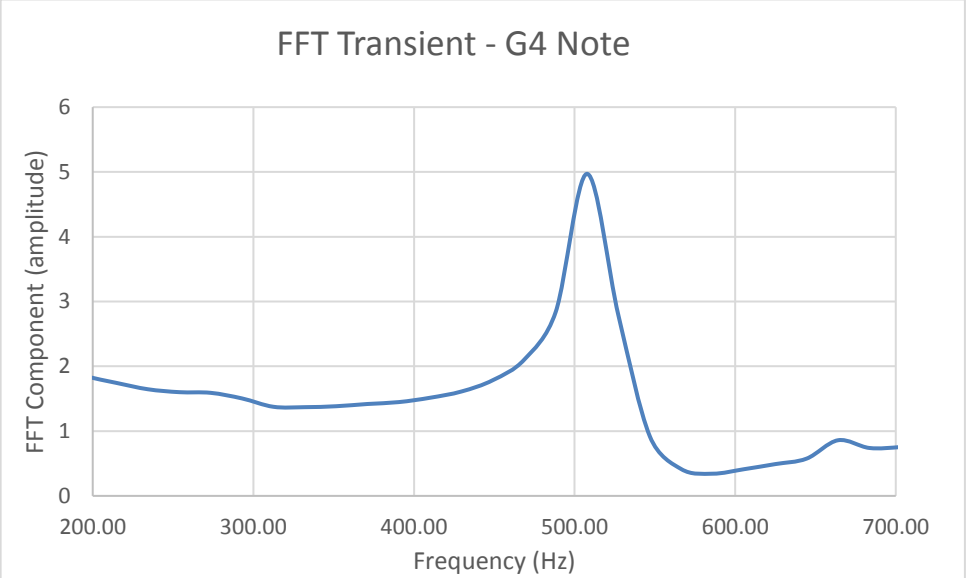

Figure 83: FFT of Transient Analysis Time History - G4

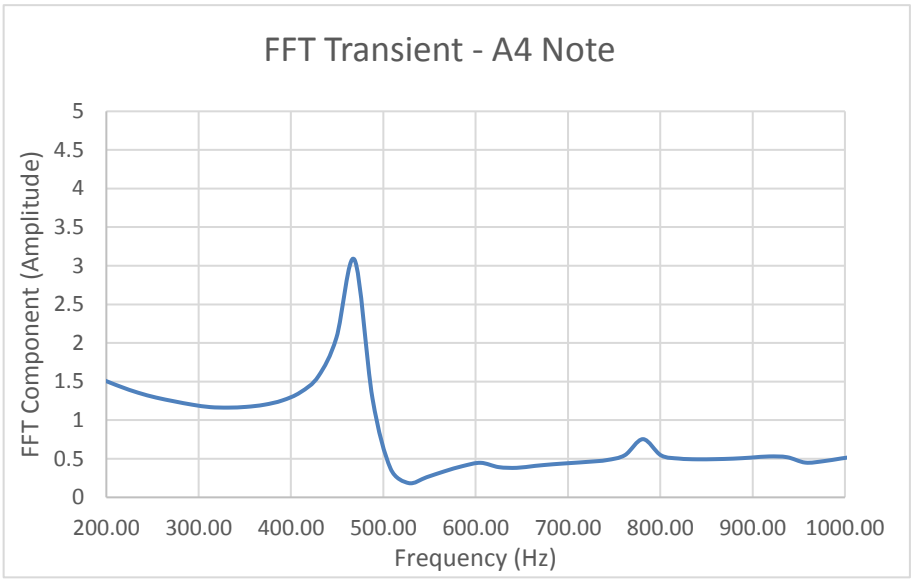

Figure 84: FFT of Transient Analysis Time History - A4

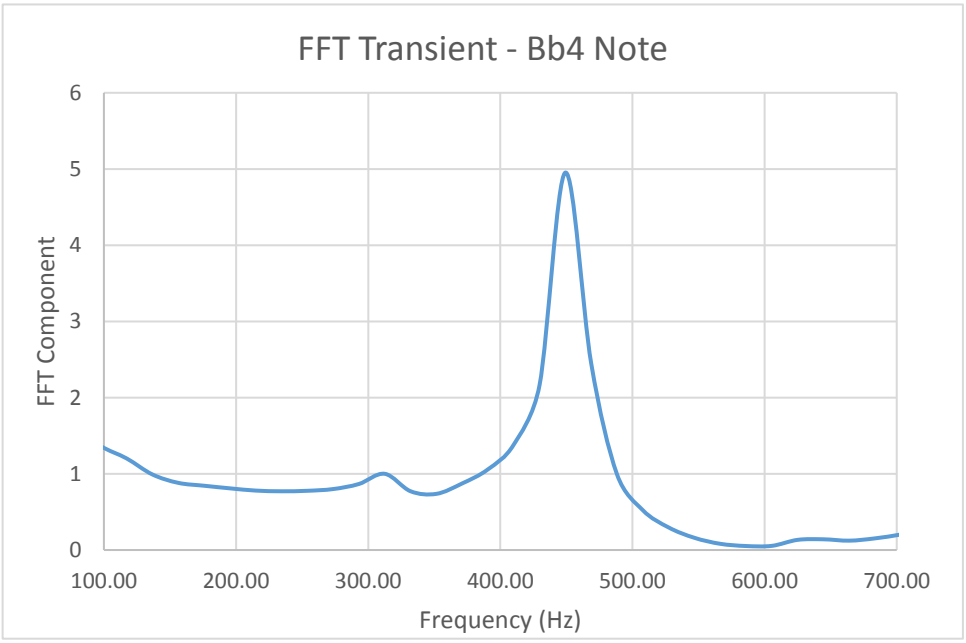

Figure 85: FFT of Transient Analysis Time History - Bb4

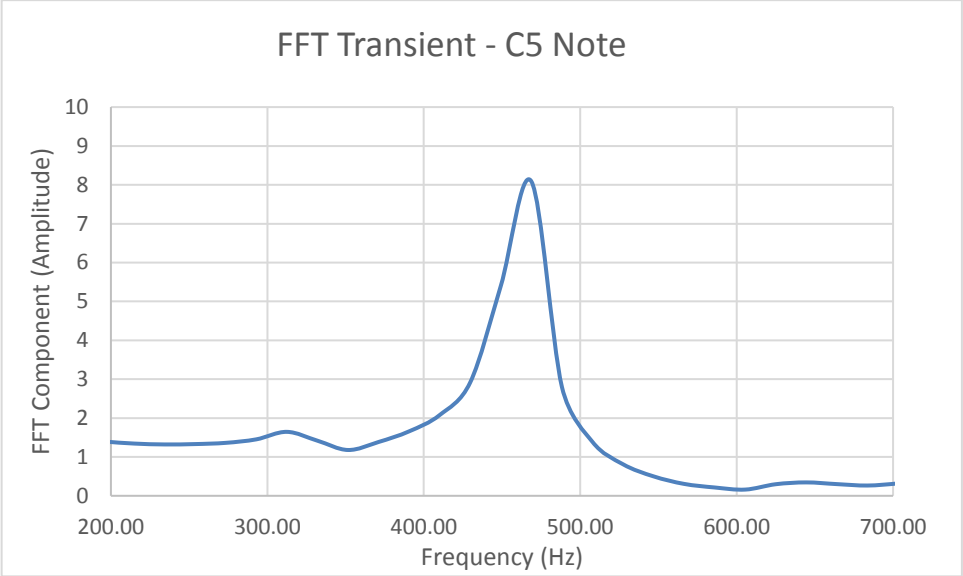

Figure 86: FFT of Transient Analysis Time History - C5

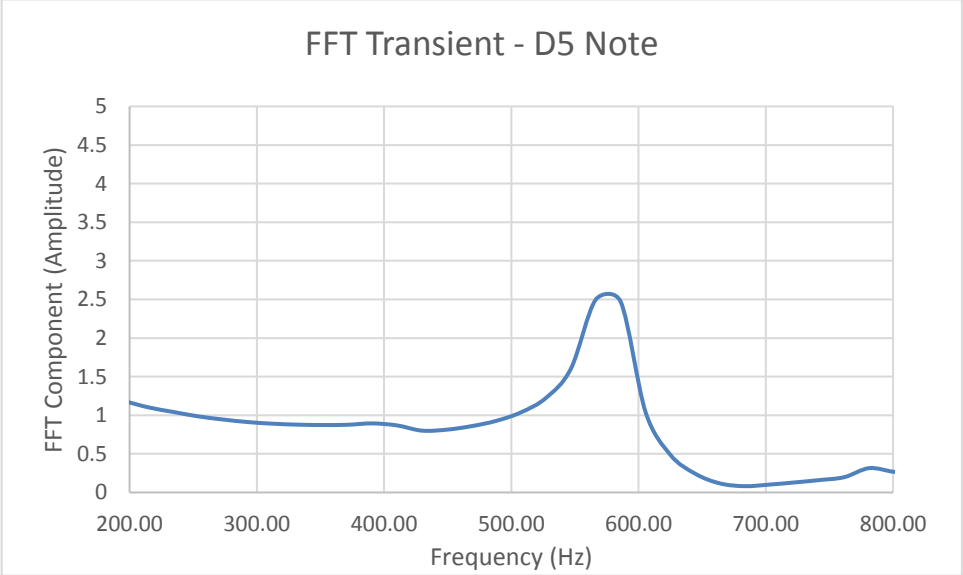

Figure 87: FFT of Transient Analysis Time History - D5

11.5 Appendix E

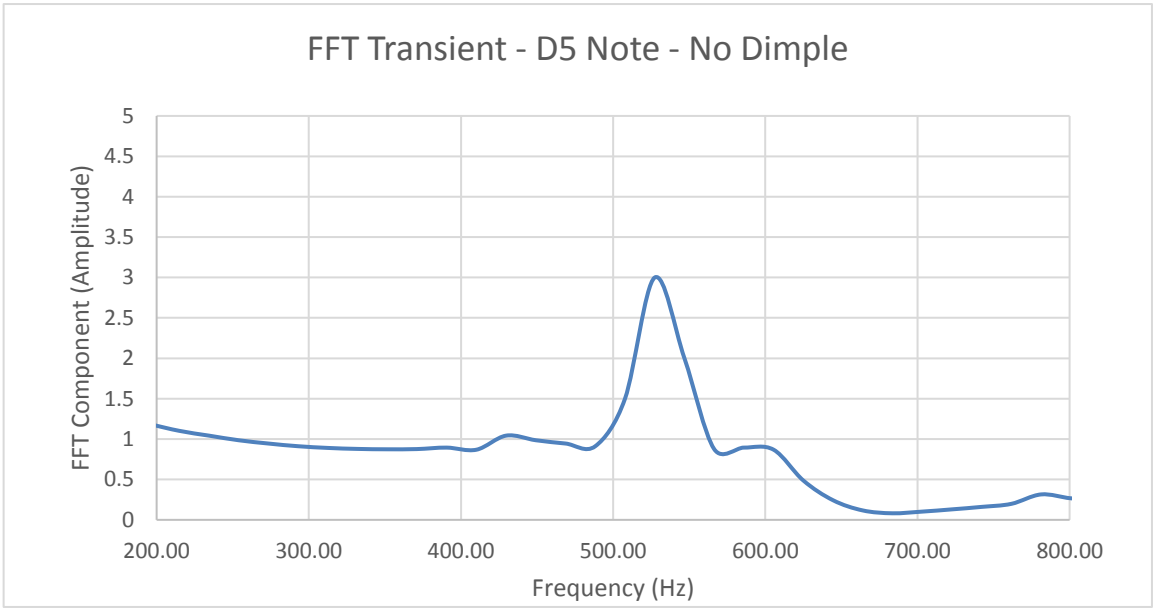

Figure 88: FFT - D5 - No Dimple

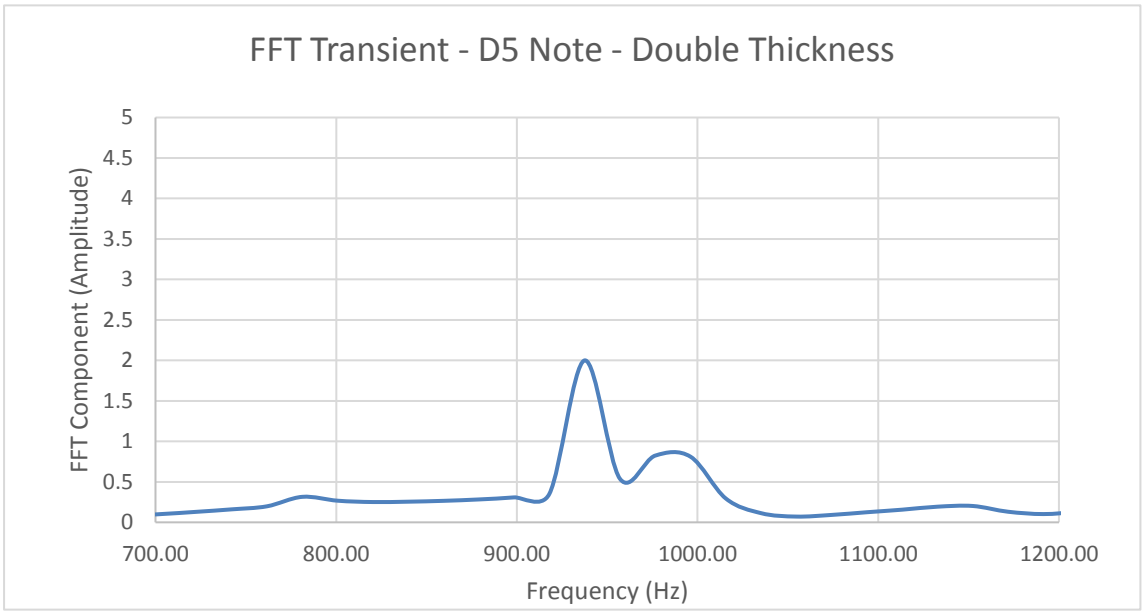

Figure 89: FFT- D5 - Double Thickness

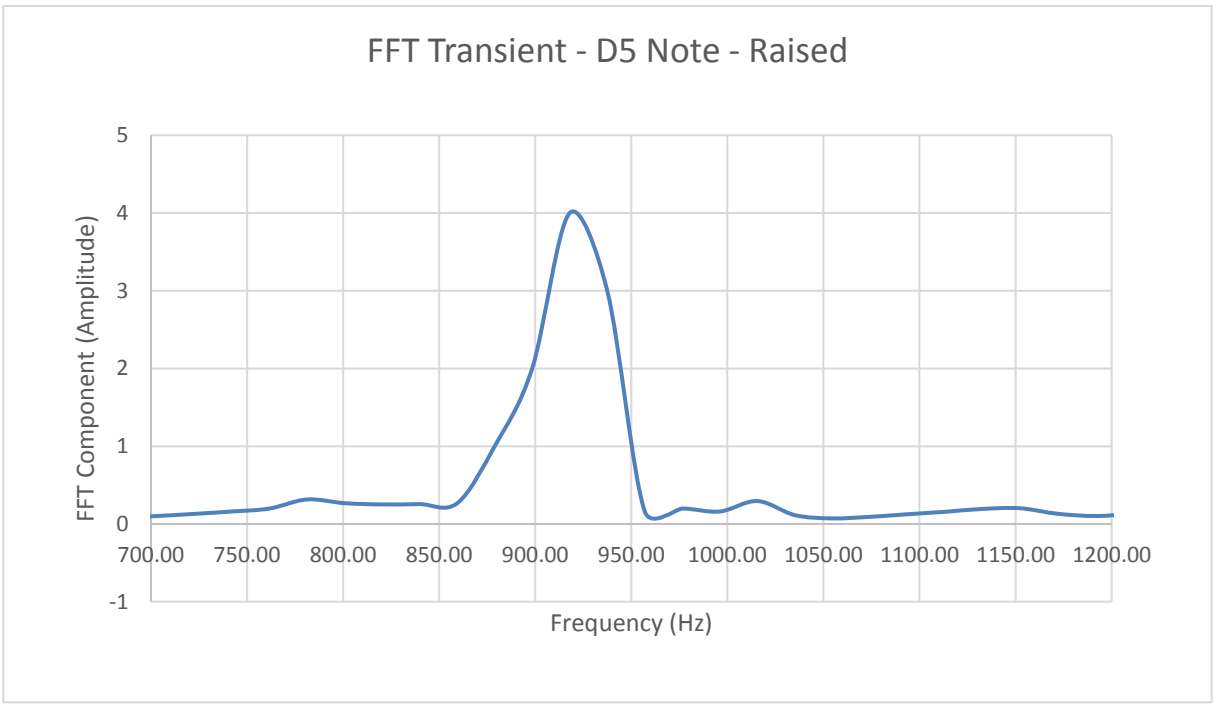

Figure 91: FFT - D5 - Raised

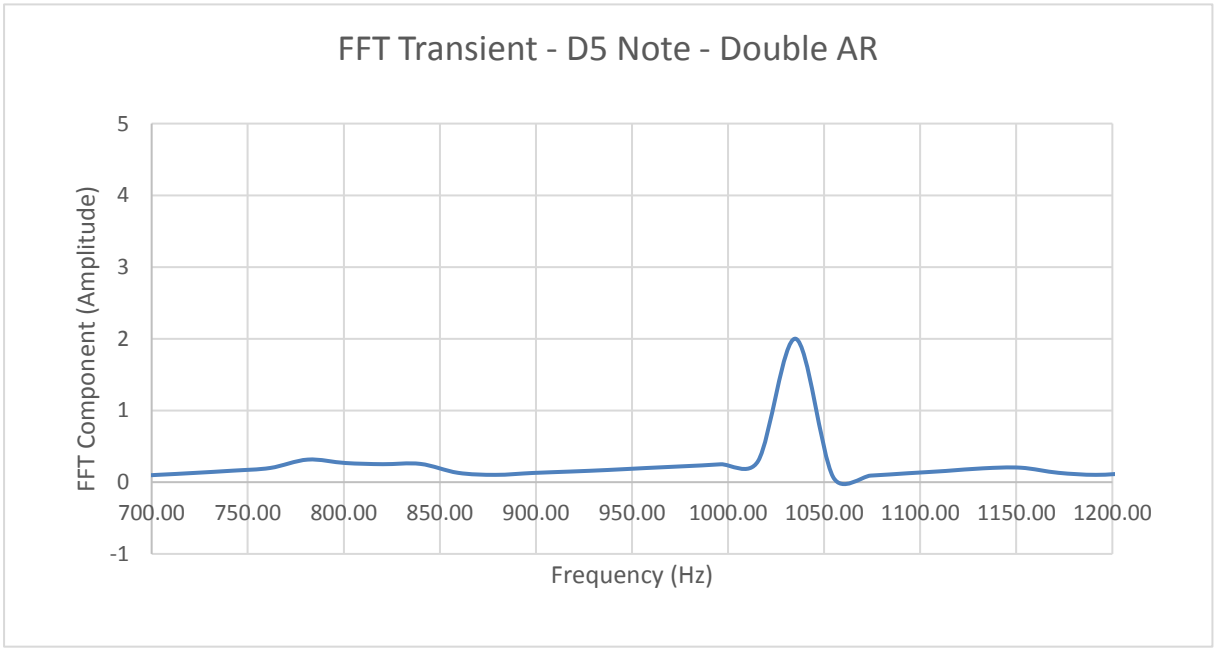

Figure 90: FFT - D5 - Double AR

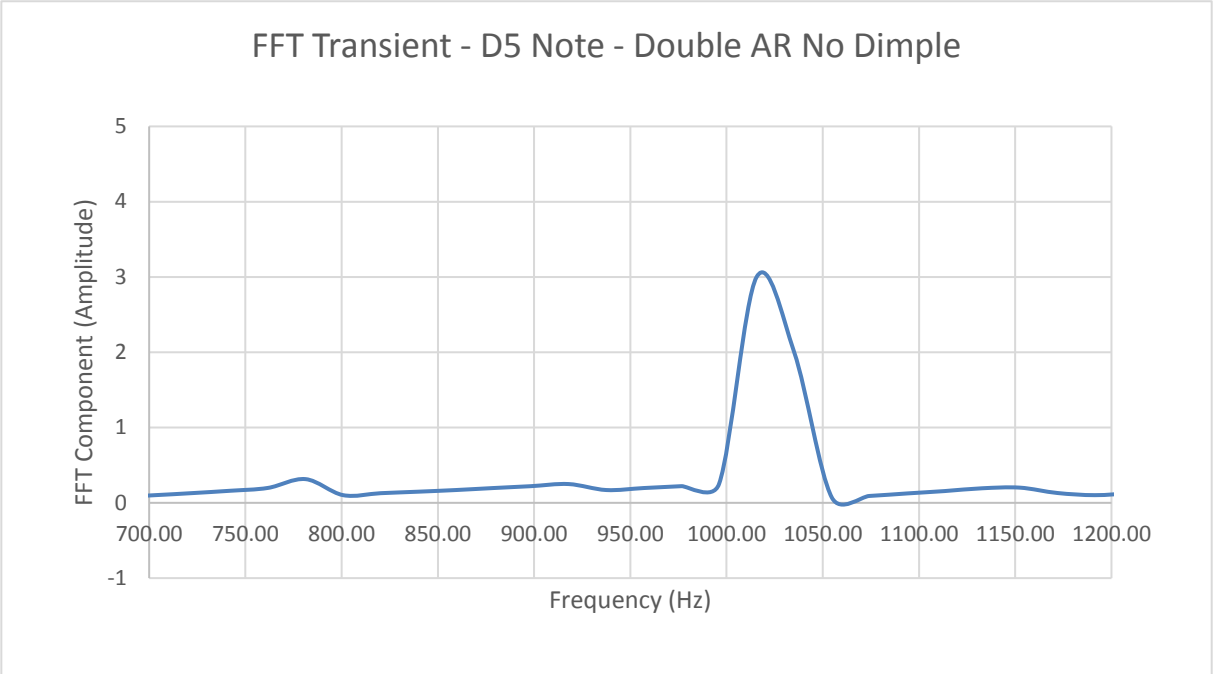

Figure 92: FFT - D5 - Double AR No Dimple

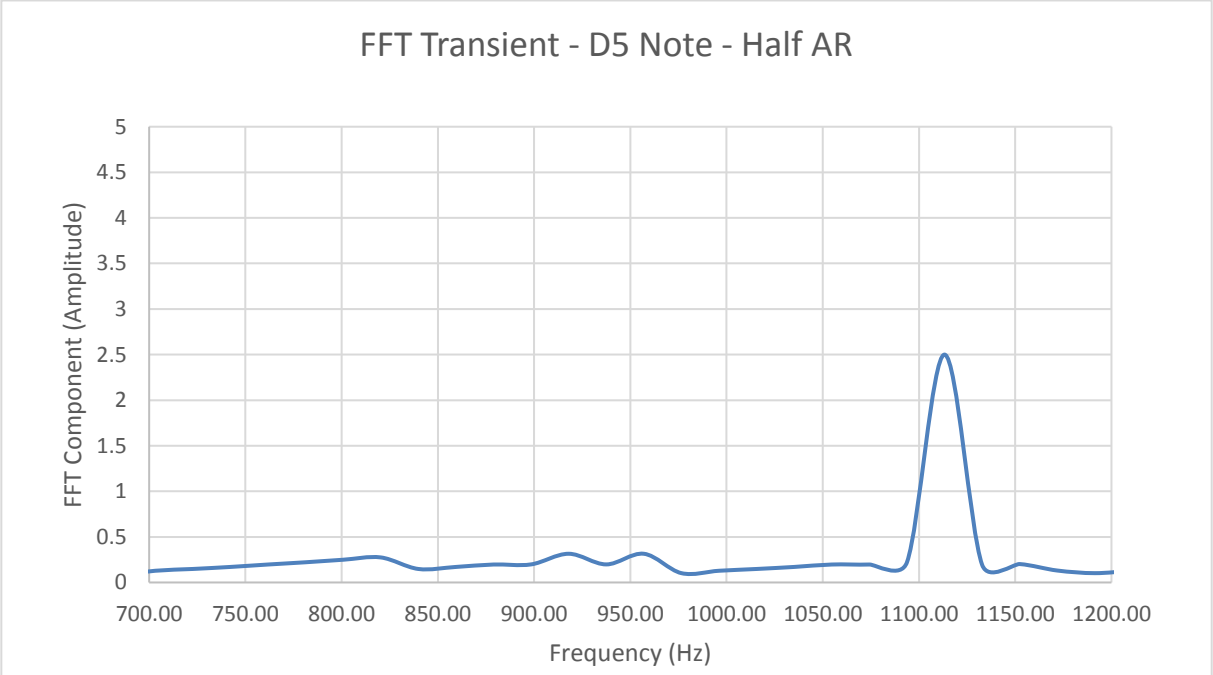

Figure 93: FFT - D5 - Half AR

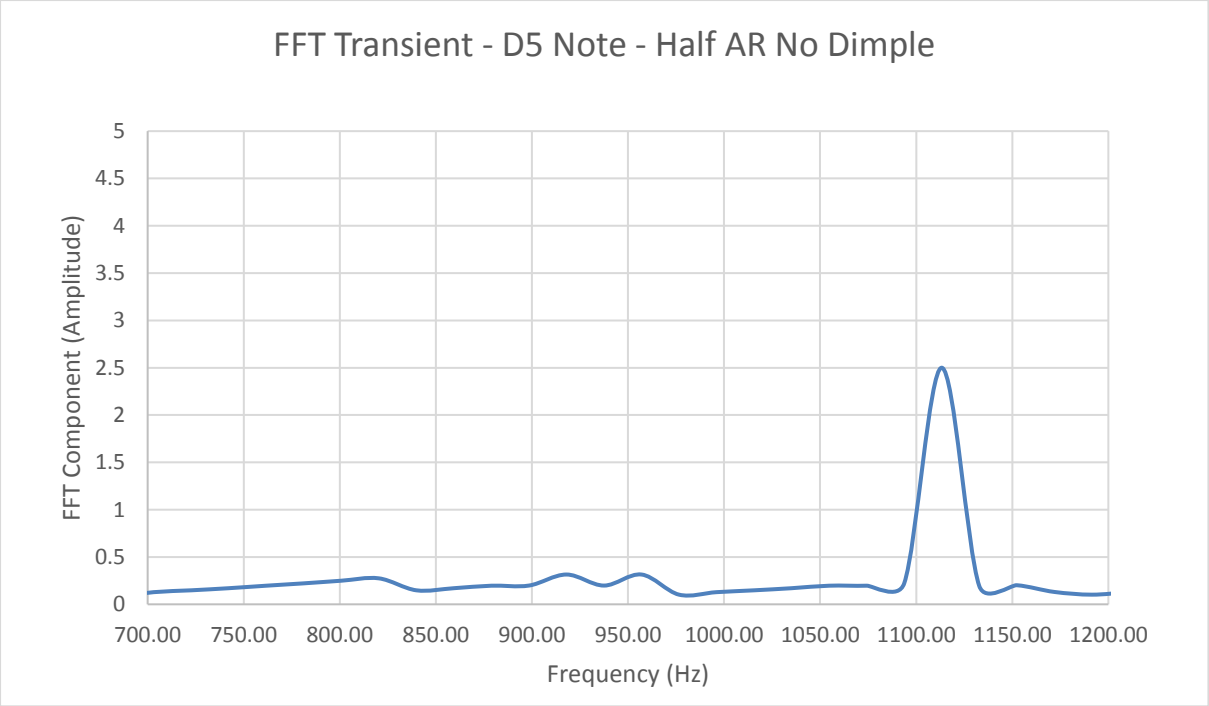

Figure 94: FFT - D5 - Half AR No Dimple